No. 03
ISSN 0801–9940 December 2008

Semi-analytical postbuckling analysis of stiffened plates with a free edge

by

Lars Brubak

RESEARCH REPORT IN MECHANICS

UNIVERSITY OF OSLO
DEPARTMENT OF MATHEMATICS
MECHANICS DIVISION

UNIVERSITETET I OSLO
MATEMATISK INSTITUTT
AVDELING FOR MEKANIKK

Mechanics Division
Dept. of Math., University of Oslo
Research Report in Mechanics, No. 03
ISSN 0801–9940 December 2008

Semi-analytical postbuckling analysis of stiffened plates with a free edge

by

Lars Brubak

Mechanics Division, Department of Mathematics,
University of Oslo

Abstract. A large deflection, semi-analytical method for pre- and postbuckling analysis of stiffened plates with a free edge is presented. The stiffeners can be oriented in both directions parallel and perpendicular to the free edge, and the stiffener spacing can be arbitrary. Both global and local buckling modes are captured by using a displacement field consisting of displacements representing a simply supported, stiffened plate and an unstiffened plate with a free edge. The out-of-plane and in-plane displacements are represented by trigonometric functions and linearly varying functions, defined over the entire plate. The formulations derived are implemented into a FORTRAN computer program, and numerical results, including load-displacement curves, stress plots and displacement shapes, are compared with results by finite element analysis for a variety of plate and stiffener geometries. Relatively high numerical accuracy is achieved with low computational efforts. In addition, introductory investigations of ultimate strength limit (USL) predictions computed by the present model are presented.

Keywords: Stiffened plates; Free edge; Postbuckling analysis; Semi-analytical method.

Contents

NOTATION

Subscripts

x, y, z	Components in Cartesian coordinates
$, xy$	Differentiation with respect to x and y
f	Flange
w	Web
0	Initial

Superscripts

a	Component representing a plate with a free edge
b	Component representing a simply supported plate
c	Component representing linear variations of in-plane displacements
me	The location at the midlength of a free edge or of an edge stiffener
pb	Bending contribution of the plate
pm	Membrane contribution of the plate
s	Stiffener
L	Linear
NL	Nonlinear

Symbols

E	Young's modulus
ν	Poisson's ratio
E_T	Hardening modulus
f_Y	Yield strength
L	Plate length
b	Plate width
t	Plate thickness
t_w	Web thickness
h_w	Web height
h	Stiffener height
t_f	Flange thickness

b_f	Flange width
A_s	Area of the cross-section of a stiffener
I	Moment of inertia about the middle plane of the plate
u, v, w	Displacements in a Cartesian coordinate system
w_i^a, w_{ij}^b	Amplitudes for the out-of-plane displacements
u_i^a, u_{ij}^b, u^c	Amplitudes for the displacements in x-direction
v_i^a, v_{ij}^b, v^c	Amplitudes for the displacements in y-direction
w_0	Model imperfection
w_{0i}^a, w_{0ij}^b	Amplitudes of the model imperfection
N_{dof}	Total number of degrees of freedom
σ_x, σ_y, τ_{xy}	In-plane stresses in a Cartesian coordinate system
ϵ_x, ϵ_y, γ_{xy}	In-plane strains in a Cartesian coordinate system
S_x	External stress in the x-direction
Λ	Load factor
Π	Total potential energy
U	Strain energy
T	Potential energy of the external loads

1 INTRODUCTION

The global capacity of plated structures depends on the buckling strength of the individual stiffened plates, and each individual plate must be dimensioned to be strong enough to sustain the external loads. As an alternative to the various finite element approaches and explicit design rules [1, 2], analysis using semi-analytical methods is becoming more common in structural analysis, in particular in computer based design codes [3, 4]. These methods are more accurate than the traditional explicit design formulas, and in addition more efficient than finite element analysis. Semi-analytical methods are usually tailor-made approaches for specific cases with certain boundary conditions and load conditions, and they are not so general as finite element approaches. This will increase the computational efficiency as compared to a more general problem description, but on the other hand, restrict the range of applicability.

In the present study, plates with a free edge are of interest. For such plates, most of the semi-analytical methods available are considering the elastic buckling (eigenvalue) characteristics of unstiffened plates. Since the accuracy and convergence of the method depend on the selection of displacement fields, many researchers have studied different proposals for admissible displacement functions for such plates. A usual assumption is to use a trigonometric series in the direction parallel to the free edge combined with polynomial functions in the perpendicular direction.

In a recent work by Mittelstedt [5], various displacement functions in the direction perpendicular to the free edge were studied, including various polynomial functions and a term with a cosine function. In that work, it was found that an ordinary polynomial function was the most appropriate displacement function. The same conclusion was also drawn by Smith, Bradford and Oehlers [6], where both ordinary and orthogonal polynomials were studied. In that paper, it was found that orthogonal polynomials were computationally more expensive than simple, ordinary polynomials, despite a reduced number of terms required for adequate convergence. Ordinary polynomials have also been applied in many other works, e.g., in Madhavan and Davidson [7, 8], Qiao and Shan [9], and Yu and Schafer [10].

All the semi-analytical methods for plates with free edges mentioned above are restricted to linear elastic buckling (eigenvalue) of unstiffened plates. In the present research work, the main focus is on postbuckling analysis of the plate response in which the displacements and stresses are predicted.

The major objective of this work is to develop a semi-analytical, large deflection (nonlinear) theory model for analysis of imperfect plates with one edge being free or provided

with an edge stiffener at the "free edge" and with or without additional stiffeners parallel or perpendicular to the free edge. The model should be capable of computing the plate response and the plate stresses. The plate stresses can be used in combination with suitable strength criteria in order to predict approximate ultimate strengths. The proposed model is based on an incremental form of the Rayleigh-Ritz method and follows the general solution strategy as outlined by Steen [11]. By using this solution procedure, the model is able to trace the pre- and postbuckling response, and consequently, it is capable of accounting for a possible reserve strength beyond the elastic buckling load typical for slender plates. The present solution strategy has also been applied by Byklum and Amdahl [12] for simply supported, regularly stiffened plates and by Brubak and Hellesland [13] for simply supported, irregularly stiffened plates. In addition, in a related semi-analytical model presented by Buermann, Rolfes, Tessmer and Schagerl [14], a similar solution strategy has been applied to stiffened cylindrical panels.

In the present semi-analytic model, the stiffeners are modelled as simple beams. This implies that the model is not able to capture local failure modes of the stiffeners. Consequently, the stiffeners must be dimensioned so that premature local stiffener buckling does not occur, for instance by satisfying certain requirements according to design rules [15, 16]. The torsional stiffness of the stiffeners may be accounted for by including the torsional energy contribution. The proposed model is able to capture the interaction between local and global plate bending, including asymmetric effects typical for cases with out-of-plane bending of plates with eccentric stiffeners. By applying rotational springs, the supported edges or a part of them may be simply supported, clamped or something in between. An initial deflection is included in the model formulation in order to describe an imperfection resulting from the fabrication process of a real structure.

2 PROBLEM FORMULATION

2.1 Introductory comments

For postbuckling analysis of thin plates, a usual approach is to describe the problem by out-of-plane displacements only. Then, the in-plane stresses must be found by solving the plate compatibility equation [17]. In previously presented semi-analytical methods for simply supported plates [12, 13], this equation have been solved by substituting an assumed Airy's stress function. For unstiffened plates with a free edge, a solution for the Airy's stress function is found by Ovesy, Loughlan and Assaee [18] using a finite strip approach. However, for semi-analytical approaches using a displacement field defined

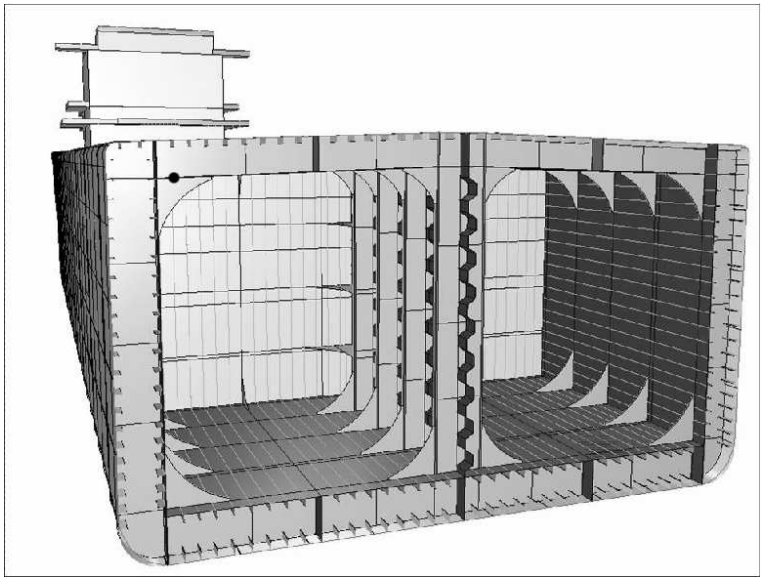

Figure 1: An illustration of a ship hull (graphics by the DNV's software program Nauticus Hull

over the entire plate, it is difficult, and maybe impossible, to find an analytical expression for the Airy's stress function that satisfies both the plate compatibility equation and the boundary conditions for a plate with a free edge.

Another approach is to use an assumed displacement field for each displacement component u, v and w. It is this approach that is presented in this report. By introducing assumed displacements also in the in-plane directions, more degrees of freedom are needed and a larger system of equations must be solved. An advantage of including in-plane displacements is that the difficulty of solving the plate compatibility equation for a stiffened plate with a free edge is avoided, and the stress computations becomes much more efficient. Once all the displacements (u, v, w) are known, the internal stresses and strains can be computed directly from Hooke's law.

The displacements are represented by adding together a displacement field for a simply supported, stiffened plate and a displacement field for an unstiffened plate with a free edge. As mentioned above, polynomial functions have been used in many research work for unstiffened plates with a free edge. However, if polynomials were used for stiffened plates, many terms are required for convergence, which, as discussed later, may cause numerical instabilities. These numerical difficulties are avoided with the present displacement fields.

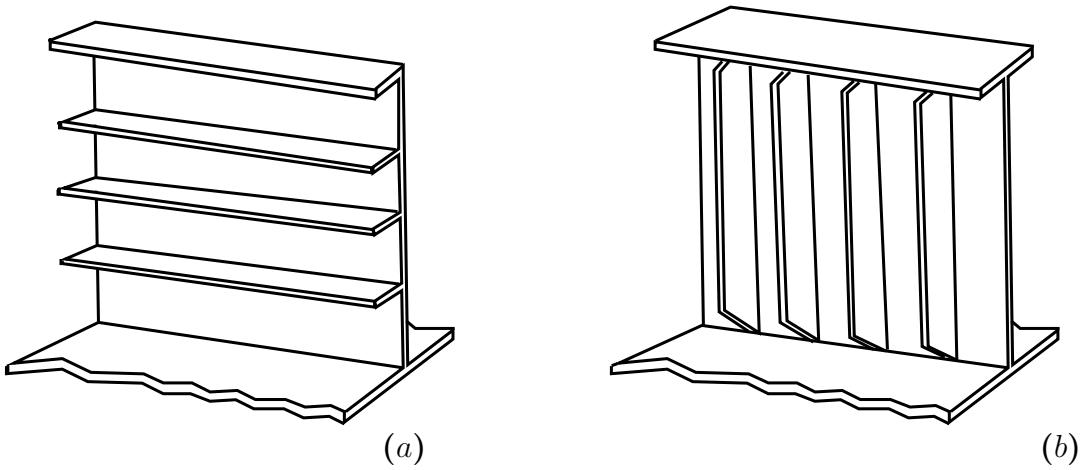

Figure 2: Typical stiffened girder examples with one free edge provided with (a) an eccentric stiffener and (b) a symmetric stiffener.

2.2 Relevant plate examples

In many branches such as marine, bridge and aerospace engineering, plated structures with stiffened plates are used as the main load-carrying components. In Fig. 1, a typical ship hull, where the structure is built up by stiffened plates, is illustrated. Due to overall bending and twisting of the ship hull, these plates are subjected to in-plane loads, and each plate must be designed to be strong enough to avoid plate collapse. A plate collapse causes material yielding and permanent displacements and this is usually not accepted. In the worst case, a local plate collapse can cause an overall collapse of the entire structure.

In ship hulls, there exist both integrated plates (i.e. plates surrounded by neighbouring plates and strong girders at all edges) and plates with a free edge. Longitudinal and transverse girders, and stringer decks are examples where the plates can have a free edge that may be provided with an edge stiffener. Girders and stringer decks are usually very important for the overall strength of the structure because they support the edges of the integrated plates. If these girders collapse, the entire structure may collapse.

Free edges of girders are often stiffened with either eccentric stiffeners or symmetric stiffeners as illustrated in Fig. 2(a) and (b), respectively. In addition, the interior plating of these girders can also be provided with horizontal and vertical stiffeners as shown in the figure, and the spacing between each stiffener may vary. These stiffeners can either be continuous or sniped at the edges.

Other examples where plates have a free edge are beams with channel sections and sections with flange outstands as illustrated in Fig. 3. These flange outstands can buckle

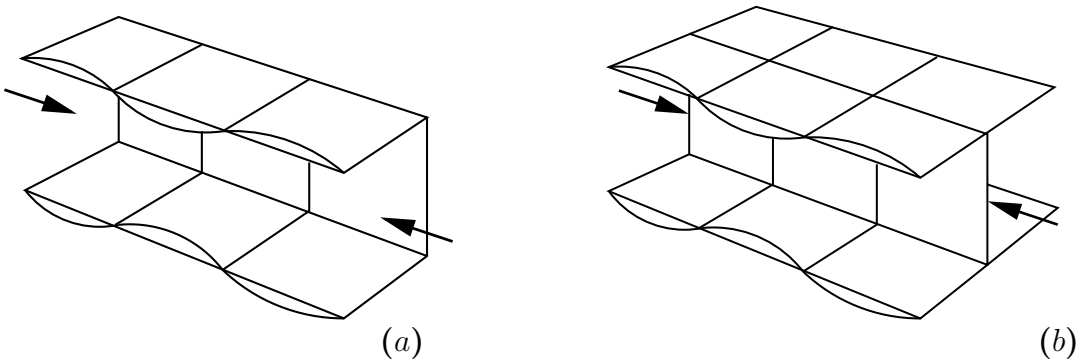

Figure 3: Local buckling of the flange outstands of a beam with (a) a channel section profile and (b) a T-section profile.

locally and this may cause an overall collapse (global buckling) of the beam. The cases mentioned above for plates with a free edge that may be stiffened are relevant examples of where the present method may be applied.

2.3 Plate definition

The rectangular plate considered can be defined with reference to Fig. 4. The plate has one unsupported edge that is free or provided with an edge stiffener, and it is supported in the out-of-plane direction at the three other edges. Two opposite supported edges, perpendicular to the free edge, are subjected to an external stress S_x.

A plate is usually a part of a larger structure and it is assumed that the supported edges remain straight due to the neighbouring plates. In addition, the loaded edges are free to move in the in-plane directions, but they are forced to remain parallel. A supported edge boundary may be simply supported, or it may be clamped or partially restrained by adding rotational spring restraints along the edges, or parts of the edges, in the same manner as described in Brubak and Hellesland [19].

The plate may be unstiffened, or it may be stiffened with one or more stiffeners oriented in the x- and y-direction. In Fig. 4(a), only one stiffener is shown in each direction. However, none or multiple stiffeners may be included. A stiffener may also be included along the "free edge". Clearly, with a stiffener present, the edge is strictly speaking not free. However, for convenience it will be referred to as a "stiffened free edge".

The spacing between the stiffeners can be arbitrarily chosen. The stiffeners may have

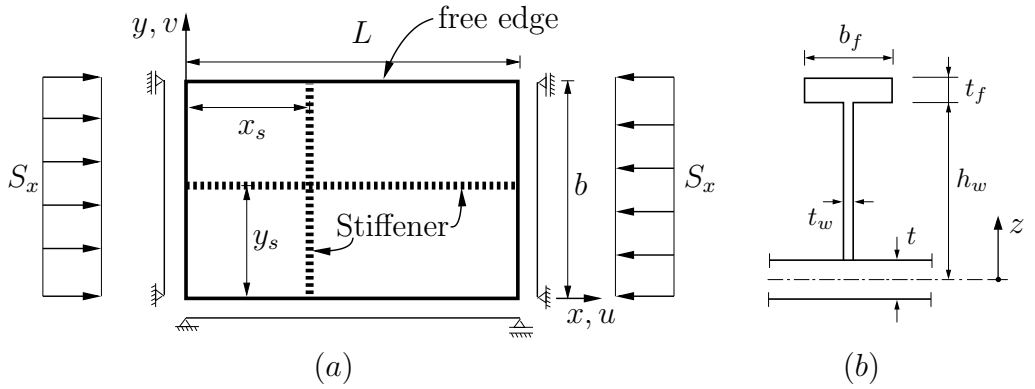

Figure 4: (a) A uniaxially loaded, stiffened plate with a free edge and three supported edges and (b) an eccentric stiffener.

different cross-section profiles, and may be eccentric, as in Fig. 4(b), or symmetric about the middle plane of the plate. The stiffeners may be end loaded (continuous stiffeners) or sniped at the ends (with no end loads).

The stiffeners are modelled as simple beams, and consequently, lateral deflections of the stiffeners are not accounted for. With this assumption, the stiffeners must be dimensioned such that premature local stiffener buckling does not occur. This can be done for instance by satisfying constructional design requirements in existing design rules, e.g., [15, 16], which are given to prevent local failure modes of the stiffeners. By using such design rules, the compressive stresses in the stiffeners will not exceed the critical stress for local stiffener buckling. Consequently, in such cases, the present stiffener modelling approach, neglecting local buckling of the stiffeners, seems reasonable.

The torsional stiffness of the stiffeners may be accounted for by including the torsional energy contribution. This contribution is neglected for the cases studied in the present report where only open stiffener profiles are considered, such as for instance T-profiles and flat bar profiles. This neglect is reasonable as the torsional stiffness of stiffeners with such profiles is relatively small. In addition, it is conservative to neglect this contribution. On the other hand, for stiffener with a closed profile, the torsional stiffness may be large and it may be too conservative to neglect this stiffness contribution.

3 MATERIAL LAW AND KINEMATIC RELATIONSHIPS

For thin isotropic plates, the stresses in the thickness direction is negligibly small and it is usual to assume a plane stress condition. Further, for a material that is assumed to be linearly elastic with Young's modulus E and Poisson's ratio ν, the well known Hooke's law is defined by

$$\sigma_x = \frac{E}{1-\nu^2}(\epsilon_x + \nu\epsilon_y) \tag{1}$$

$$\sigma_y = \frac{E}{1-\nu^2}(\epsilon_y + \nu\epsilon_x) \tag{2}$$

$$\tau_{xy} = \frac{E}{2(1+\nu)}\gamma_{xy} = G\gamma_{xy} \tag{3}$$

where σ_x, σ_y and τ_{xy} are the in-plane stresses, and ϵ_x, ϵ_y and γ_{xy} the in-plane strains, defined positive in tension. The total strain at a distance z from the middle plane of the plate can be written as

$$\epsilon_x = \epsilon_x^{pm} - zw_{,xx}\ , \quad \epsilon_y = \epsilon_y^{pm} - zw_{,yy}\ , \quad \gamma_{xy} = \gamma_{xy}^{pm} - 2zw_{,xy} \tag{4}$$

where the first terms, with the super index 'pm', represent the membrane strains and the second terms expressed by out-of-plane displacements w are the bending strains. These out-of-plane displacements w are additional to an initial imperfection. The conventional "comma" notation is used for partial differentiation, i.e., $w_{,xy}$ for $\partial^2 w/\partial x\partial y$, etc. The bending strain distribution complies with Kirchhoff's assumption [20] that normals to the middle plane remain normal to the deflected middle plane. For the membrane strains, the classical large deflection theory [21] is used (large rotations, but small in-plane strains). The in-plane membrane strains are defined by

$$\epsilon_x^{pm} = u_{,x} + \frac{1}{2}w_{,x}^2 + w_{0,x}w_{,x} \tag{5}$$

$$\epsilon_y^{pm} = v_{,y} + \frac{1}{2}w_{,y}^2 + w_{0,y}w_{,y} \tag{6}$$

$$\gamma_{xy}^{pm} = u_{,y} + v_{,x} + w_{,x}w_{,y} + w_{0,x}w_{,y} + w_{0,y}w_{,x} \tag{7}$$

for a plate with an initial out-of-plane imperfection w_0. Here, u and v are the displacements of the middle plane of the plate in the x- and y-direction, respectively. These formulations were given by Marguerre [17] in order to include initial imperfections in the von Karman's plate theory [20].

4 DISPLACEMENTS AND IMPERFECTION

4.1 Displacement fields

The displacement field in each direction consists of a field representing an unstiffened plate with a free edge, identified by a super index 'a', and a simply supported, stiffened plate, identified by a super index 'b'. In addition, a linear in-plane displacement field, identified by a super index 'c', is added to the displacement field in the x- and y-direction in order to account for linear variations. The displacement fields are given by

$$w = w^a + w^b \tag{8}$$

$$u = u^a + u^b + u^c \tag{9}$$

$$u = v^a + v^b + v^c \tag{10}$$

where

$$w^a(x,y) = \sum_{i=1}^{M_{wa}} w_i^a \frac{y}{b} \sin(\frac{\pi i x}{L}) \tag{11}$$

$$w^b(x,y) = \sum_{i=1}^{M_{wb}} \sum_{j=1}^{N_{wb}} w_{ij}^b \sin(\frac{\pi i x}{L}) \sin(\frac{\pi j y}{b}) \tag{12}$$

$$u^a(x,y) = \sum_{i=1}^{M_{ua}} u_i^a \frac{y}{b} \sin(\frac{\pi i x}{L}) \tag{13}$$

$$u^b(x,y) = \sum_{i=1}^{M_{ub}} \sum_{j=1}^{N_{ub}} u_{ij}^b \sin(\frac{\pi i x}{L}) \sin(\frac{\pi j y}{b}) \tag{14}$$

$$u^c(x,y) = u^c \frac{x}{L} \tag{15}$$

$$v^a(x,y) = \sum_{i=1}^{M_{va}} v_i^a \frac{y}{b} \cos(\frac{\pi i x}{L}) \tag{16}$$

$$v^b(x,y) = \sum_{i=1}^{M_{vb}} \sum_{j=1}^{N_{vb}} v_{ij}^b \sin(\frac{\pi i x}{L}) \sin(\frac{\pi j y}{b}) \tag{17}$$

$$v^c(x,y) = v^c \frac{y}{b} \tag{18}$$

where w_i^a, w_{ij}^b, u_i^a, u_{ij}^b, u^c, v_i^a, v_{ij}^b, v^c are amplitudes, L the plate length and b the plate width. With these displacement fields, the total number of degrees of freedom is

$$N_{\text{dof}} = M_{ua} + (M_{ub} \times N_{ub}) + M_{va} + (M_{vb} \times N_{vb}) + M_{wa} + (M_{wb} \times N_{wb}) + 2 \tag{19}$$

For the displacement fields representing a simply supported plate (Eqs. 12, 14 and 17), similar fields with only one term in each direction are used in Bazant [21] to study simply supported, unstiffened plates. By including more terms in the displacement fields in each direction, it is also possible to model stiffened plates in the same manner as in Brubak et al. [13, 19, 22]. For the displacement fields representing a plate with a free edge (Eqs. 11, 13 and 16), each displacement component consists of a trigonometric series in the x-direction in the same manner as in Ovesy, Loughlan and GhannadPour [23], and a linear variation in y-direction.

Both the displacement fields representing a simply supported plate (with super index 'a') and an unstiffened plate with a free edge (with super index 'b') account for the in-plane and out-of-plane variations due to out-of-plane bending. In addition, the displacements fields defined with the super index 'c' (Eqs. 15 and 18) are included in order to account for linear varying, in-plane displacements. For instance, if an unstiffened plate without initial imperfections is analysed by the present model, no out-of-plane displacements occur and the only non-zero displacement amplitudes are u^c and v^c. The latter component v^c accounts for the extension of the plate in y-direction due to Poisson's ratio.

Boundary conditions

The displacement fields represent a plate with three simply supported edges and one free edge. The displacements at the supported boundaries can be related to the coordinate system in Fig. 4 and expressed by

$$u(0,y) = 0, \quad u(L,y) = u^c, \quad v(0,y) = 0 \tag{20}$$

$$w(0,y) = 0, \quad w(L,y) = 0, \quad w(x,0) = 0 \tag{21}$$

Although the plate has three simply supported edges, it is also possible to model rotationally restrained edges by using rotational springs. In the out-of-plane displacement fields, each term in the series of sine functions represents a simply supported condition, and consequently, does not satisfy the kinematic boundary conditions for rotationally restrained edges. However, by adding together the terms, the sine series are, in combination with rotational springs along the supports, nearly able also to describe fully or partially restrained conditions. If plate edges, or portions of edges, are partly or fully clamped, the additional strain energy contributions from the rotational springs have to be added.

For rotationally fully clamped plates, it would be more appropriate to assume an out-of-plane displacement field defined with a series of cosine functions that satisfy the kinematic boundary conditions. To achieve the same accuracy with a sine field that does

not satisfy the kinematic boundary conditions, a higher number of degrees of freedom (number of terms) will normally be required. Rotational edge restraints are discussed in more detail by Brubak et al. [19, 24], and by Byklum and Amdahl [12].

Discussion/comments

Some comments of the chosen displacement fields might be in order. In the assumed displacement field representing a plate with one free edge, variations in the y-direction (perpendicular to the free edge) are accounted for by including linear polynomial functions. As mentioned before, polynomial functions in the y-direction have been used for analysing plates with a free edge in many research works, e.g., Mittelstedt [5], Madhavan and Davidson [7, 8], Qiao and Shan [9], and Yu and Schafer [10]. In these works, unstiffened plates were studied, and for such plates it is not necessary to used many terms in order to achieve satisfactory results.

In preliminary stages of the present work, displacements with polynomial functions with many terms were studied. In that study, an eigenvalue problem was established for an assumed displacement field defined by

$$w^{po}(x,y) = \sum_{i=1}^{M_w} \sum_{j=1}^{N_w} w_{ij}^{po} \left(\frac{y}{b}\right)^j \sin(\frac{\pi i x}{L}) \tag{22}$$

where w_{ij}^{po} denotes the displacement amplitudes. In order to describe the displacements for an unstiffened plate, a polynomial with 3 or 4 terms in Eq. 22 will normally be enough. For such few terms, no numerical problems occurred in the test study. However, by using Eq. 22 for a stiffened plate, many terms must be included to describe the displacements. In principle, the more terms that are included in the polynomial function, the more exact the solution becomes. However, numerical tests using the polynomial function showed that numerical problems occur if many polynomial terms are included. As a result of this, it was decided to replace the displacement field in Eq. 22 by the combined displacement field defined by Eq. 11 and 12.

For the assumed displacement fields used in the present method (Eqs. 8-18), numerical problems did not occur. The approximation of using only a linear variation in the y-direction is partly compensated for by adding the trigonometric series representing a simply supported stiffened plate (u^b, v^b, w^b). This will be demonstrated later.

4.2 Imperfection shape

The initial imperfection shape is represented by a similar field as that used for the additional out-of-plane displacements. This imperfection can be written as

$$w_0 = w_0^a + w_0^b \tag{23}$$

where

$$w_0^a(x,y) = \sum_{i=1}^{M_{wa}} w_{0i}^a \frac{y}{b} \sin(\frac{\pi i x}{L}) \tag{24}$$

$$w_0^b(x,y) = \sum_{i=1}^{M_{wb}} \sum_{j=1}^{N_{wb}} w_{0ij}^b \sin(\frac{\pi i x}{L}) \sin(\frac{\pi j y}{b}) \tag{25}$$

Here, w_{0i}^a and w_{0ij}^b are displacement amplitudes. These amplitudes must be found in order to describe the imperfection.

In the results presented later, the first eigenmode is used for the imperfection shape as such. The maximum amplitude of the imperfection is a specified value. In a design situation, this value can be taken according to a relevant design code [1, 2]. The eigenmode is computed in the same manner as described in detail in Brubak et al. [19]. The resulting eigenvalue problem can be written in the common, bold face notation as

$$(\mathbf{K}_e^M + \Lambda^e \mathbf{K}_e^G)\mathbf{w}^e = \mathbf{0} \tag{26}$$

where Λ^e is the eigenvalue and $\mathbf{w}^e$ the corresponding eigenmode. $\mathbf{K}_e^M$ and $\mathbf{K}_e^G$ are the material and geometrical stiffness matrix, respectively. These matrices are given in Appendix E. In this eigenvalue problem, the amplitudes for the out-of-plane displacements are the only unknowns.

In the eigenvalue problem, the stiffeners are modelled as simple beams with flexural stiffness only against out-of-plane bending. This means that the axial stiffener stiffness is neglected. An eccentric stiffener is included in the same manner as a symmetric stiffener, but with an effective moment of inertia I_e computed with an effective plate width b_e. In the same manner as in Brubak et al. [19], an effective plate width $b_e = 30t$ is used for a stiffener located in the interior plating, where t is the plate thickness. For an edge stiffener at the free edge, the effective plate width is reduced to $b_e = 15t$ as proposed by Eiding [25]. Similar reduction for the effective plate width for edge stiffeners was used by Rhodes [26] in another context.

In order to obtain a more correct interaction between the stiffener and the plate in an eigenvalue procedure, a method such as presented by Bedair [27] could have been

used. In that method, both out-of-plane and in-plane displacements are introduced as unknowns. The approximation of neglecting the axial stiffener stiffness and of using an effective moment of inertia, in the present procedure for obtaining the imperfection shape, is considered more than adequate. This has also also been verified by Brubak and Hellesland [19, 22]

In principle, any imperfection shape can be used in the present model. Another common approach for stiffened plates is to use an imperfection shape in which a global and a local imperfection mode is added together (Byklum [28], Paik and Lee [29]). The global mode may be taken equal to the displacement field of a plate without stiffeners. The local mode can be found by performing a linear elastic buckling analysis where the out-of-plane displacements along the stiffeners are prevented by using strong translational springs. Alternatively, measured imperfections in a real plate may approximately be represented by the assumed displacement field. Any imperfection shape can be modelled by using enough terms in the displacement field.

5 SOLUTION PROCEDURE

5.1 Incremental response propagation

The postbuckling response is traced using an incremental procedure presented by Steen [11] in which an arc length parameter is used as a propagation (incrementation) parameter. By using an arc length parameter, this procedure is more general than methods with pure load or pure displacement control, and a complex plate response can be handled, including snap-through and snap-back equilibrium curves. This procedure has been applied in several other research works, in which the out-of-plane displacements were the only assumed displacements, e.g., Byklum and Amdahl [12], Brubak and Hellesland [13], Byklum, Steen and Amdahl [30], and Steen, Byklum and Hellesland [31]. Unlike in those studies, also the in-plane displacements are included in the assumed displacement fields in the present work. This complicates the expressions in the incremental response propagation and coupling terms between the in-plane and out-of-plane displacements appear in the equations that describe the plate response.

In the large deflection theory, the equilibrium equations obtained using the Rayleigh-Ritz method are nonlinear in the displacements. In order to avoid solving nonlinear equations directly, the equilibrium equations are solved incrementally by computing the rate form of the equilibrium equations with respect to an arc length parameter η. The change in the arc length parameter can be related directly to a change in the external

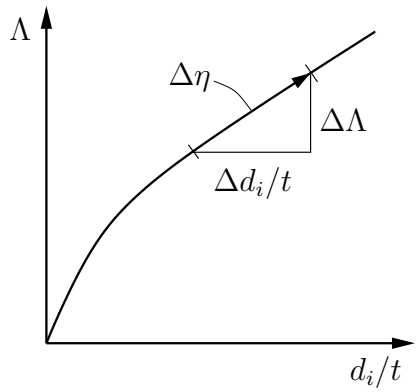

Figure 5: Illustration of the relationship between $\Delta\eta$, a load increment $\Delta\Lambda$ and an increment in the displacements for a case with one amplitude d_i.

stresses and displacements. For an external applied stress that is changing proportionally with a load parameter Λ, this relation is illustrated graphically in Fig. 5. In the limit, as the increment size approaches zero, it can be expressed as

$$\dot{\Lambda}^2 + \sum_{i=1}^{N_{\text{dof}}} \frac{\dot{d}_i^2}{t^2} = 1 \tag{27}$$

where N_{dof} is the total number of degrees of freedom, d_i represents the elements in a vector consisting of an assembly of all the displacement amplitudes and $\dot{d}_i$ is the rates of the displacement components. The displacement amplitude vector, defined by these components, can be written as

$$\begin{aligned}[d_i] =& \left[d_1, d_2, d_3, ..., d_{N_{\text{dof}}} \right] \\ =& \Big[u_1^a, ..., u_{M_{ua}}^a, u_{11}^b, u_{12}^b, ..., u_{M_{ub}N_{ub}}^b, u^c, v_1^a, ..., v_{M_{va}}^a, v_{11}^b, \\ & v_{12}^b, ..., v_{M_{vb}N_{vb}}^b, v^c, w_1^a, ..., w_{M_{va}}^a, w_{11}^b, w_{12}^b, ..., w_{M_{wb}N_{wb}}^b \Big]\end{aligned} \tag{28}$$

where, for instance, $d_1 = u_1^a$ and $d_{N_{\text{dof}}} = w_{M_{wb}N_{wb}}^b$. In Eq. 27, the plate thickness t is introduced in order to obtain dimensional consistency. A dot above a symbol ($\dot{\Lambda}$, etc.) means differentiation with respect to the arc length parameter η, which can be considered a pseudo-time.

In the incremental procedure, the load parameter Λ and displacement amplitudes d_i are functions of the arc length parameter η. For an increment $\Delta\eta$ along the equilibrium curve from point "k" to"$k+1$", a Taylor series expansion gives

$$d_i^{k+1} = d_i^k + \dot{d}_i^k \Delta\eta + \frac{1}{2}\ddot{d}_i^k \Delta\eta^2 + ... \tag{29}$$

$$\Lambda^{k+1} = \Lambda^k + \dot{\Lambda}^k \Delta\eta + \frac{1}{2}\ddot{\Lambda}^k \Delta\eta^2 + ... \tag{30}$$

The second and higher order terms are neglected in the present work, resulting in a first order expansion. The approximation based on only the first order expansion is usually referred to as the Euler or Euler-Cauchy method. In other works, such as in Steen [11] and Byklum [28], it is shown how to include the second order terms. However, in the latter work, it was found that significant computational gains (efficiency) are not achieved by retaining the second order terms as compared to the Euler method with smaller increments.

The accuracy of the present method can also be improved by using equilibrium corrections after each increment, for instance such as in Riks' arc length method [32], or alternatively by using an improved Euler method (Heun's method), which is a predictor-corrector method [33]. However, these improvements are also computationally costly and will not likely result in significant computational gains although they allow for larger increments to be used.

5.2 Incremental equilibrium equations

Equilibrium is satisfied using the principle of stationary potential energy (Rayleigh-Ritz method) on an incremental form (rate form) as mentioned above. The incremental form of the stationary potential energy principle, $\delta\dot{\Pi} = 0$, where Π is the total potential energy, leads to N_{dof} linear equations in $N_{\text{dof}} + 1$ unknowns. The additional equation required is given by Eq. 27. The incremental form of the stationary potential energy principle gives

$$\frac{\partial\dot{\Pi}}{\partial d_i} = \frac{\partial}{\partial\eta}\frac{\partial\Pi}{\partial d_i} = K_{ij}\dot{d}_j + G_i\dot{\Lambda} = 0 \tag{31}$$

where

$$K_{ij} = \frac{\partial^2\Pi}{\partial d_i \partial d_j} \text{ and } G_i = \frac{\partial^2\Pi}{\partial d_i \partial\Lambda} \tag{32}$$

Here, K_{ij} is a generalised, incremental (tangential) stiffness matrix, $-G_i\dot{\Lambda}$ is a generalised, incremental load vector. Above, the index notation with the Einstein summation rule for repeated indexes is adopted.

Alternatively, in the common, bold face matrix notation, the final set of equations, including Eq. 27, can be given by

$$\mathbf{K}\dot{\mathbf{d}} + \mathbf{G}\dot{\Lambda} = 0 \tag{33}$$

$$\dot{\Lambda}^2 + \frac{1}{t^2}\dot{\mathbf{d}}^T\dot{\mathbf{d}} = 1 \tag{34}$$

where Eq. 33 may be written in submatrix and subvector form as follows

$$\mathbf{K} = \begin{bmatrix} \mathbf{K}_{uu} & \mathbf{K}_{uv} & \mathbf{K}_{uw} \\ \mathbf{K}_{vu} & \mathbf{K}_{vv} & \mathbf{K}_{vw} \\ \mathbf{K}_{wu} & \mathbf{K}_{wv} & \mathbf{K}_{ww} \end{bmatrix} \tag{35}$$

and

$$\mathbf{d} = \begin{bmatrix} \mathbf{u} \\ \mathbf{v} \\ \mathbf{w} \end{bmatrix} \tag{36}$$

$$-\dot{\Lambda}\mathbf{G} = -\dot{\Lambda} \begin{bmatrix} \mathbf{G}_u \\ \mathbf{G}_v \\ \mathbf{G}_w \end{bmatrix} \tag{37}$$

In these expressions, the incremental stiffness matrix $\mathbf{K}$ is divided into submatrices, $\mathbf{K}_{uu}$, $\mathbf{K}_{uv}$, etc., and the incremental load vector $-\dot{\Lambda}\mathbf{G}$ and the displacement vector $\mathbf{d}$ into subvectors. Further, for each displacement component (u, v, w), these submatrices and subvectors are subdivided into new submatrices and subvectors corresponding to the displacement assumptions (Section 4.1) previously labelled with super indexes 'a', 'b' and 'c'. For the displacements, this subdivision is expressed by

$$\mathbf{u} = \begin{bmatrix} \mathbf{u}_a \\ \mathbf{u}_b \\ \mathbf{u}_c \end{bmatrix} = \left[u_1^a, ..., u_{M_{ua}}^a, u_{11}^b, u_{12}^b, ..., u_{M_{ub}N_{ub}}^b, u^c \right]^T \tag{38}$$

$$\mathbf{v} = \begin{bmatrix} \mathbf{v}_a \\ \mathbf{v}_b \\ \mathbf{v}_c \end{bmatrix} = \left[v_1^a, ..., v_{M_{va}}^a, v_{11}^b, v_{12}^b, ..., v_{M_{vb}N_{vb}}^b, v^c \right]^T \tag{39}$$

$$\mathbf{w} = \begin{bmatrix} \mathbf{w}_a \\ \mathbf{w}_b \end{bmatrix} = \left[w_1^a, ..., w_{M_{wa}}^a, w_{11}^b, w_{12}^b, ..., w_{M_{wb}N_{wb}}^b \right]^T \tag{40}$$

The vectors $-\dot{\Lambda}\mathbf{G}_u$, $-\dot{\Lambda}\mathbf{G}_v$ and $-\dot{\Lambda}\mathbf{G}_w$ are subdivided in a similar manner. All the bold face vectors and subvectors in the expressions above are column vectors. More details of the subdivision of the matrices and vectors are given in Appendix A.

The incremental stiffness matrix and incremental load vector consist of contributions both from the plate and the stiffener, and can be expressed as

$$\mathbf{K} = \mathbf{K}^{pb} + \mathbf{K}^{pm} + \mathbf{K}^{s} \tag{41}$$

$$-\dot{\Lambda}\mathbf{G} = -\dot{\Lambda}\mathbf{G}^{p} - \dot{\Lambda}\mathbf{G}^{s} \tag{42}$$

where $\mathbf{K}^{pb}$ and $\mathbf{K}^{pm}$ are the incremental bending stiffness matrix and the incremental membrane stiffness matrix of the plate, respectively, and $\mathbf{K}^{s}$ is the incremental stiffness matrix of the stiffeners. In Eq. 42, the incremental load vector is separated into a plate contribution $-\dot{\Lambda}\mathbf{G}^{p}$ and a stiffener contribution $-\dot{\Lambda}\mathbf{G}^{s}$. The latter contribution is zero if the stiffeners are not end loaded, which is the case for sniped stiffeners.

The bending stiffness contribution of the plate $\mathbf{K}^{pb}$ is independent of the displacement amplitudes and this is a constant contribution to the incremental stiffness matrix. On the other hand, both the incremental membrane stiffness contribution of the plate $\mathbf{K}^{pm}$ and the incremental stiffness matrix of the stiffener $\mathbf{K}^{s}$ is dependent on the displacement amplitudes. These two matrices can be divided into a linear (L) and a nonlinear contribution (NL), and they can be written as

$$\mathbf{K}^{pm} = \mathbf{K}^{pmL} + \mathbf{K}^{pmNL} \tag{43}$$

$$\mathbf{K}^{s} = \mathbf{K}^{sL} + \mathbf{K}^{sNL} \tag{44}$$

The linear contributions are constant, and the nonlinear contributions are dependent of the displacement amplitudes. The analytical expressions of the stiffness matrices and the load vectors for the plate are given in Appendix C. For the stiffeners, the stiffness matrix is given in Appendix D, and it is divided into contributions $\mathbf{K}^{sL,x}$ and $\mathbf{K}^{sNL,x}$, for the stiffeners in the x-direction, and contributions $\mathbf{K}^{sL,y}$ and $\mathbf{K}^{sNL,y}$, for stiffeners in the y-direction.

5.3 Procedure for solving the equations

In order to trace the equilibrium curve, the solution of a system of equations must be found. As mentioned above, Eq. 31 (or 33) represents $N_{\text{dof}} \times N_{\text{dof}}$ linear equations in the $N_{\text{dof}} \times N_{\text{dof}} + 1$ unknowns ($\dot{d}_j$ and $\dot{\Lambda}$) and Eq. 27 is the additional equation required. The solution of Eq. 31 is given by

$$\dot{d}_j = -\dot{\Lambda} K_{ij}^{-1} G_i = \dot{\Lambda} Q_j \quad \text{where } Q_j = -K_{ij}^{-1} G_i \tag{45}$$

By substituting Eq. 45 into Eq. 27, the following equation is obtained

$$\dot{\Lambda}^2 (t^2 + \sum_{j=1}^{N_{\text{dof}}} Q_j^2) = t^2 \tag{46}$$

from which the load rate parameter $\dot{\Lambda}$ can be determined as

$$\dot{\Lambda} = \pm \frac{t}{\sqrt{t^2 + \sum_{j=1}^{N_{\text{dof}}} Q_j^2}} \tag{47}$$

There are two possible solutions with the same numerical value, but with opposite signs. One solution is in the direction of an increasing arc length and one in the opposite direction. The solution of interest corresponds to that giving a continuous increase of the arc length. This is assumed to be the solution which results in the smoothest equilibrium curve. In the same manner as in Steen [11], this is expressed by the requirement that the absolute value of the angle between the tangents of two consecutive states ("$k-1$" and "k") in the load-displacement ($\Lambda - d_j/t$) space is smaller than 90 degrees. Thus, for the correct sign of the load rate $\dot{\Lambda}^k$ at state "k", the following criterion must be satisfied:

$$\sum_{j=1}^{N_{\text{dof}}} \dot{\Lambda}^k \left(\frac{Q_j^k \dot{d}_j^{k-1}}{t^2} + \dot{\Lambda}^{k-1}\right) > 0 \tag{48}$$

An equivalent criterion for choosing the correct sign is given in Byklum et al. [12].

When $\dot{\Lambda}^k$ at stage "k" is found, the displacement rate amplitudes $\dot{d}_j^k$ are given by Eq. 45. The displacement amplitudes and load parameter at the next stage are then found from obtained from linear Taylor series expansion as

$$d_j{}^{k+1} = d_j{}^k + \dot{d}_j{}^k \Delta\eta; \qquad \Lambda^{k+1} = \Lambda^k + \dot{\Lambda}^k \Delta\eta \tag{49}$$

In this manner, the solution propagation is continued until a specified limit, or given criterion, is reached. The present solution procedure is capable of passing limit points, including tracing of snap-through and snap-back equilibrium curves.

6 POTENTIAL ENERGY

6.1 Potential energy of the plate

6.1.1 Introduction

The potential energy of the plate consists of a strain energy contribution and an energy contribution due to external loads. The potential strain energy of the plate gives contribution to the incremental stiffness matrix, and the potential energy of the external stresses along the plate edges contribute to the incremental load vector. Each contribution of the potential energy of the plate is given below, and due to the large and complex expressions, the rate form of these contributions are given separately in Appendix C.

For thin plates, the potential strain energy U^p can be given by

$$U^p = \frac{1}{2} \int_V \boldsymbol{\sigma}^T \boldsymbol{\epsilon} \, dV \tag{50}$$

where $\boldsymbol{\sigma} = [\sigma_x, \sigma_y, \tau_{xy}]^T$, $\boldsymbol{\epsilon} = [\epsilon_x, \epsilon_y, \gamma_{xy}]^T$ and V is the volume of the plate. It is common to divide the strain energy into a membrane contribution and a bending contribution. Then, Eq. 50 can be written as

$$\begin{aligned} U^p &= \frac{1}{2}\int_V (\boldsymbol{\sigma}^{pm} + \boldsymbol{\sigma}^{pb})^T (\boldsymbol{\epsilon}^{pm} + \boldsymbol{\epsilon}^{pb})\, dV \\ &= \frac{1}{2}\int_V (\boldsymbol{\sigma}^{pm})^T \boldsymbol{\epsilon}^{pm}\, dV + \frac{1}{2}\int_V (\boldsymbol{\sigma}^{pb})^T \boldsymbol{\epsilon}^{pb}\, dV \\ &= U^{pm} + U^{pb} \end{aligned} \tag{51}$$

where U^{pm} and U^{pb} are the potential membrane and bending strain energy, respectively. The coupling terms between the membrane and bending contribution disappear when integrating over the plate thickness, since the bending stresses are zero at the middle plane of the plate and are varying linearly in the thickness direction.

6.1.2 Potential bending strain energy

By substituting Hooke's law into the bending part of Eq. 51 and then integrating this contribution over the plate thickness, the elastic strain energy contribution from bending of the plate can be written as [20]

$$U^{pb} = \frac{D}{2}\int_0^b \int_0^L \left((w_{,xx} + w_{,yy})^2 - 2(1-\nu)(w_{,xx}w_{,yy} - w_{,xy}^2) \right) dx\, dy \tag{52}$$

where $D = Et^3/12(1-\nu^2)$ is the plate bending stiffness and t is the plate thickness. By substituting the assumed displacement field, an analytical solution of this integral may be derived. This energy contribution is of quadratic order in the displacement amplitudes. Thereby, it gives a constant contribution to the incremental plate stiffness matrix since this matrix is obtained by differentiation twice with respect to the displacement amplitudes (Eq. 32). Consequently, it is necessary to computed this matrix only once. The bending stiffness matrix of the plate on rate form is given in Appendix C.

6.1.3 Potential membrane strain energy

By substituting Hooke's law into the membrane part of Eq. 51, the elastic membrane strain energy of the plate can be written as [20]

$$U^{pm} = \frac{C}{2}\int_0^b \int_0^L \left((\epsilon_x^{pm})^2 + (\epsilon_x^{pm})^2 - 2\nu(\epsilon_x^{pm})(\epsilon_y^{pm}) - \frac{1-\nu}{2}(\gamma_{xy}^{pm})^2 \right) dx\, dy \tag{53}$$

where $C = Et/(1-\nu^2)$ is the extensional stiffness of the plate. By substituting the membrane strains from Eqs. 5-7 and the assumed displacement fields into this equation, an analytical solution of this integral may be derived. The resulting expression can be separated into a term U^{pmL} that is quadratic in the displacement amplitudes and a term U^{pmNL} that is of a higher order in the amplitudes. The membrane strain energy can then be written as

$$U^{pm} = U^{pmL} + U^{pmNL} \tag{54}$$

The first term in Eq. 54 gives constant contribution $\mathbf{K}^{pmL}$ to the total incremental plate stiffness matrix in Eq. 32. Thus, this matrix must be calculated only once, and does not affect the computation time significantly. The second term in Eq. 54 contributes to the nonlinear, incremental stiffness matrix $\mathbf{K}^{pmNL}$. This matrix is dependent of the displacement amplitudes and consequently, it must be calculated for every increment in the solution propagation described in Chapter 5. Thus, this matrix affects the computational efficiency significantly.

6.1.4 Potential energy of an external, in-plane plate load in x-direction

The potential energy of an external, in-plane load acting on the plate in the x-direction is given by

$$T^{p,x} = -\Lambda S_{x0} t b \Delta u \tag{55}$$

where S_{x0} is a reference stress, $\Delta u = u^c$ is the plate shortening in the x-direction and Λ is the load factor. Eq. 55 gives a contribution to the incremental load vector $-\dot{\Lambda}\mathbf{G}$. An analytical expression for this vector is given in Appendix C.

6.1.5 Potential energy of an external lateral pressure in z-direction

The potential energy of an external lateral pressure acting on the plate in the z-direction can be given by

$$T^{p,z} = -\int_0^b \int_0^L p\, w\, dx\, dy \tag{56}$$

where $p = p(x, y)$ is the lateral pressure. This contribution gives a constant contribution to the incremental load vector. More details on how to include an external, lateral pressure can be found in Byklum [28]. This load case is not included in the present report.

6.2 Potential energy of stiffeners

6.2.1 Introduction

The potential energy of the stiffener consists of a strain energy contribution and an energy contribution due to external stiffener loads. The potential strain energy of the stiffener gives a contribution to the incremental stiffness matrix, and the rate form of this energy contribution is given separately in Appendix D. In the present report, end loaded stiffeners are not considered. However, the potential energy of external stiffener loads for a stiffener in the x-direction is given below.

6.2.2 Potential strain energy of a stiffener parallel to the free edge

The elastic strain energy of a stiffener parallel to free edge is given by [13, 34]

$$\begin{aligned} U^{s,x} =& \frac{E}{2}\int_0^L \int_{A_s} \epsilon_x^2 \, dA_s dx \\ =& \frac{EI}{2}\int_0^L z^2 w_{,xx}^2 \, dx - e_c E A_s \int_0^L \epsilon_x^{pm} w_{,xx} \, dx + \frac{EA_s}{2}\int_0^L (\epsilon_x^{pm})^2 \, dx \end{aligned} \tag{57}$$

where I is the moment of inertia about $z = 0$ (at the midplane of the plate), A_s is the stiffener cross-section area and e_c is the distance from the middle plane of the plate to the centre of area of the stiffener. The integrand in Eq. 57, must be evaluated at the stiffener location $y = y_s$ defined in Fig. 4. By substituting the strain ϵ_x^{pm} from Eq. 5 and the assumed displacement field into Eq. 57, an analytical solution can be derived. In a similar manner as for the membrane strain energy of the plate, the strain energy of the stiffener can be separated into a term that is quadratic in the displacement amplitude and a term of a higher order. Then, $U^{s,x}$ can be written as

$$U^{s,x} = U^{sL,x} + U^{sNL,x} \tag{58}$$

where $U^{sL,x}$ and $U^{sNL,x}$ give contributions to the linear, incremental stiffness matrix $\mathbf{K}^{sL,x}$, and to the nonlinear, incremental stiffness matrix $\mathbf{K}^{sNL,x}$, respectively. These two matrices are given in Appendix D.

The torsional stiffness of the stiffeners may be accounted for in a simplified manner by including the St. Venant torsion energy contribution given by

$$U^{sT,x} = \frac{GJ}{2}\int_0^L w_{,xy}^2 dx \tag{59}$$

where J is the torsion constant and $G = E/2(1+\nu)$. The integrand must be evaluated at the stiffener location $y = y_s$. The strain energy due to torsion of a stiffener is quadratic

in the displacement amplitudes. It will therefore give a contribution only to the linear incremental stiffness matrix $\mathbf{K}^{sL}$. This contribution may be significant in conjunction with torsionally stiff, closed stiffener profiles. In the open stiffener profile examples of the present paper, the torsional stiffener stiffness is neglected. This is normally acceptable for such profiles.

6.2.3 Potential strain energy of a stiffener perpendicular to the free edge

The elastic strain energy of a stiffener perpendicular to free edge is given by

$$\begin{aligned} U^{s,y} =& \frac{E}{2}\int_0^b \int_{A_s} \epsilon_y^2 \, dA_s dy \\ =& \frac{EI}{2}\int_0^b z^2 w_{,yy}^2 \, dy - e_c E A_s \int_0^b \epsilon_y^{pm} w_{,yy} \, dy + \frac{EA_s}{2}\int_0^b (\epsilon_y^{pm})^2 \, dy \end{aligned} \tag{60}$$

In similar manner as for a stiffener parallel to the free edge, the integrand must be evaluated at the stiffener location $x = x_s$ defined in Fig. 4. Further, this contribution can also be separated into a term that is quadratic and a term of a higher order, and then, $U^{s,y}$ can be written as

$$U^{s,y} = U^{sL,y} + U^{sNL,y} \tag{61}$$

where $U^{sL,y}$ and $U^{sNL,y}$ give contributions to the linear, incremental stiffness matrix $\mathbf{K}^{sL,y}$, and to the nonlinear, incremental stiffness matrix $\mathbf{K}^{sNL,y}$, respectively. These two matrices are given in Appendix D.

The torsional stiffness of the stiffeners may be accounted for in a simplified manner by including the energy contribution (St. Venant torsion) given by

$$U^{sT,y} = \frac{GJ}{2}\int_0^b w_{,xy}^2 dy \tag{62}$$

The integrand must be evaluated at the stiffener location $x = x_s$.

6.3 Potential energy of external stiffener loads for a stiffener in x-direction

The stiffeners may be end loaded (typical for continuous stiffeners) if the stiffener ends are attached to a surrounding structure. For a continuous longitudinal stiffener parallel to the free edge, the potential energy of the external loads can be taken according to

$$T^{s,x} = -P_{sx}\Delta u - P_{sx} e_c w_{2,x} + P_{sx} e_c w_{1,x} \tag{63}$$

where P_{sx} is the resultant force (positive in compression) acting on the stiffener. In this expression, $w_{1,x}$ and $w_{2,x}$ are the rotations of the stiffener end located at $x = 0$ and $x = L$, respectively. The two last terms in Eq. 63 are due to the rotation of the stiffener about the y-axis at the stiffener ends. This expression is similar to an expression for potential energy of external stiffener loads previously given by Brubak and Hellesland [13], and by Steen [34] for a stiffened plate with only one degree of freedom.

7 FINITE ELEMENT MODEL

For verification of the present semi-analytical model, a variety of plate and stiffener dimensions have been considered. Computed results by the present model have been compared with finite element analyses (FEA) using ANSYS [35] in which both plate and stiffeners were modelled using Shell93 elements. In these comparisons, many different results are studied, including load-displacement curves, displacement plots for a given load, internal stresses and elastic buckling stress (eigenvalue) limit (ESL). In addition, introductory investigation of ultimate strength limit (USL) predictions are presented.

In the cases studied, the finite element model is supported in the out-of-plane direction along three edges and it has one edge being free or provided with an edge stiffener. In the same manner as for the proposed model, the plate is subjected to an external axial stress at the two opposite, supported edges, perpendicular to the free edge. The supported edges are forced to remain straight during deformation, and further, the loaded edges remain parallel. The plate is also supported in the in-plane directions, just enough to prevent rigid body motions. In the cases studied, the ends of the stiffeners are completely free and they are not subjected to any external loads.

In the presented results, the number of degrees of freedom used in ANSYS for a stiffened plate is typically about 15000, which is believed to be a sufficiently large number to ensure satisfactory results. A typical element mesh is shown later (Fig. 19(b)). Probably, sufficient accuracy could have been obtained with fewer degrees of freedom in the finite element model. In comparison, 259 degrees of freedom are used in the proposed model in all cases.

8 LOAD-DISPLACEMENT RESULTS

8.1 Introduction

The present method has been implemented into a FORTRAN computer program, and numerical results obtained by the method have been compared with finite element analyses results from ANSYS for a variety of cases. The load-deflection response for elastic plates computed by the present method is compared with those obtained by large deflection, finite element analysis using ANSYS.

The present load-deflection results are computed without accounting for material yielding, and the response curves are arbitrarily terminated when the external stress S_x reaches the yield stress $f_Y = 235$ MPa. The adopted elastic material properties in each computation are Young's modulus $E = 208000$ MPa and Poisson's ratio $\nu = 0.3$.

The imperfection shape is taken equal to the first eigenmode of the plate also in the nonlinear ANSYS element analyses. For verification purposes, the specified maximum amplitude is taken equal to $w_{0,\text{spec}} = 5$mm both in the proposed model and ANSYS.

In the analysis by the present model, the total number of degrees of freedom is defined by the number of terms in the assumed displacement fields as given by Eq. 19. The chosen number of terms in each displacement field is

$$M_{wa} = 1, \quad M_{wb} = N_{wb} = 6, \quad M_{ua} = M_{ub} = N_{ub} = M_{va} = M_{vb} = N_{vb} = 10 \tag{64}$$

which results in 259 degrees of freedom. Convergence test have shown that these degrees of freedom give satisfactory results for the plates studied. In these cases, the most severe test case with respect to the number of degrees of freedom is a plate with two regular stiffeners and a stiffened free edge. If plates with more than three stiffeners or plates with clamped edges are analysed, it may be necessary to increase the number of the degrees of freedom.

The present model is also able to analyse plates with simple supports at all four edges, simply by setting $M_{wa} = M_{ua} = M_{va} = 0$. This can be done directly in the FORTRAN computer code. The edge located at $y = b$ will then be simply supported and forced to remain straight during deformation.

As mentioned above, the choice of the number of degrees of freedom will affect the computation time. Another parameter that affects the computation efficiency of the present model, is the incremental step size $\Delta\eta$. A rather small value of $\Delta\eta = 0.04$ is used in the present comparisons with ANSYS results. This value has been found to be satisfactory in previous investigations [13].

First in this section, unstiffened plates with a free edge is studied, and next, plates at which the free edge is stiffened with a single edge stiffener. At last, results for plates with two regular stiffeners oriented in the x-direction and a stiffened free edge are presented.

In addition, similar comparisons between results by the present model (with the input values mentioned above) and by ANSYS have been made for unstiffened plates with simple supports at all the edges, and good agreement was achieved. Those results are not included in the present report.

8.2 Unstiffened plates with a free edge

Unstiffened plates with three simply supported edge and one free edge are analysed, and results are presented for four typical cases with plate geometries and dimensions defined in Fig. 6. These plates have intermediate to relatively large slenderness values in order to study cases with rather nonlinear load-displacements curves. These represent relatively severe test cases for the present model.

The displacement shapes of the plates computed by ANSYS and by the present model are very similar. A typical case is shown in Fig. 7(a) and (b), in which the additional out-of-plane displacements fields w are plotted for Plate 1 subjected to an external stress $S_x = f_y$. Similar comparisons of the in-plane displacement fields in the x- and y-direction have also been made. Again, the results, not included in the present report, are very similar to each other.

In Figs. 8-11, response curves are shown in which the external stress S_x is plotted both versus the end shortening Δ_x and versus the additional out-of-plane displacement w_{me} at the midlength of the free edge. The results are given in a non-dimensional form. In the figures, t is the plate thickness, f_Y the yield stress and $\epsilon_Y = f_Y/E$ ($= 0.00113$) is the yield strain. The agreement between the response curves computed by the present model (thick solid curves) and by ANSYS (open dots) is good. It can be seen that the curves obtained by the present model is slightly to the non-conservative side. By increasing the number of terms (degrees of freedom) in the displacement fields, the agreement will improve slightly. However, the present discrepancy is considered as acceptable. The end shortening Δ_x is the reduction of the distance between two opposite edges and it can be considered as a "global displacement", while the out-of-plane displacement w_{me} is a "local displacement" at the midlength of the free edge. Consequently, it is expected that the agreement between the present model and ANSYS generally is better for the load-shortening curves than for the load-deflection curves. This will especially be true for stiffened plates, as will be seen later.

	L	b	t
Plate 1	1000	1000	12
Plate 2	1000	1000	20
Plate 3	1000	1000	30
Plate 4	2000	1000	30

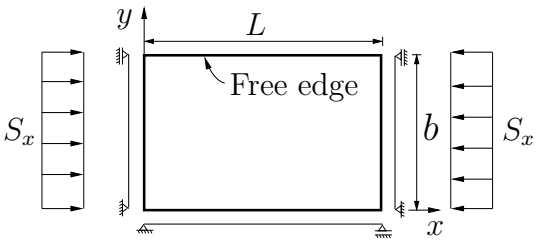

Figure 6: Overview and dimensions [mm] of unstiffened plates with a free edge.

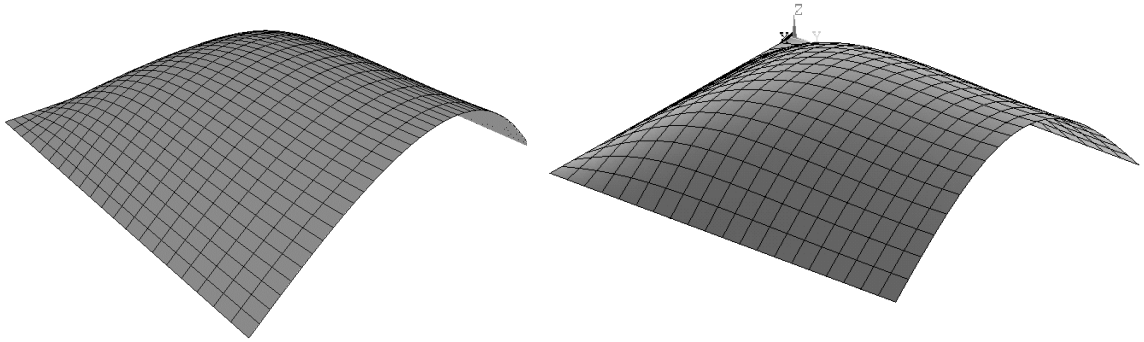

(a) (b)

Figure 7: The bending mode of Plate 1 subjected to an external load $S_x = f_Y$ computed (a) by the present model and (b) by ANSYS.

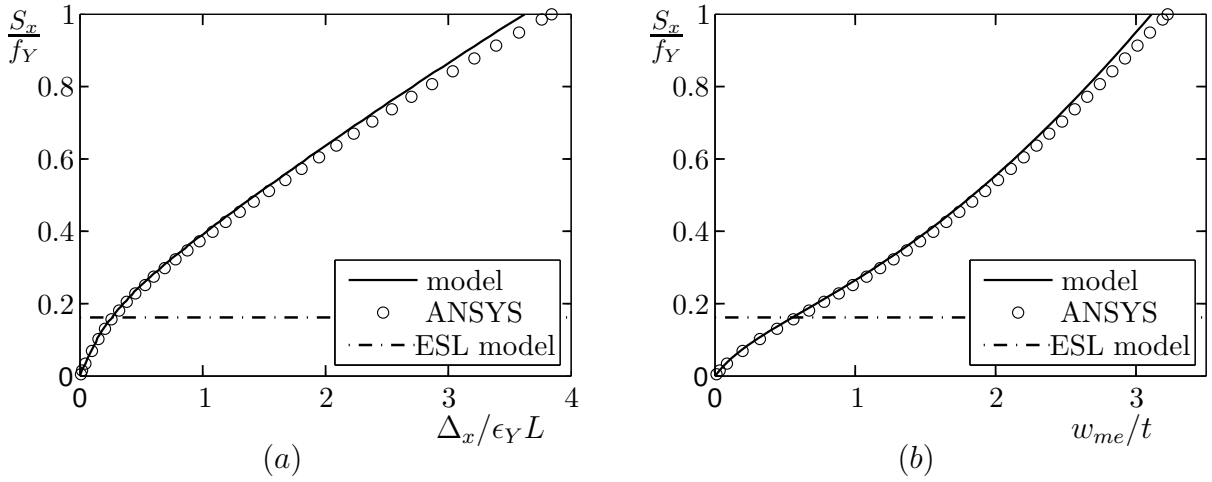

Figure 8: (*a*) Load-shortening and (*b*) load-deflection curves of Plate 1 (slender plate) subjected to a uniaxial load S_x.

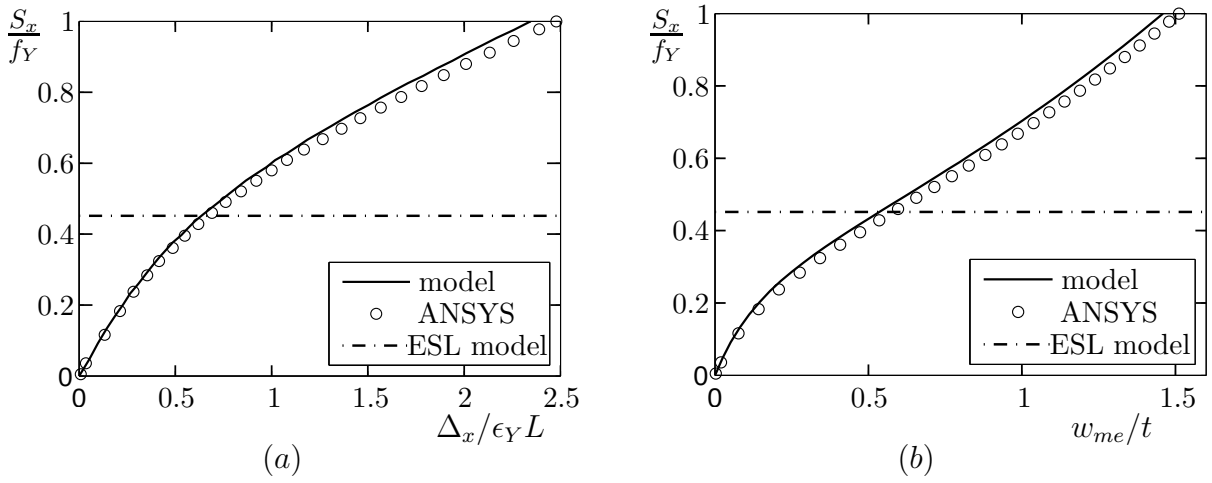

Figure 9: (*a*) Load-shortening and (*b*) load-deflection curves of Plate 2 (slender plate) subjected to a uniaxial load S_x.

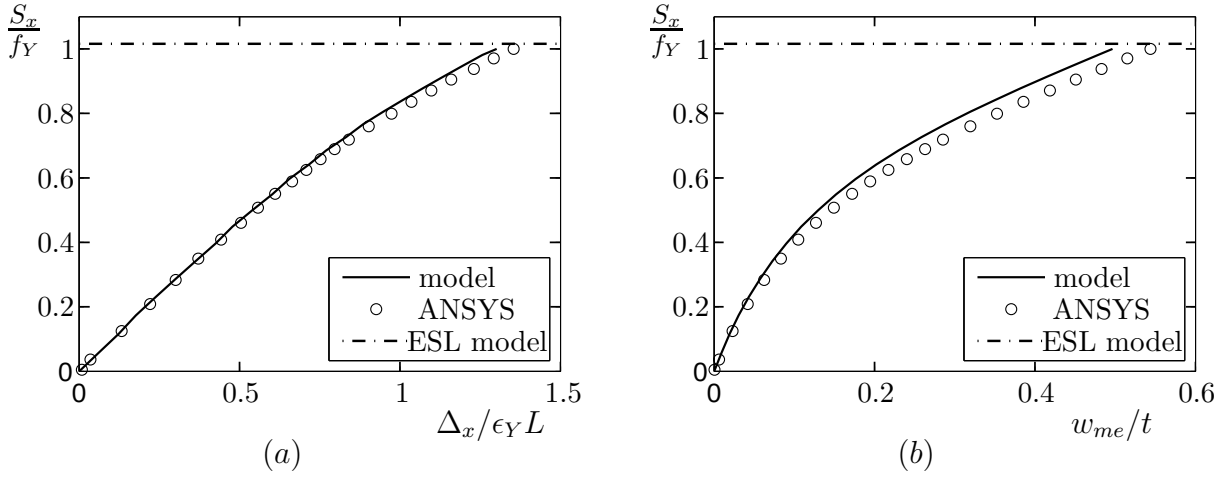

Figure 10: (a) Load-shortening and (b) load-deflection curves of Plate 3 (moderately slender plate) subjected to a uniaxial load S_x.

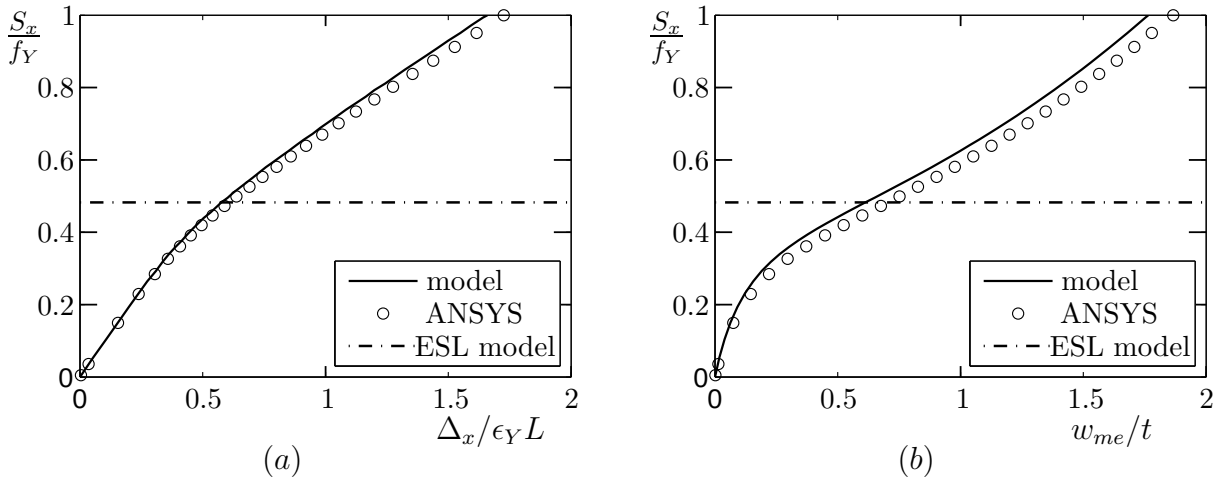

Figure 11: (a) Load-shortening and (b) load-deflection curves of Plate 4 (slender plate) subjected to a uniaxial load S_x.

	L	b	t	h_w	t_w
Plate 5	1000	1000	12	156	10
Plate 6	1000	1000	20	160	10
Plate 7	1000	1000	30	165	10
Plate 8	2000	1000	30	165	10

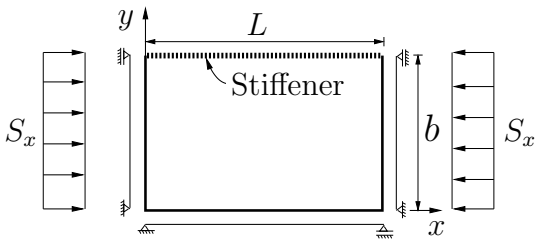

Figure 12: Overview and dimensions [mm] of plates with a free edge provided with an eccentric, flat bar edge stiffener of height $h = 150$ mm.

The relative elastic buckling stress (eigenvalue) limit (ESL) computed by the present model is also included in the figures (the horizontal dash-dotted lines). This stress level (S_x/f_Y) gives an indication of the plate slenderness. The corresponding first eigenmode computed by ANSYS and by the present model is quite similar, and as mentioned before, this mode is used as the imperfection shape. When the external stress is close to the elastic buckling stress limit, it can be seen by inspection of the load-shortening curves that the in-plane plate stiffness is reduced. For these load levels, the slope of the load-deflection curves is smallest and the change in the out-of-plane displacements is largest. For external loads far above the ESL value, the slope of the load-deflection curves will actually increase which can be seen in Fig. 8(b). This behaviour is due to nonlinear membrane effects, and is typical for slender plates with large out-of-plane displacements.

8.3 Plates with a stiffened free edge

The unstiffened plates with three simply supported edges and one free edge, in the previous section, were relatively slender. A usual and effective way to increase the stiffness and strength of a plate with a free edge is to provide the edge with an edge stiffener. If this edge stiffener is strong enough to prevent out-of-plate displacements, the plate will almost behave as a simply supported plate. In this section, four plates with an edge stiffener will be studied, and results by the present model will be compared with ANSYS results. An overview of the plates and the plate dimensions are given in Fig. 12. The dimensions of the plates alone are the same as for the unstiffened plates (Plate 1-4) in the previous section. But now, an eccentric, flat bar stiffener is attached to the free edge in each case. The height of the stiffener web itself is 150 mm.

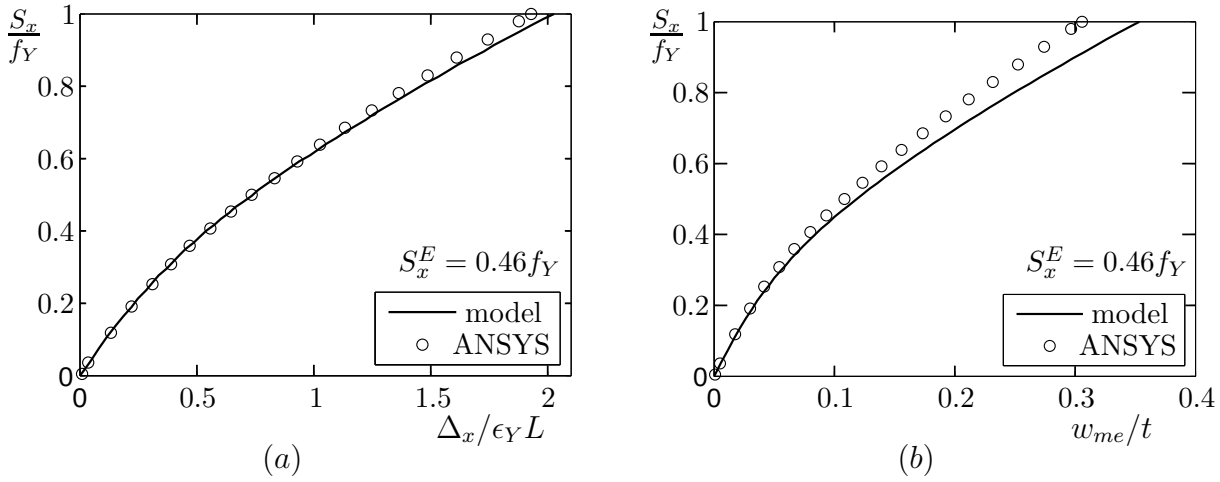

Figure 13: (a) Load-shortening and (b) load-deflection curves of Plate 5 (slender plate) subjected to a uniaxial load S_x.

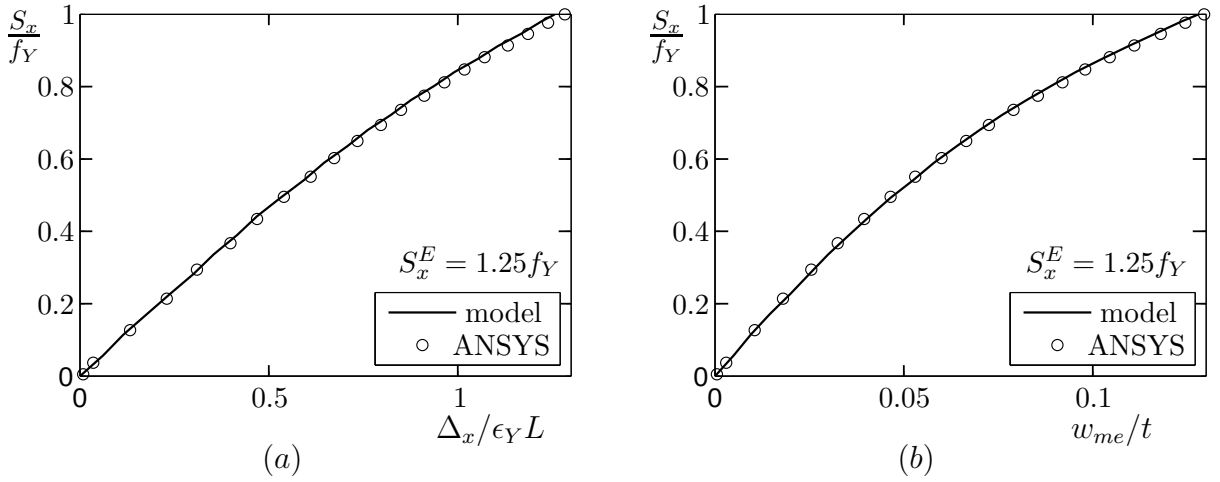

Figure 14: (a) Load-shortening and (b) load-deflection curves of Plate 6 (non-slender plate) subjected to a uniaxial load S_x.

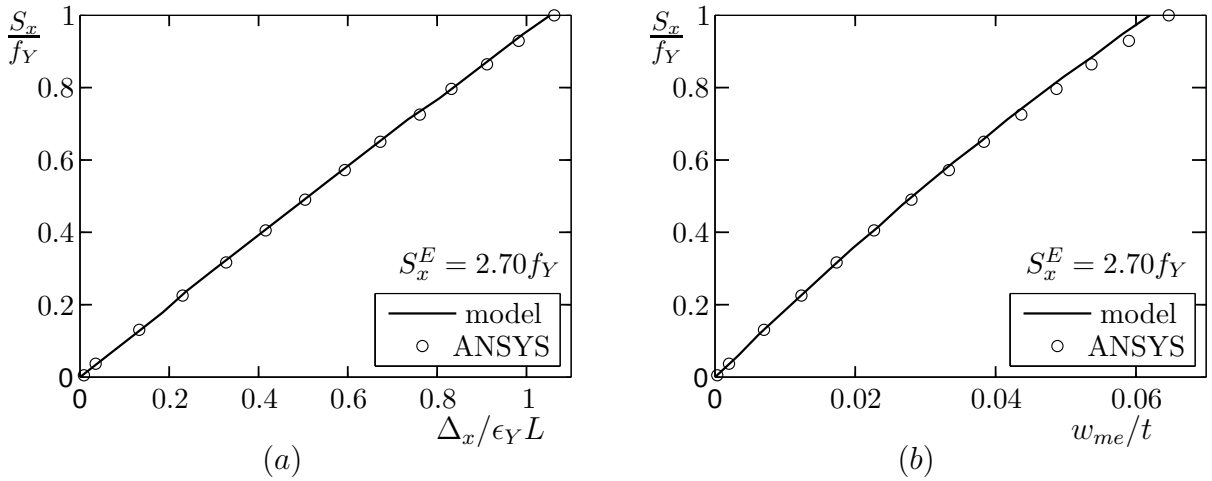

Figure 15: (a) Load-shortening and (b) load-deflection curves of Plate 7 (non-slender plate) subjected to a uniaxial load S_x.

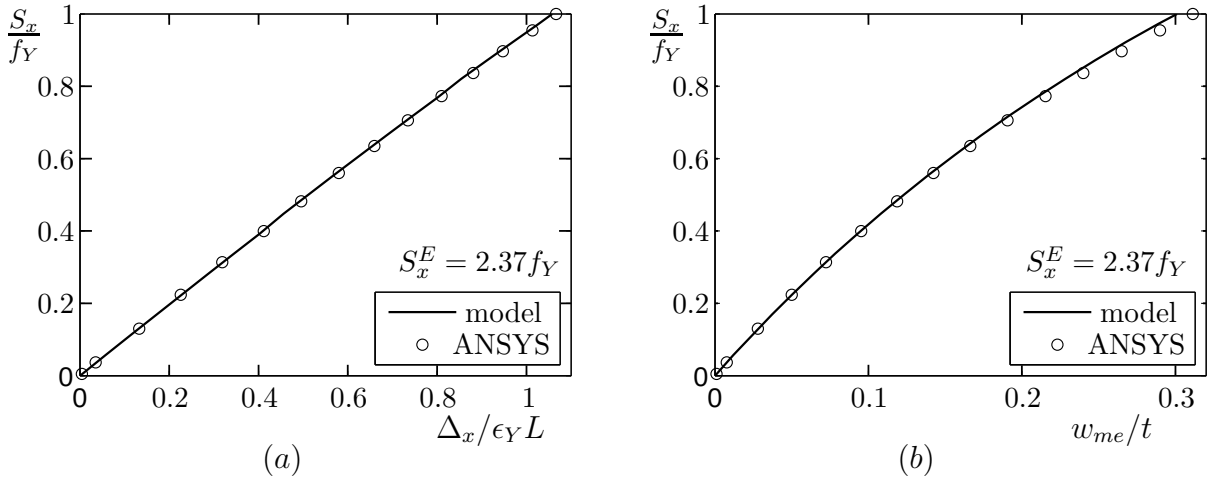

Figure 16: (a) Load-shortening and (b) load-deflection curves of Plate 8 (non-slender plate) subjected to a uniaxial load S_x.

In Figs. 13-16, similar response curves to those presented above for unstiffened plates are presented for the four plates with a stiffened free edge. It can be seen that the agreement between the results of the present model and ANSYS is good. The location of the out-of-plane displacement w_{me} is at the midlength of the stiffened edge. Compared to the unstiffened plates, the out-of-plane displacement w_{me} is now much smaller than for the corresponding unstiffened plate with the same plate dimensions. The bending modes are predominantly local in which the largest out-of-plane displacements are located in the interior plating.

In the figures, the agreement is generally better for the load-shortening curves ($S_x - \Delta_x$) than for the load-deflection curves ($S_x - w_{me}$). As mentioned before, this is to be expected since Δ_x is a global displacement and w_{me} is a local displacement. This is especially the case for plates with relatively stiff edge stiffeners nearly preventing completely out-of-plane displacements, such as for instance, in Fig. 13(b), where there is a clear difference between the model and ANSYS results. For this plate, the out-of-plane displacements are largest in the interior of the plate. The out-of-plane displacement w_{me} at the stiffened edge is therefore not a particularly good parameter for comparison in such cases when the comparisons are between very small values. The overall out-of-plane bending shape computed by the present model and by ANSYS have also been compared, and found to be very similar. The agreement is better for the out-of-plane displacement in the interior of the plate.

For information, the plate stiffness and the elastic buckling stress, computed by the present model and denoted by S_x^E is also included in the figures. For the plates in Figs. 13-16, the elastic buckling stress limit (ESL) is much larger than that computed previously for the unstiffened plates. For Plate 6, 7 and 8, the elastic buckling stress is not reached before the external stress becomes equal the yield stress f_Y.

8.4 Plates with two regular stiffeners and a stiffened free edge

Similar results to those presented for the plates in the two previous sections, have been obtained for four plates with a free edge stiffened by an edge stiffener and two regular stiffeners. The stiffener profiles are eccentric flat bars. An overview of the plate and dimensions are given in Fig. 17. Compared to the stiffener dimensions for the plates above with one stiffener, the stiffener height for present Plate 9-12 is smaller in order to study cases with a global bending behaviour. In these four cases, the height of the stiffener web itself is 50 mm. The fifth Plate 13 is provided with stiffeners with a web height equal to 100 mm, and it will be shown that the bending mode for this plate is a

	L	b	t	h_w	t_w
Plate 9	1000	1000	12	56	10
Plate 10	1000	1000	20	60	10
Plate 11	1000	1000	30	65	10
Plate 12	2000	1000	30	65	10
Plate 13	1000	1000	12	106	10

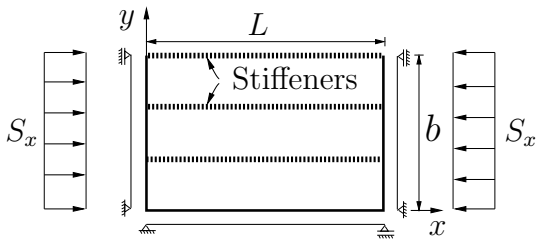

Figure 17: Overview and dimensions [mm] of plates with a free edge provided with three eccentric, flat bar stiffeners of height $h = 50$ mm for Plates 9-12 and $h = 100$ mm for Plate 13.

combination of a local and a global bending mode.

Also for these plates, the bending modes of the plates computed by ANSYS and by the present model are very similar. A typical case of a global bending mode is shown in Fig. 18(a) and (b), in which the additional out-of-plane displacements w are plotted for Plate 9 subjected to an external stress $S_x = f_y$. In this case, the stiffeners are not strong enough to prevent large plate deflections along the stiffeners. In Fig. 19(a) and (b), similar plots are shown for Plate 13. It can be seen that the bending mode in this case, is a combination of a global and a local bending mode.

For Plates 9-13, the load-shortening and the load-deflection curves are presented in Figs. 20-24. The agreement between the present model and ANSYS results is seen to be good, except maybe for the load-deflection curve of Plate 13 presented in Fig. 24(b). The displacement w_{me} is a local displacement at the midlength of the stiffened edge, and as mentioned before, it is not a particularly good parameter for comparison in cases when the comparisons are between very small values. This is the case for this plate, since the displacement w_{me} is rather small due to the relatively stiff stiffeners partly preventing out-of-plane displacements. However, the results are conservative compared to the ANSYS results, and the comparison is the most conservative case observed by the present model. Moreover, the load-shortening curve computed for Plate 13 by the present model in seen (Fig. 24(a)) to be in good agreement with ANSYS. The end shortening Δ_x in that response curve can be considered as a global displacement, and consequently better agreement was to be expected.

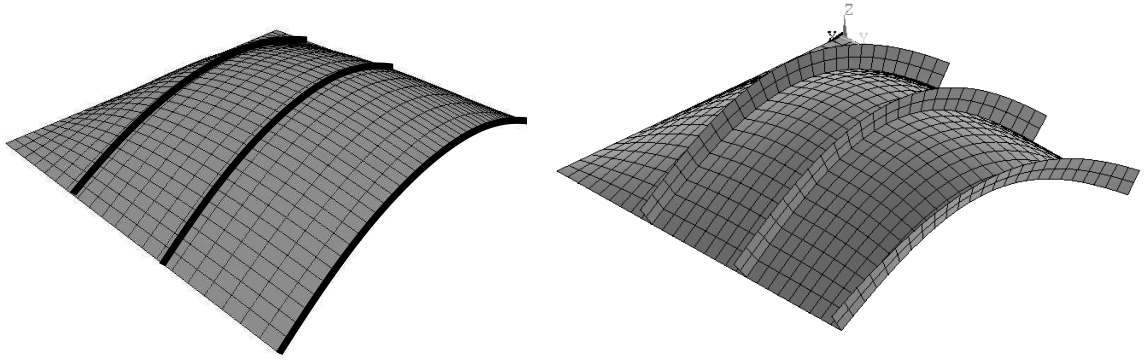

(a) (b)

Figure 18: The bending mode (predominantly global) of Plate 9 subjected to an external load $S_x = f_Y$ computed (a) by the present model and (b) by ANSYS.

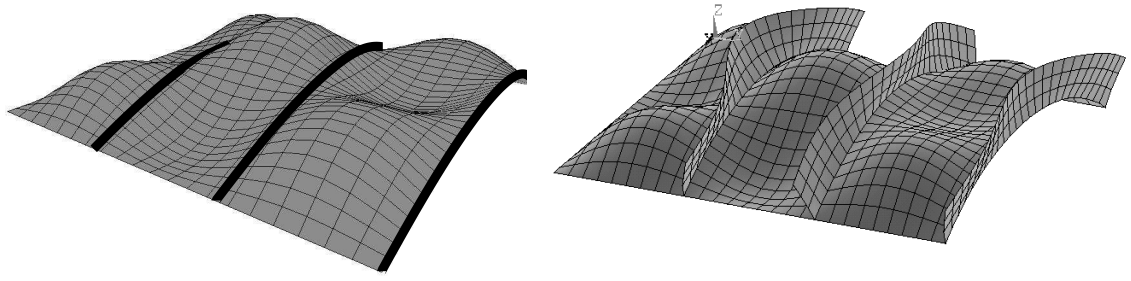

(a) (b)

Figure 19: The bending mode (combined global and local) of Plate 13 subjected to an external load $S_x = f_Y$ computed (a) by the present model and (b) by ANSYS.

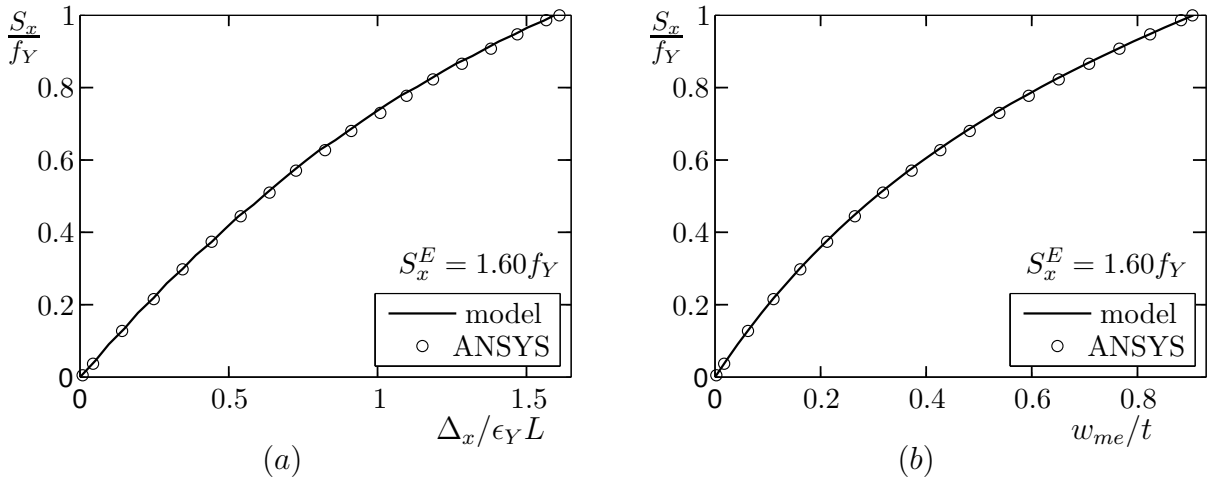

Figure 20: (a) Load-shortening and (b) load-deflection curves of Plate 9 (non-slender plate) subjected to a uniaxial load S_x.

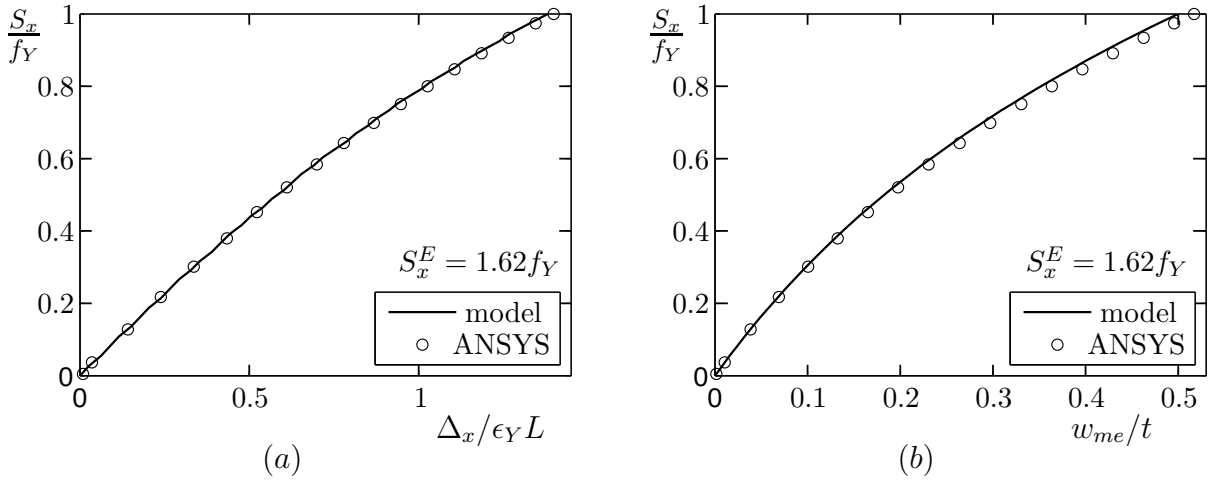

Figure 21: (a) Load-shortening and (b) load-deflection curves of Plate 10 (non-slender plate) subjected to a uniaxial load S_x.

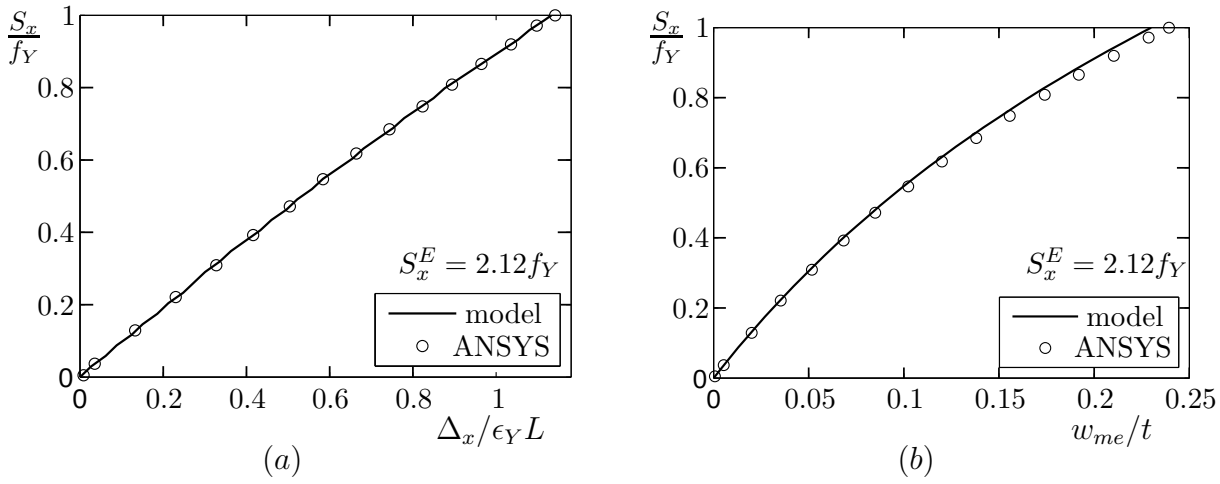

Figure 22: (a) Load-shortening and (b) load-deflection curves of Plate 11 (non-slender plate) subjected to a uniaxial load S_x.

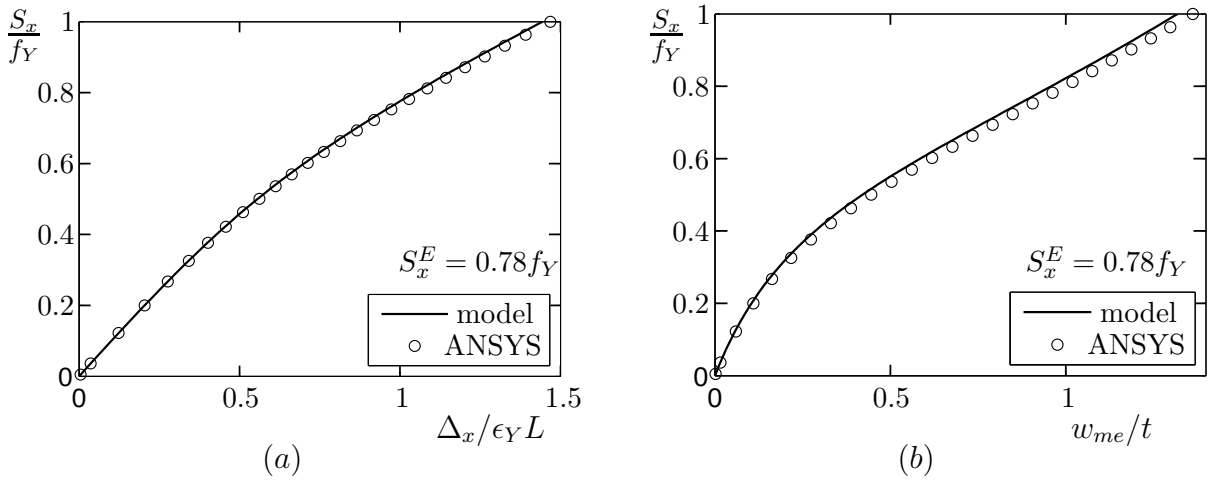

Figure 23: (a) Load-shortening and (b) load-deflection curves of Plate 12 (moderately slender plate) subjected to a uniaxial load S_x.

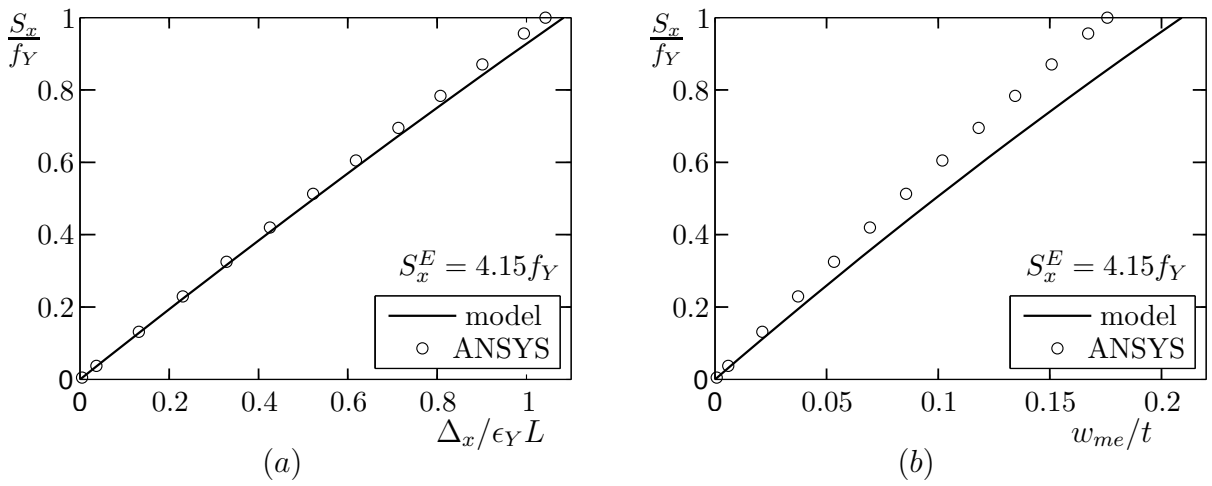

Figure 24: (a) Load-shortening and (b) load-deflection curves of Plate 13 (non-slender plate) subjected to a uniaxial load S_x.

9 STRESS AND STRENGTH PREDICTIONS

9.1 Introduction

The main emphasis of the present study has been to develop a model for displacement and stress predictions of stiffened plates with a free edge that may be provided with an edge stiffener. In addition, introductory investigations of ultimate strength limit (USL) predictions computed by the present model are considered. In those investigations, first yield of the von Mises' membrane stress is used as a strength criterion. These investigations indicate that it may be necessary with a more in-depth study of various strength criteria, in particular, for unstiffened plates with a free edge.

Due to the limited time frame, the investigations of stress and strength predictions are limited to such unstiffened plates. A more extensive study is required for stress and strength predictions of plates provided with stiffeners.

For each plate studied below, input parameters, including material properties, imperfection amplitude, etc., are given in Section 8.1.

9.2 Internal stress computations

In the results presented above (Chapter 8), load-displacement curves computed by the present model were verified by comparisons with finite element analysis results. In the present section, the accuracy of the internal stresses computed by the present model is

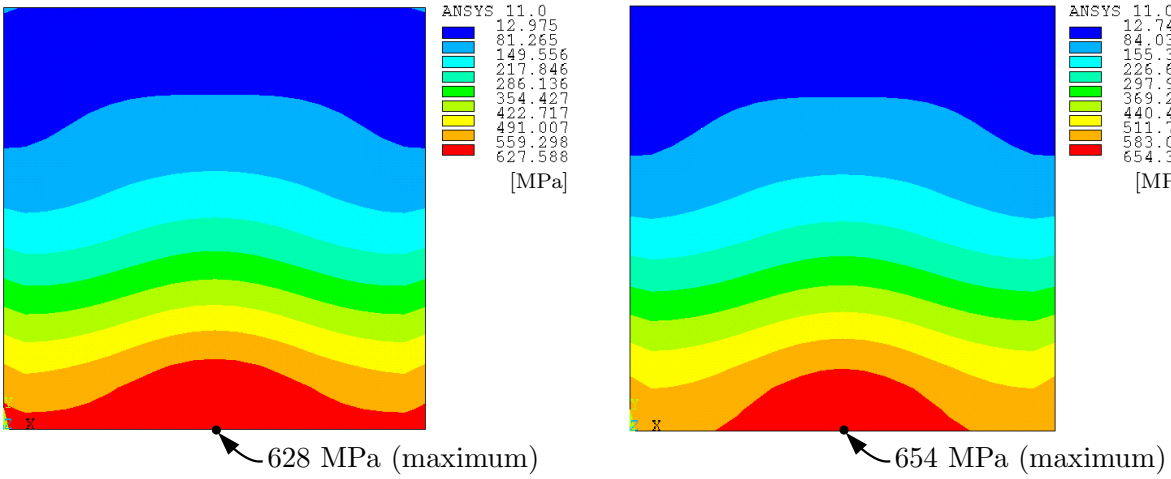

(a) ANSYS model 1 (b) ANSYS model 2

Figure 25: (a) Nodal solutions of the von Mises' membrane stresses computed by ANSYS for Plate 2 subjected to an external stress $S_x = f_Y$, with a coupling prescribing linear in-plane edge displacements and (b) the similar stress plot without such coupling.

investigated. It is important that the internal stresses are computed with satisfactory accuracy, if these stresses are to be used for instance in criteria for stress limitations or in ultimate strength predictions.

In the present model, the in-plane displacements along the supported edges vary linearly. The effect of this restriction on the internal stresses, has been studied using finite element analyses. In these analyses, two elastic element models with different boundary conditions are studied. Both element models have the same properties as described in Chapter 7, but in one of the models, there are couplings between the nodes in order to prescribe linearly varying in-plane edge displacements along the three simply supported edges. The element model with prescribed linearly varying in-plane edge displacements is referred to as "ANSYS model 1", and the other model is referred to as "ANSYS model 2".

From the finite element analyses, it was found that the maximum von Mises' membrane stress at a specified load level is smallest for the plate with linearly varying edge displacements. This is illustrated in Fig. 25 for Plate 2 subjected to an external in-plane stress $S_x = f_Y$, at which the nodal solution of the von Mises' membrane stress computed by ANSYS is shown. The maximum von Mises' membrane stress is about 628 MPa for "ANSYS model 1" and, in comparison, it is about 654 MPa for "ANSYS model 2". The stress level in both cases is unrealistically large, and the stress plots in the figure are only

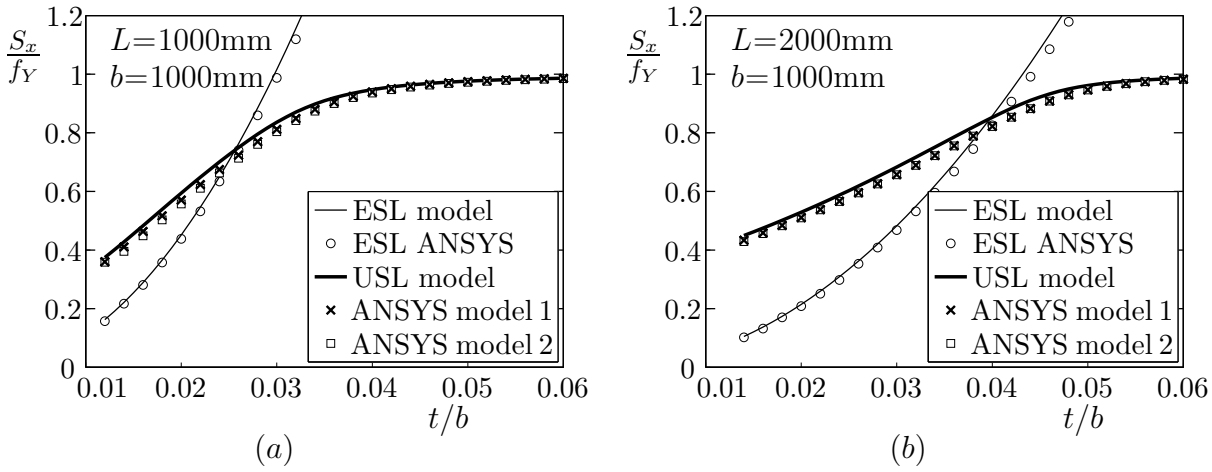

Figure 26: Elastic buckling stress limits (ESL) and applied in-plane uniaxial stresses causing first yield of the von Mises' membrane stress for (a) a quadratic plate and (b) a rectangular plate.

included in order to illustrate the effect of prescribed linearly varying edge displacements on the internal stresses.

In the context of strength predictions, the maximum von Mises' membrane stress will generally not exceed the yield strength. For such stress levels, the difference in stresses of the two element models is not large. This is illustrated in Fig. 26 in which the applied in-plane stress causing first yield of the von Mises' membrane stress is plotted both for "ANSYS model 1" (crosses) and for "ANSYS model 2" (squares). These curves are obtained by varying the plate thickness for both a quadratic plate ($L = b = 1000$ mm) in Fig. 26(a) and a rectangular plate ($L = 2b = 2000$ mm) in Fig. 26(b). It can be seen that the results computed by "ANSYS model 1" and "ANSYS model 2" are close to each other. This means that the effect of specifying linearly varying in-plane edge displacements on the internal stresses is rather small for the stress levels causing first yield of the von Mises' membrane stress.

In the figure, similar results computed by the present model are included (thick solid curves). The agreement between the model results and the corresponding finite element analysis results is good. Similar results have also been obtained for other plate dimensions, and good agreement is also achieved in these cases. This demonstrates that the internal stresses by the present model is computed with satisfactory accuracy. The model results, representing the applied in-plane stress causing first yield of the von Mises' membrane stress, are approximate ultimate limit strength (USL) predictions. Such strength

predictions will be discussed in more detail in the section below.

Elastic buckling stress limit (ESL) results computed by the present model (thin solid curve) and by ANSYS (open dots) are also included in Fig. 26. It can be seen that the agreement between the model and ANSYS results is good. As mentioned previously, the ESL results give an indication of the plate slenderness.

9.3 Strength predictions

9.3.1 Fully nonlinear finite element analysis

It is widely accepted that fully nonlinear finite element analyses, including both geometrical and material nonlinearities, predict the ultimate strength limit (USL) of stiffened plates with high numerical accuracy. In such analysis, the plate response is traced and the USL is reached when the external loads reach a maximum value (limit point).

Due to increasing out-of-plane displacements in analysis of imperfect, stiffened plates subjected to in-plane loads, stresses are redistributed from the interior of the plate to the parts with the largest stiffness. These parts are at the supported edges and, in addition, at the stiffeners in local bending cases. The stiffest parts are the critical parts of the plate, since when the cross-section capacity of these parts are exhausted the plate will usually collapse.

The stress redistribution is caused by both geometrical and material nonlinearities. Due to geometrical nonlinear effects, membrane stresses are redistributed from the interior of the plate to the critical parts. In addition, bending about the midplane of the plate may cause yielding in the interior portions of the plate in cases with significant out-of-plane displacements and thus significant bending stress. In such cases, with material nonlinear effects, additional stresses must be redistributed to the critical parts.

9.3.2 Previous strength criteria

Strength criteria can be used in combination with the incremental postbuckling procedure outlined above (Chapter 5) to predict the ultimate strength of stiffened plates with a free edge that may be provided with an edge stiffener. Typically, such strength criteria are applied in the critical parts of the plate. As mentioned above, the critical parts are the parts of the plate with the largest stiffness, and when the capacity of the critical parts is exhausted, no more stresses can be redistributed. Then, an additional in-plane loading cannot be applied without causing collapse.

In previous studies [12, 28], first yield of the von Mises' membrane stress was used as

a strength criterion for regularly stiffened and unstiffened, simply supported plates. For such plates, it was found that this criterion applied at the critical parts of the plate gave good agreement with fully nonlinear finite element analysis in most cases.

For irregularly stiffened, simply supported plates, various strength criteria were investigated in Brubak and Hellesland [36]. For such plates, it was found that the bending stresses at the critical parts are important for the ultimate strength. In order to account for this, strength criteria with these bending stresses included, were studied. Good agreement with fully nonlinear finite element analysis was achieved in most cases.

The criteria for irregularly stiffened, simply supported plates can also be used for regularly stiffened and unstiffened, simply supported plates subjected to in-plane loads. For such plates, the bending stresses at the critical parts are normally small (or zero). Then it makes little difference whether the bending stresses are included in the strength criterion or not, and it is first yield of the von Mises' membrane stress that is most relevant as a strength criterion.

Bending stresses in the interior of the plate may in some cases, have some influence on the ultimate strength. This is typical for cases with large bending stresses in the interior of the plate, which result in yielding and subsequent additional redistribution of stresses to the critical parts. In Byklum and Amdahl [12], it was found that the bending stresses and resulting yielding in the interior of the plate are important for strength predictions of long, simply supported plates subjected to predominant loading on the long edges, as illustrated in Fig. 27(a). For these load cases, such plates can have relatively large slenderness values, although the plate is rather thick, causing large displacements and bending stresses. For such cases, it may be rather non-conservative to neglect material yielding due to bending in the interior plate.

For plates with a free edge, as illustrated in Fig. 27(b), the interior bending stresses may be important for the ultimate strength in the same manner as for the long, simply supported plates discussed above. Some introductory investigations on strength predictions of plates with a free edge are presented in the section below.

9.3.3 Strength prediction results

Calculated ultimate strength limit (USL) results are examined for selected unstiffened plates with three simply supported edges and one free edge. For such plates, the bending stresses along the edges (critical parts) are zero, and then the strength criteria mentioned above and discussed in detail elsewhere [36] are identically equal to the criterion for first yield of the von Mises' membrane stress. It is this criterion that is used in the USL

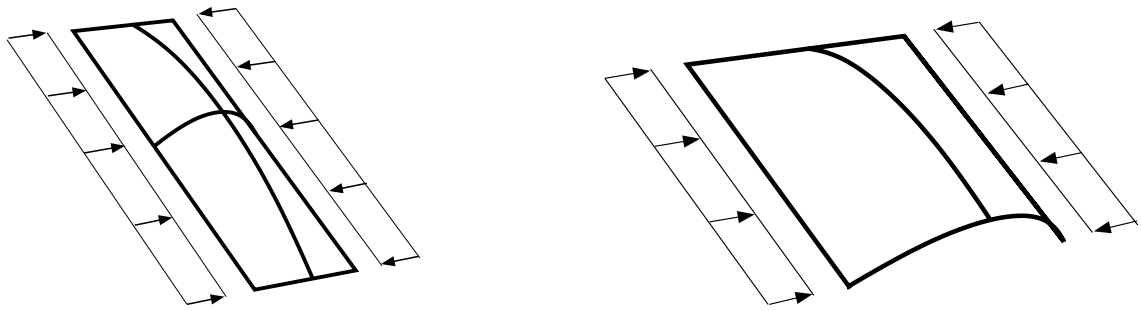

(a) (b)

Figure 27: (a) Illustration of the bending mode for a long simply supported, unstiffened plate subjected to in-plane stresses at the long edges and (b) the same for a uniaxially loaded unstiffened plate with a free edge.

predictions by the present model.

Computed USL predictions by the present model are compared to those obtained by fully nonlinear element analysis using ANSYS. The ANSYS analysis is performed with bilinear stress-strain relationship having the same material properties E, ν and f_Y as above (Section 8.1), and additionally, a hardening modulus $E_T = 1000$ MPa.

In Fig. 28, analysis results are presented for both quadratic and rectangular plates with various thicknesses. These plates are identical to those studied above in conjunction with the investigation of the internal stresses. Thus, the ESL results by the present model (thin solid curves) and by ANSYS (open dotes) shown in figure are equal to those in Section 9.2.

In the figure, USL predictions by the present method (thick, full curves) are shown. These are the same USL model results as presented in Section 9.2. The USL model results are now compared with USL predictions obtained by fully nonlinear element analysis using ANSYS (filled dots). It can be seen that the agreement is relatively good for the most slender plates. More specifically, good agreement is achieved for the quadratic plates with thickness smaller than about 20 mm ($t/b < 0.02$) and for the rectangular plates with thickness smaller than about 30 mm ($t/b < 0.03$). For intermediate and rather thick plates, it can be seen that the results computed by present method with first yield of the von Mises' membrane stress as the strength criterion are non-conservative compared to the USL ANSYS results. The USL results computed by the model and ANSYS will

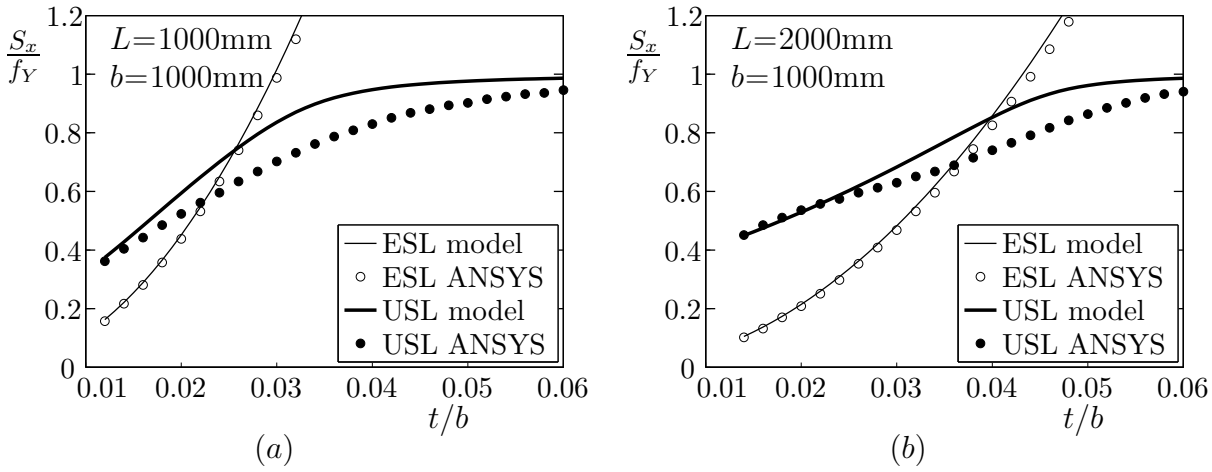

Figure 28: Elastic buckling stress limits (ESL) and ultimate strength limits (USL) for (a) a quadratic plate and (b) a rectangular plate.

converge as the plate thickness becomes large, i.e., as the results approach the "squash load" ($S_x = f_Y$).

In the region with the greatest discrepancy (intermediate slenderness and rather thick plates), the bending stresses in the interior of the plate are rather important for the ultimate strength. As mentioned above, material nonlinear effects are accounted for in the ANSYS analysis, and stresses in the interior plate are redistributed due to yielding caused by bending about the midplane of the plate. These effects are not accounted for in the present model, and the results become non-conservative in cases with large bending stresses, which is typical for intermediate to rather thick, unstiffened plates with a free edge. This indicates that it may be necessary to establish a strength criterion that accounts for these stresses. For instance, a criterion for stress limitation of the bending stresses in the interior of the plate.

In the present strength predictions, both slender and thick, unstiffened plates with a free edge were studied by varying the plate thickness. In such analysis, the effect of increasing the plate thickness on the ultimate strength can be studied. However, in a design situation, it is more common and more effective to use stiffened plates, instead of using thick, unstiffened plates, in order to achieve the required strength. For stiffened plates, the out-of-plane displacements and the bending stresses in the interior of the plate are usually not so large as for unstiffened plates with a free edge, and then, better agreement between the present method and finite element analysis is expected.

However, for global bending cases of the stiffened plates, the bending stresses in the

stiffeners may cause yielding, which usually will affect the ultimate strength. In Brubak and Hellesland [36], this plasticity is reflected quite well in a simplified manner by reducing the stiffness (removing area) of the stiffener. This simplified treatment of plasticity is not dependent on the boundary conditions, and it is expected that good results also will be achieved for stiffened plates with free edge provided with an edge stiffener.

9.3.4 Future work

In order to establish strength criteria that account for the bending stresses in the interior plate, more extensive investigations must be performed. The time frame available did not allow for in-depth investigations and this may be a topic for future work. In addition, it is necessary to study stress and strength predictions of stiffened plates for a variety of plate and stiffener dimensions. For strength analysis of stiffened plates with a free edge, the simplified treatment of plasticity [36] in a stiffener mentioned above may be applied. However, this implies a rather extensive verification study by comparisons with fully finite element analysis.

10 CONCLUDING REMARKS

An efficient computational model is presented for large deflection postbuckling analysis of imperfect, stiffened plates with an edge being free or provided with an edge stiffener. The applicability of the present method is documented for several cases by comparison with finite element analysis results using ANSYS. The model is able to trace the plate response beyond the elastic buckling load. It is able to capture both local and global displacement modes as well as the asymmetric global bending behaviour of plates with eccentric stiffeners. Due to the computational efficiency of the present model, it is also suited for design optimisation and reliability studies that normally require large number of case studies.

Introductory studies of ultimate strength limit (USL) predictions by the present model are presented. In these studies, first yield of the von Mises membrane stress was used as strength criterion. Preliminary results indicate that this strength criterion may be somewhat non-conservative for thick, unstiffened plates with a free edge. Alternative criteria for such cases are possible topics for further study.

ACKNOWLEDGEMENTS

First, I would like to thank Professor Jostein Hellesland at the University of Oslo for his interest, suggestions and valuable discussions during the study. I would also like to thank Dr. Scient. Eivind Steen at Det Norske Veritas (DNV) for his interest and for initially suggesting the topic of the research work. Valuable discussions with Henrik Eiding (M.Sc.) in conjunction with his master thesis are also highly appreciated.

REFERENCES

[1] prEN 1993-1-5, Eurocode 3: Design of steel structures. Part 1.5: Plated structural elements, CEN, European Committee for Standardisation, Brussels, 2005

[2] Det Norske Veritas. DNV Rules for classification of ships, Det Norske Veritas, Høvik, Norway, 2002

[3] E. Steen and E. Byklum and K.G. Vilming and T.K. Østvold, Computerized buckling models for ultimate strength assessments of stiffened ship hull panels, Proceedings of The Ninth International Symposium on Practical Design of Ships and other Floating Structures, Lübeck-Travemünde, Germany, Sept. 12-17, 2004; 235–242

[4] J.K. Paik, ALPS/ULSAP user's manual, Ship Structural Mechanics Lab., Department of Naval Architecture and Ocean Engineering, Pusan National University, Busan, Korea, 2003

[5] C. Mittelstedt. Stability behaviour of arbitrarily laminated composite plates with free and elastically restrained unloaded edges, International Journal of Mechanical Sciences, 2007; 49(7): 819–833

[6] S.T. Smith, M.A. Bradford and D.J. Oehlers. Numerical convergence of simple and orthogonal polynomials for the unilateral plate buckling problem using the Rayleigh-Ritz method, International Journal for Numerical Methods in Engineering, 1999; 44(11): 1685–1707

[7] M. Madhavan and J.S. Davidson. Elastic buckling of I-beam flanges subjected to a linearly varying stress distribution, Journal of Constructional Steel Research, 2007; 63(10): 1373–1383

[8] M. Madhavan and J.S. Davidson. Buckling of centerline-stiffened plates subjected to uniaxial eccentric compression, Thin-Walled Structures, 2008; 43(5): 1264–1276

[9] P. Qiao and L. Shan. Explicit local buckling analysis and design of fiber-reinforced plastic composite structural shapes, Composite Structures, 2005; 70(4): 468–483

[10] C. Yu and B.W. Schafer. Effect of longitudinal stress gradients on elastic buckling of thin plates, Journal of Engineering Mechanics, ASCE, 2007; 133(4): 452–463

[11] E. Steen. Application of the perturbation method to plate buckling problems, Research Report in Mechanics, No. 98-1, Mechanics Division, Dept. of Mathematics, University of Oslo, Norway, 1998, 60 pp.

[12] E. Byklum and J. Amdahl. A simplified method for elastic large deflection analysis of plates and stiffened panels due to local buckling, Thin-Walled Structures, 2000; 40(11): 925–953

[13] Lars Brubak and Jostein Hellesland. Semi-analytical postbuckling and strength analysis of arbitrarily stiffened plates in local and global bending, Thin-Walled Structures, 2007; 45(6), 620–633

[14] P. Buermann, R. Rolfes, J. Tessmer and M. Schagerl. A semi-analytical model for local post-buckling analysis of stringer- and frame-stiffened cylindrical panels Thin-Walled Structures, 2006; 44(1): 102–114

[15] prEN 1993-1-1, Eurocode 3: Design of steel structures. Part 1.1: General rules and rules for buildings, CEN, European Committee for Standardisation, Brussels, 2003

[16] Det Norske Veritas. Recommended practice DNV-RP-C201, Buckling strength of plated structures, Høvik, Norway, 2002

[17] K. Marguerre. Zur theorie der gekrümmten platte grosser formänderung, Proceedings of The 5^{th} International Congress for Applied Mechanics, 1938; 93–101

[18] H.R. Ovesy, J. Loughlan, H. Assaee. The compressive post-local bucking behaviour of thin plates using a semi-energy finite strip approach, Thin-Walled Structures, 2004; 42(3): 449–474

[19] L. Brubak, J. Hellesland and E. Steen. Semi-analytical buckling strength analysis of plates with arbitrary stiffener arrangements, Journal of Constructional Steel Research, 2007; 63(4): 532–543

[20] D.O. Brush and B.O. Almroth. Buckling of bars, plates and shells, McGraw-Hill Book Company, 1975

[21] Z.P. Bažant and L. Cedolin. Stability of structures, Oxford University Press, 1991

[22] Lars Brubak and Jostein Hellesland. Approximate buckling strength analysis of arbitrarily stiffened, stepped plates, Engineering Structures, 2007; 29(9): 2321–2333

[23] H.R. Ovesy, J. Loughlan, S.A.M. GhannadPour. Geometric non-linear analysis of channel sections under end shortening, using different versions of the finite strip method Computers and Structures, 2006; 84(13-14): 855–872

[24] L. Brubak. Semi-analytical buckling strength analysis of plates with constant or varying thickness and arbitrarily oriented stiffeners. Research report in mechanics, No. 05-6, Mechanics Division, Dept. of Mathematics, University of Oslo, Norway, 2005, 65 pp.

[25] H.M. Eiding. Knekning av avstivede plater med variable randbetingelser (Buckling of stiffened plates with various boundary conditions), Mechanics Division, Department of Mathematics, University of Oslo, Norway, 2007, 87 pp.

[26] L.K. Seah and J. Rhodes. Simplified buckling analysis of plate with compound edge stiffeners, Journal of Engineering Mechanics, 1993; 119(1): 19–37

[27] O.K. Bedair. The elastic behaviour of multi-stiffened plates under uniform compression, Thin-Walled Structures, 1997; 27(4): 311–335

[28] E. Byklum. Ultimate strength analysis of stiffened steel and aluminium panels using semi-analytical methods, Dr. Ing. thesis, Norwegian University of Science and Technology, Trondheim, Norway, 2002

[29] J.K. Paik and M.S. Lee, A Semi-analytical method for the elastic-plastic large deflection analysis of stiffened panels under combined biaxial compression/tension, biaxial in-plate bending, edge shear, and lateral pressure loads, Thin-Walled Structures, 2005; 43(3): 375–410

[30] E. Byklum, E. Steen and J. Amdahl. A semi-analytical model for global buckling and postbuckling analysis of stiffened panels, Thin-Walled Structures, 2004; 42(5): 701–717

[31] E. Steen, E. Byklum and J. Hellesland. Elastic postbuckling stiffness of biaxially compressed rectangular plates, Engineering Structures, 2008; 30(10): 2631–2643

[32] E. Riks. An incremental approach to the solution of snapping and buckling problems, International Journal of Solids and Structures, 1979; 15: 529–551

[33] E. Kreyszig. Advanced Engineering Mathematics, 7th ed., John Wiley & Sons, Inc., 1993

[34] E. Steen. Elastic buckling and postbuckling of eccentrically stiffened plates, International Journal of Solids and Structures, 1989; 25(7): 751–768

[35] ANSYS Inc., ANSYS Documentation 11.0, Southpointe, Canonsburg, PA, 2007.

[36] Lars Brubak and Jostein Hellesland. Strength criteria in semi-analytical, large deflection analysis of stiffened plates in local and global bending, Thin-Walled Structures, 2008; 46(12), 1382–1390

A Subdivision of matrices and vectors

In the solution procedure outlined in Chapter 5, the incremental stiffness matrix $\mathbf{K}$ in Eq. 33 must be computed. For each displacement component (u, v, w), this matrix is divided into submatrices, and it can be written as

$$\mathbf{K} = \begin{bmatrix} \mathbf{K}_{uu} & \mathbf{K}_{uv} & \mathbf{K}_{uw} \\ \mathbf{K}_{vu} & \mathbf{K}_{vv} & \mathbf{K}_{vw} \\ \mathbf{K}_{wu} & \mathbf{K}_{wv} & \mathbf{K}_{ww} \end{bmatrix} \tag{65}$$

Further, the submatrices ($\mathbf{K}_{uu}$, $\mathbf{K}_{uu}$, etc.) are subdivided into new submatrices corresponding to the displacement assumptions (Section 4.1) previously labelled with super indexes 'a', 'b' and 'c', and they can be written as

$$\mathbf{K}_{uu} = \begin{bmatrix} \mathbf{K}_{uaua} & \mathbf{K}_{uaub} & \mathbf{K}_{uauc} \\ \mathbf{K}_{ubua} & \mathbf{K}_{ubub} & \mathbf{K}_{ubuc} \\ \mathbf{K}_{ucua} & \mathbf{K}_{ucub} & \mathbf{K}_{ucuc} \end{bmatrix}, \quad \mathbf{K}_{vv} = \begin{bmatrix} \mathbf{K}_{vava} & \mathbf{K}_{vavb} & \mathbf{K}_{vavc} \\ \mathbf{K}_{vbva} & \mathbf{K}_{vbvb} & \mathbf{K}_{vbvc} \\ \mathbf{K}_{vcva} & \mathbf{K}_{vcvb} & \mathbf{K}_{vcvc} \end{bmatrix} \tag{66}$$

$$\mathbf{K}_{ww} = \begin{bmatrix} \mathbf{K}_{wawa} & \mathbf{K}_{wawb} \\ \mathbf{K}_{wbwa} & \mathbf{K}_{wbwb} \end{bmatrix}, \quad \mathbf{K}_{uv} = \mathbf{K}_{vu}^T = \begin{bmatrix} \mathbf{K}_{uava} & \mathbf{K}_{uavb} & \mathbf{K}_{uavc} \\ \mathbf{K}_{ubva} & \mathbf{K}_{ubvb} & \mathbf{K}_{ubvc} \\ \mathbf{K}_{ucva} & \mathbf{K}_{ucvb} & \mathbf{K}_{ucvc} \end{bmatrix} \tag{67}$$

$$\mathbf{K}_{uw} = \mathbf{K}_{wu}^T = \begin{bmatrix} \mathbf{K}_{uawa} & \mathbf{K}_{uawb} \\ \mathbf{K}_{ubwa} & \mathbf{K}_{ubwb} \\ \mathbf{K}_{ucwa} & \mathbf{K}_{ucwb} \end{bmatrix}, \mathbf{K}_{vw} = \mathbf{K}_{wv}^T = \begin{bmatrix} \mathbf{K}_{vawa} & \mathbf{K}_{vawb} \\ \mathbf{K}_{vbwa} & \mathbf{K}_{vbwb} \\ \mathbf{K}_{vcwa} & \mathbf{K}_{vcwb} \end{bmatrix} \tag{68}$$

The submatrices ($\mathbf{K}_{uaua}$, $\mathbf{K}_{uaub}$, etc.) obtained in the subdivision for each displacement field are computed by differentiation of the strain energy contributions, twice with respect to the displacement amplitudes (Eq. 32) . For instance, the linear plate membrane stiffness contribution of $\mathbf{K}_{uava}$ is obtained by the expression

$$\mathbf{K}_{uava}^{pmL} = \frac{\partial^2 U^{pmL}}{\partial u_f^a \partial v_p^a} = \begin{bmatrix} \frac{\partial^2 U^{pmL}}{\partial u_1^a \partial v_1^a} & \cdots & \frac{\partial^2 U^{pmL}}{\partial u_1^a v_{Nva}^a} \\ \vdots & & \vdots \\ \frac{\partial^2 U^{pmL}}{\partial u_{Nua}^a \partial v_1^a} & \cdots & \frac{\partial^2 U^{pmL}}{\partial u_{Nua}^a v_{Nva}^a} \end{bmatrix} \tag{69}$$

The two first subscripts (ua) of the matrix $\mathbf{K}_{uava}^{pmL}$ indicate the displacement field u^a (Eq. 13) and the two last subscripts (va) indicate the displacement field v^a (Eq. 16). The size of this matrix is equal to $N_{ua} \times N_{va}$, where N_{ua} and N_{va} are the number of terms in the displacement fields u^a and v^a, respectively. A more detailed overview of the composition of the submatrices is given in Appendix B. The expressions for all the submatrices are given in Appendix C and D.

In a similar manner as for the incremental stiffness matrix, the incremental load vector $-\dot{\Lambda}\mathbf{G}$ is divided into subvectors for each displacement component (u, v, w) as given in Eq. 37. Alternatively, it can be written as

$$-\dot{\Lambda}\mathbf{G}^T = -\dot{\Lambda}[\mathbf{G}_u^T, \mathbf{G}_v^T, \mathbf{G}_w^T] \tag{70}$$

These subvectors are subdivided for each displacement field (with super indexes 'a', 'b' and 'c'), and they can be written as

$$-\dot{\Lambda}\mathbf{G}_u^T = -\dot{\Lambda}\left[\mathbf{G}_{ua}^T, \mathbf{G}_{ub}^T, \mathbf{G}_{uc}^T\right], \quad -\dot{\Lambda}\mathbf{G_v}^T = -\dot{\Lambda}\left[\mathbf{G}_{va}^T, \mathbf{G}_{vb}^T, \mathbf{G}_{vc}^T\right], \quad -\dot{\Lambda}\mathbf{G_w}^T = -\dot{\Lambda}\left[\mathbf{G}_{wa}^T, \mathbf{G}_{wb}^T\right] \tag{71}$$

The subvectors ($-\dot{\Lambda}\mathbf{G}_{ua}$, $-\dot{\Lambda}\mathbf{G}_{ub}$, etc.) obtained in the subdivision for each displacement field are computed by differentiation of the potential energy of the external loads, with respect to the displacement amplitudes and the load factor (Eq. 32). For instance, the plate contribution of the subvector $-\dot{\Lambda}\mathbf{G}_{ua}$ for a load applied at the plate edge in x-direction is obtained by the expression

$$-\dot{\Lambda}\mathbf{G}_{ua}^p = -\dot{\Lambda}\frac{\partial^2 T^{p,x}}{\partial u_f^a \partial \Lambda} = -\dot{\Lambda}\begin{bmatrix} \frac{\partial^2 T^{p,x}}{\partial u_1^a \partial \Lambda} \\ \vdots \\ \frac{\partial^2 T^{p,x}}{\partial u_{Nua}^a \partial \Lambda} \end{bmatrix} \tag{72}$$

All the subvectors of the incremental load vector of the plate are given in Appendix C.

B Composition of submatrices and subvectors

According to the principle of stationary potential energy, equilibrium requires that the total potential energy $\Pi = U + T$, has a stationary value. This requirement on rate form, $\delta\dot{\Pi} = \delta\dot{U} + \delta\dot{T} = 0$, leads to the $N_{\text{dof}} \times N_{\text{dof}}$ equations given by

$$\frac{\partial \dot{\Pi}}{\partial d_i} = \frac{\partial}{\partial \eta}\frac{\partial \Pi}{\partial d_i} = K_{ij}\dot{d}_j + G_i\dot{\Lambda} = 0 \tag{73}$$

where

$$K_{ij} = \frac{\partial^2 \Pi}{\partial d_i \partial d_j} \text{ and } G_i = \frac{\partial^2 \Pi}{\partial d_i \partial \Lambda} \tag{74}$$

In the expression above (Eq. 73), the index notation with the Einstein summation rule for repeated indexes is adopted. However, after substituting the potential energy into Eq. 73, the summation symbol ($\sum$) is used instead of Einstein summation rule for the convenience of the reader.

The composition of the submatrices and subvectors is explained by an example where the chosen matrix $\mathbf{K}^{sL,y}_{vawb}$ will be built. In line with Eqs. 73-74, this matrix can be obtained by the expression

$$\mathbf{K}^{sL,y}_{vawb}\dot{\mathbf{w}}^b = \frac{\partial^2 U^{sL,y}}{\partial v^a_f \partial w^b_{pq}}\dot{w}^b_{pq} \tag{75}$$

where $U^{sL,y}$ is a stiffener strain energy contribution that is quadratic in the displacements. The composition of this submatrix represents a difficult example, since the displacement amplitudes for two different displacement fields v^a and w^b and, in addition, the initial imperfection field w^a_0, are involved. In order to make it easier to distinguish between the indexes used for the rows and the columns, the product of the submatrix and the displacement rate subvector is given. By substituting $U^{sL,y}$ into Eq. 75, this can be written as

$$\begin{aligned}\mathbf{K}^{sL,y}_{vawb}\dot{\mathbf{w}}^b =& \frac{\partial^2 U^{sL,y}}{\partial v^a_f \partial w^b_{pq}}\dot{w}^b_{pq} \\ =& \sum_{p=1}^{M_{wb}}\sum_{q=1}^{N_{wb}} e_c E A_s \left(\frac{q\pi}{b}\right)^2 \frac{1}{b} I^s_q \cos(\frac{f\pi}{L}x_s)\sin(\frac{p\pi}{L}x_s)\dot{w}^b_{pq} \\ &+ \sum_{p=1}^{M_{wb}}\sum_{q=1}^{N_{wb}}\sum_{m=1}^{M_{wb}} w^b_{0mq} E A_s \left(\frac{q\pi}{b}\right)^2 \frac{1}{2}\cos(\frac{f\pi}{L}x_s)\sin(\frac{p\pi}{L}x_s)\sin(\frac{m\pi}{L}x_s)\dot{w}^b_{pq}\end{aligned} \tag{76}$$

where 'f' indicates the row number ($f = 1, 2, ..., M_{va}$), and 'p' and 'q' indicate the column number ($[p, q] = [1, 1], [1, 2]..., [M_{wb}, N_{wb}]$). Thus, the total number of rows is M_{va} and the total number of columns is $M_{wb}N_{wb}$, and the size of the matrix is $M_{va} \times M_{wb}N_{wb}$. The matrix alone can be written as

$$\begin{aligned}\mathbf{K}^{sL,y}_{vawb} =& \frac{\partial^2 U^{sL,y}}{\partial v^a_f \partial w^b_{pq}} \\ =& e_c E A_s \left(\frac{q\pi}{b}\right)^2 \frac{1}{b} I^s_q \cos(\frac{f\pi}{L}x_s)\sin(\frac{p\pi}{L}x_s) \\ &+ \sum_{m=1}^{M_{wb}} w^b_{0mq} E A_s \left(\frac{q\pi}{b}\right)^2 \frac{1}{2}\cos(\frac{f\pi}{L}x_s)\sin(\frac{p\pi}{L}x_s)\sin(\frac{m\pi}{L}x_s)\end{aligned} \tag{77}$$

All the expressions for the submatrices and subvectors are given in Appendix C and D. The composition of these expressions is similar to the example given above. Thus, the row number is indicated by 'f' for a corresponding displacement amplitude with one subscript ($f = 1, 2, ...$), and by 'f' and 'g' for a corresponding displacement amplitude with two subscripts ($[f, g] = [1, 1], [1, 2]...$). In a similar manner, 'p' and 'q' are used to indicate the column number.

C Rate form of energy contributions of the plate

C.1 The generalised, incremental membrane stiffness matrix $\mathbf{K}^{pm}$

C.1.1 Introduction

The generalised, incremental membrane stiffness matrix $\mathbf{K}^{pm}$ is divided into the submatrices given below. In the solution procedure for postbuckling analysis described in Chapter 5, $\mathbf{K}^{pm}$ must be added to the generalised, incremental stiffness matrix $\mathbf{K}$ given in Eq. 41.

In the expressions below, the integrals are replace with simplified expressions (I^s_m, I^{cs}_{mn}, etc). For instance,

$$I^s_m = \int_0^b \sin(\frac{m\pi}{b}y)\,dy = \frac{b}{m\pi}[1-(-1)^m] \tag{78}$$

is introduced. The expressions for all the integrals can be found in Appendix F. In addition , the Kronecker delta defined by

$$\delta_{ij} = \begin{cases} 1 & \text{if } i=j \\ 0 & \text{otherwise} \end{cases} \tag{79}$$

is used. Details on how to build the matrices is given in Appendix A and B.

C.1.2 Definition of the $\mathbf{K}^{pmL}_{uu}$-matrix

The matrix $\mathbf{K}^{pmL}_{uu}$ is symmetrical, and the size of this matrix is $(M_{ua}+M_{ub}N_{ub}+1)\times(M_{ua}+M_{ub}N_{ub}+1)$. The matrix is a constant contribution and consists of the submatrices given in index notation in the following expressions

$$\mathbf{K}^{pmL}_{uaua}\dot{\mathbf{u}}^a = \frac{\partial^2 U^{pmL}}{\partial u^a_f \partial u^a_p}\dot{u}^a_p = \sum_{p=1}^{M_{ua}} C\left[\left(\frac{f\pi}{L}\right)^2\frac{b}{3}\frac{L}{2}+\frac{1-\nu}{2}\frac{1}{b}\frac{L}{2}\right]\delta_{fp}\dot{u}^a_p \tag{80}$$

$$\mathbf{K}^{pmL}_{ubub}\dot{\mathbf{u}}^b = \frac{\partial^2 U^{pmL}}{\partial u^b_{fg}\partial u^b_{pq}}\dot{u}^b_{pq} = \sum_{p=1}^{M_{ub}}\sum_{q=1}^{N_{ub}} C\left[\left(\frac{f\pi}{L}\right)^2+\frac{1-\nu}{2}\left(\frac{g\pi}{b}\right)^2\right]\frac{Lb}{4}\delta_{fp}\delta_{gq}\dot{u}^b_{pq} \tag{81}$$

$$\mathbf{K}^{pmL}_{ucuc}\dot{\mathbf{u}}^c = \frac{\partial^2 U^{pmL}}{\partial u^c \partial u^c}\dot{u}^c = C\frac{b}{L}\dot{u}^c \tag{82}$$

$$\mathbf{K}^{pmL}_{uaub}\dot{\mathbf{u}}^b = \frac{\partial^2 U^{pmL}}{\partial u^a_f \partial u^b_{pq}}\dot{u}^b_{pq} = \sum_{p=1}^{M_{ub}}\sum_{q=1}^{N_{ub}} C\left(\frac{f\pi}{L}\right)^2\frac{L}{2}I^{ys}_q\delta_{fp}\dot{u}^b_{pq} \tag{83}$$

$$\mathbf{K}^{pmL}_{ubua}\dot{\mathbf{u}}^a = \frac{\partial^2 U^{pmL}}{\partial u^b_{fg}\partial u^a_p}\dot{u}^a_p = \sum_{p=1}^{M_{ua}} C\left(\frac{f\pi}{L}\right)^2 \frac{L}{2} I^{ys}_g \delta_{fp}\dot{u}^a_p \tag{84}$$

$$\mathbf{K}^{pmL}_{uauc} = 0, \quad \mathbf{K}^{pmL}_{ucua} = 0, \quad \mathbf{K}^{pmL}_{ubuc} = 0, \quad \mathbf{K}^{pmL}_{ucub} = 0 \tag{85}$$

In these expressions, the matrices $\mathbf{K}^{pmL}_{uaua}$ and $\mathbf{K}^{pmL}_{ubub}$ are diagonal matrices.

C.1.3 Definition of the $\mathbf{K}^{pmL}_{uv}$-matrix

The size of the matrix $\mathbf{K}^{pmL}_{uv}$ is $(M_{ua} + M_{ub}N_{ub} + 1) \times (M_{va} + M_{vb}N_{vb} + 1)$. The matrix is a constant contribution and consists of the submatrices given in index notation in the following expressions

$$\mathbf{K}^{pmL}_{uava}\dot{\mathbf{v}}^a = \frac{\partial^2 U^{pmL}}{\partial u^a_f \partial v^a_p}\dot{v}^a_p = \sum_{p=1}^{M_{va}} C\frac{f\pi}{L}\frac{L}{4}\frac{3\nu - 1}{2}\delta_{fp}\dot{v}^a_p \tag{86}$$

$$\mathbf{K}^{pmL}_{uavb}\dot{\mathbf{v}}^b = \frac{\partial^2 U^{pmL}}{\partial u^a_f \partial v^b_{pq}}\dot{v}^b_{pq} = \sum_{p=1}^{M_{vb}}\sum_{q=1}^{N_{vb}} C\left[\nu\frac{f\pi}{L}\frac{q\pi}{b}I^{yc}_q I^{cs}_{fp} + \frac{1-\nu}{2}\frac{p\pi}{L}\frac{1}{b}I^{s}_q I^{cs}_{pf}\right]\dot{v}^b_{pq} \tag{87}$$

$$\mathbf{K}^{pmL}_{ubva}\dot{\mathbf{v}}^a = \frac{\partial^2 U^{pmL}}{\partial u^b_{fg}\partial v^a_p}\dot{v}^a_p = \sum_{p=1}^{M_{va}} C\left[\nu\frac{f\pi}{L}\frac{1}{b}\frac{L}{2}I^{s}_g - \frac{1-\nu}{2}\frac{f\pi}{L}\frac{g\pi}{b}\frac{L}{2}I^{yc}_g\right]\delta_{fp}\dot{v}^a_p \tag{88}$$

$$\mathbf{K}^{pmL}_{ubvb}\dot{\mathbf{v}}^b = \frac{\partial^2 U^{pmL}}{\partial u^b_{fg}\partial v^b_{pq}}\dot{v}^b_{pq} = \sum_{p=1}^{M_{vb}}\sum_{q=1}^{N_{vb}} C\left[\nu\frac{f\pi}{L}\frac{q\pi}{b}I^{cs}_{fp}I^{cs}_{qg} + \frac{1-\nu}{2}\frac{g\pi}{b}\frac{p\pi}{L}I^{cs}_{pf}I^{cs}_{gq}\right]\dot{v}^b_{pq} \tag{89}$$

$$\mathbf{K}^{pmL}_{ucvc}\dot{\mathbf{v}}^a = \frac{\partial^2 U^{pmL}}{\partial u^c \partial v^c}\dot{v}^c = C\nu\dot{v}^c \tag{90}$$

$$\mathbf{K}^{pmL}_{uavc} = 0, \quad \mathbf{K}^{pmL}_{ucva} = 0, \quad \mathbf{K}^{pmL}_{ubvc} = 0, \quad \mathbf{K}^{pmL}_{ucvb} = 0 \tag{91}$$

This matrix is not symmetrical, but total incremental stiffness matrix $\mathbf{K}$, consisting of an assembly of all the submatrices, is symmetrical.

C.1.4 Definition of the $\mathbf{K}^{pmL}_{vu}$-matrix

Due to symmetry, the matrix can be given by

$$\mathbf{K}^{pmL}_{vu} = (\mathbf{K}^{pmL}_{uv})^T \tag{92}$$

where $\mathbf{K}^{pmL}_{uv}$ is given in Section C.1.3. The size of this matrix is $(M_{va} + M_{vb}N_{vb} + 1) \times (M_{ua} + M_{ub}N_{ub} + 1)$.

C.1.5 Definition of the $\mathbf{K}_{vv}^{pmL}$-matrix

The matrix $\mathbf{K}_{vv}^{pmL}$ is symmetrical, and the size of this matrix is $(M_{va} + M_{vb}N_{vb} + 1) \times (M_{va} + M_{vb}N_{vb} + 1)$. The matrix is a constant contribution and consists of the submatrices given in index notation in the following expressions

$$\mathbf{K}_{vava}^{pmL}\dot{\mathbf{v}}^a = \frac{\partial^2 U^{pmL}}{\partial v_f^a \partial v_p^a}\dot{v}_p^a = \sum_{p=1}^{M_{va}} C\left[\frac{1}{b} + \frac{1-\nu}{2}\left(\frac{f\pi}{L}\right)^2\frac{b}{3}\right]\frac{L}{2}\delta_{fp}\dot{v}_p^a \tag{93}$$

$$\mathbf{K}_{vbvb}^{pmL}\dot{\mathbf{v}}^b = \frac{\partial^2 U^{pmL}}{\partial v_{fg}^b \partial v_{pq}^b}\dot{v}_{pq}^b = \sum_{p=1}^{M_{vb}}\sum_{q=1}^{N_{vb}} C\left[\left(\frac{g\pi}{b}\right)^2 + \frac{1-\nu}{2}\left(\frac{f\pi}{L}\right)^2\right]\frac{Lb}{4}\delta_{fp}\delta_{gq}\dot{v}_{pq}^b \tag{94}$$

$$\mathbf{K}_{vcvc}^{pmL}\dot{\mathbf{v}}^c = \frac{\partial^2 U^{pmL}}{\partial v^c \partial v^c}\dot{v}^c = C\frac{L}{b}\dot{v}^c \tag{95}$$

$$\mathbf{K}_{vavb}^{pmL}\dot{\mathbf{v}}^a = \frac{\partial^2 U^{pmL}}{\partial v_f^a \partial v_{pq}^b}\dot{v}_{pq}^b = -\sum_{p=1}^{M_{vb}}\sum_{q=1}^{N_{vb}} C\frac{1-\nu}{2}\frac{f\pi}{L}\frac{p\pi}{L}I_q^{ys}I_{pf}^{cs}\dot{v}_{pq}^b \tag{96}$$

$$\mathbf{K}_{vbva}^{pmL}\dot{\mathbf{v}}^a = \frac{\partial^2 U^{pmL}}{\partial v_{fg}^b \partial v_p^a}\dot{v}_p^a = -\sum_{p=1}^{M_{va}} C\frac{1-\nu}{2}\frac{f\pi}{L}\frac{p\pi}{L}I_g^{ys}I_{fp}^{cs}\dot{v}_p^a \tag{97}$$

$$\mathbf{K}_{vavc}^{pmL} = 0, \quad \mathbf{K}_{vcva}^{pmL} = 0, \quad \mathbf{K}_{vbvc}^{pmL} = 0, \quad \mathbf{K}_{vcvb}^{pmL} = 0 \tag{98}$$

C.1.6 Definition of the $\mathbf{K}_{uw}^{pmL}$-matrix

The size of the matrix $\mathbf{K}_{uw}^{pmL}$ is $(M_{ua} + M_{ub}N_{ub} + 1) \times (M_{wa} + M_{wb}N_{wb})$. The matrix is a constant contribution and consists of the submatrices given in index notation in the following expressions

$$\begin{aligned}
\mathbf{K}_{uawa}^{pmL}\dot{\mathbf{w}}^a &= \frac{\partial^2 U^{pmL}}{\partial u_f^a \partial w_p^a}\dot{w}_p^a \\
&= \sum_{p=1}^{M_{wa}}\sum_{m=1}^{M_{wa}} w_{0m}^a C\left[\frac{f\pi}{L}\frac{p\pi}{L}\frac{m\pi}{L}\frac{b}{4}I_{fpm}^{ccc} + \frac{1-\nu}{2}\left(\frac{1}{b}\right)^2\frac{b}{2}\frac{m\pi}{L}I_{mfp}^{css}\right. \\
&\qquad \left. + \nu\frac{f\pi}{L}\left(\frac{1}{b}\right)^2\frac{b}{2}I_{fpm}^{css} + \frac{1-\nu}{2}\frac{p\pi}{L}\left(\frac{1}{b}\right)^2\frac{b}{2}I_{pfm}^{css}\right]\dot{w}_p^a \\
&+ \sum_{p=1}^{M_{wa}}\sum_{m=1}^{M_{wb}}\sum_{n=1}^{N_{wb}} w_{0mn}^b C\left[\frac{f\pi}{L}\frac{p\pi}{L}\frac{m\pi}{L}I_n^{yys}I_{fpm}^{ccc} + \frac{1-\nu}{2}\left(\frac{1}{b}\right)^2\frac{m\pi}{L}I_n^s I_{mfp}^{css}\right. \\
&\qquad \left. + \nu\frac{f\pi}{L}\frac{1}{b}\frac{n\pi}{b}I_n^{yc}I_{fpm}^{css} + \frac{1-\nu}{2}\frac{p\pi}{L}\frac{n\pi}{b}\frac{1}{b}I_n^{yc}I_{pfm}^{css}\right]\dot{w}_p^a
\end{aligned} \tag{99}$$

$$\mathbf{K}^{pmL}_{uawb}\dot{\mathbf{w}}^b = \frac{\partial^2 U^{pmL}}{\partial u^a_f \partial w^b_{pq}}\dot{w}^b_{pq}$$

$$= \sum_{p=1}^{M_{wb}}\sum_{q=1}^{N_{wb}}\sum_{m=1}^{M_{wa}} w^a_{0m} C\left[\frac{f\pi}{L}\frac{p\pi}{L}\frac{m\pi}{L} I^{yys}_q I^{ccc}_{fpm} + \frac{1-\nu}{2}\frac{q\pi}{b}\frac{m\pi}{L}\frac{1}{b} I^{yc}_q I^{css}_{mfp}\right.$$

$$\left. +\nu\frac{f\pi}{L}\frac{q\pi}{b}\frac{1}{b} I^{yc}_q I^{css}_{fpm} + \frac{1-\nu}{2}\left(\frac{1}{b}\right)^2\frac{p\pi}{L} I^{s}_q I^{css}_{pfm}\right]\dot{w}^b_{pq} \tag{100}$$

$$+\sum_{p=1}^{M_{wb}}\sum_{q=1}^{N_{wb}}\sum_{m=1}^{M_{wb}}\sum_{n=1}^{N_{wb}} w^b_{0mn} C\left[\frac{f\pi}{L}\frac{p\pi}{L}\frac{m\pi}{L} I^{yss}_{qn} I^{ccc}_{fpm} + \frac{1-\nu}{2}\frac{1}{b}\frac{q\pi}{b}\frac{m\pi}{L} I^{cs}_{qn} I^{css}_{mfp}\right.$$

$$\left. +\nu\frac{f\pi}{L}\frac{q\pi}{b}\frac{n\pi}{b} I^{ycc}_{qn} I^{css}_{fpm} + \frac{1-\nu}{2}\frac{p\pi}{L}\frac{n\pi}{b}\frac{1}{b} I^{cs}_{nq} I^{css}_{pfm}\right]\dot{w}^b_{pq}$$

$$\mathbf{K}^{pmL}_{ubwa}\dot{\mathbf{w}}^a = \frac{\partial^2 U^{pmL}}{\partial u^b_{fg} \partial w^a_p}\dot{w}^a_p$$

$$= \sum_{p=1}^{M_{wa}}\sum_{m=1}^{M_{wa}} w^a_{0m} C\left[\frac{f\pi}{L}\frac{p\pi}{L}\frac{m\pi}{L} I^{yys}_g I^{ccc}_{fpm} + \frac{1-\nu}{2}\frac{g\pi}{b}\frac{m\pi}{L}\frac{1}{b} I^{yc}_g I^{css}_{mfp}\right.$$

$$\left. +\nu\frac{f\pi}{L}\left(\frac{1}{b}\right)^2 I^{s}_g I^{css}_{fpm} + \frac{1-\nu}{2}\frac{g\pi}{b}\frac{p\pi}{L}\frac{1}{b} I^{yc}_g I^{css}_{pfm}\right]\dot{w}^a_p \tag{101}$$

$$+\sum_{p=1}^{M_{wa}}\sum_{m=1}^{M_{wb}}\sum_{n=1}^{N_{wb}} w^b_{0mn} C\left[\frac{f\pi}{L}\frac{p\pi}{L}\frac{m\pi}{L} I^{yss}_{qn} I^{ccc}_{fpm} + \frac{1-\nu}{2}\frac{1}{b}\frac{g\pi}{b}\frac{m\pi}{L} I^{cs}_{gn} I^{css}_{mfp}\right.$$

$$\left. +\nu\frac{f\pi}{L}\frac{n\pi}{b}\frac{1}{b} I^{cs}_{ng} I^{css}_{fpm} + \frac{1-\nu}{2}\frac{g\pi}{b}\frac{p\pi}{L}\frac{n\pi}{b} I^{ycc}_{gn} I^{css}_{pfm}\right]\dot{w}^a_p$$

$$\mathbf{K}^{pmL}_{ubwb}\dot{\mathbf{w}}^b = \frac{\partial^2 U^{pmL}}{\partial u^b_{fg} \partial w^b_{pq}}\dot{w}^b_{pq}$$

$$= \sum_{p=1}^{M_{wb}}\sum_{q=1}^{N_{wb}}\sum_{m=1}^{M_{wa}} w^a_{0m} C\left[\frac{f\pi}{L}\frac{p\pi}{L}\frac{m\pi}{L} I^{yss}_{gq} I^{ccc}_{fpm} + \frac{1-\nu}{2}\frac{g\pi}{b}\frac{q\pi}{b}\frac{m\pi}{L} I^{ycc}_{gq} I^{css}_{mfp}\right.$$

$$\left. +\nu\frac{f\pi}{L}\frac{q\pi}{b}\frac{1}{b} I^{cs}_{qg} I^{css}_{fpm} + \frac{1-\nu}{2}\frac{g\pi}{b}\frac{p\pi}{L}\frac{1}{b} I^{cs}_{gq} I^{css}_{pfm}\right]\dot{w}^b_{pq} \tag{102}$$

$$+\sum_{p=1}^{M_{wb}}\sum_{q=1}^{N_{wb}}\sum_{m=1}^{M_{wb}}\sum_{n=1}^{N_{wb}} w^b_{0mn} C\left[\frac{f\pi}{L}\frac{p\pi}{L}\frac{m\pi}{L} I^{ccc}_{fpm} I^{sss}_{gqn} + \frac{1-\nu}{2}\frac{g\pi}{b}\frac{q\pi}{b}\frac{m\pi}{L} I^{css}_{mfp} I^{scc}_{ngq}\right.$$

$$\left. +\nu\frac{f\pi}{L}\frac{q\pi}{b}\frac{n\pi}{b} I^{css}_{fpm} I^{scc}_{gqn} + \frac{1-\nu}{2}\frac{g\pi}{b}\frac{p\pi}{L}\frac{n\pi}{b} I^{scc}_{qgn} I^{css}_{pfm}\right]\dot{w}^b_{pq}$$

$$\begin{aligned}
\mathbf{K}^{pmL}_{ucwa}\dot{\mathbf{w}}^a &= \frac{\partial^2 U^{pmL}}{\partial u^c \partial w^a_p}\dot{w}^a_p \\
&= \sum_{p=1}^{M_{wa}} w^a_{0p} C\left[\frac{1}{L}\left(\frac{p\pi}{L}\right)^2 \frac{Lb}{6} + \nu\frac{1}{L}\frac{1}{b}\frac{L}{2}\right]\dot{w}^a_p \\
&+ \sum_{p=1}^{M_{wawb}}\sum_{n=1}^{N_{wb}} w^b_{0pn} C\left[\frac{1}{L}\left(\frac{p\pi}{L}\right)^2 I^{ys}_n \frac{L}{2}\right]\dot{w}^a_p
\end{aligned} \tag{103}$$

$$\begin{aligned}
\mathbf{K}^{pmL}_{ucwb}\dot{\mathbf{w}}^b &= \frac{\partial^2 U^{pmL}}{\partial u^c \partial w^b_{pq}}\dot{w}^b_{pq} \\
&= \sum_{p=1}^{M_{wawb}}\sum_{q=1}^{N_{wb}} w^a_{0p} C\left[\frac{1}{L}\left(\frac{p\pi}{L}\right)^2 I^{ys}_q \frac{L}{2}\right]\dot{w}^b_{pq} \\
&+ \sum_{p=1}^{M_{wb}}\sum_{q=1}^{N_{wb}} w^b_{0pq} C\left[\frac{1}{L}\left(\frac{p\pi}{L}\right)^2 + \nu\frac{1}{L}\left(\frac{q\pi}{b}\right)^2\right]\frac{Lb}{4}\dot{w}^b_{pq}
\end{aligned} \tag{104}$$

C.1.7 Definition of the $\mathbf{K}^{pmL}_{wu}$-matrix

Due to symmetry, the matrix can be given by

$$\mathbf{K}^{pmL}_{wu} = (\mathbf{K}^{pmL}_{uw})^T \tag{105}$$

where $\mathbf{K}^{pmL}_{uw}$ is given in Section C.1.6. The size of this matrix is $(M_{wa} + M_{wb}N_{wb}) \times (M_{ua} + M_{ub}N_{ub} + 1)$.

C.1.8 Definition of the $\mathbf{K}^{pmL}_{vw}$-matrix

The size of the matrix $\mathbf{K}^{pmL}_{vw}$ is $(M_{va} + M_{vb}N_{vb} + 1) \times (M_{wa} + M_{wb}N_{wb})$. The matrix is a constant contribution and consists of the submatrices given in index notation in the

following expressions

$$\begin{aligned}
\mathbf{K}^{pmL}_{vawa}\dot{\mathbf{w}}^a &= \frac{\partial^2 U^{pmL}}{\partial v^a_f \partial w^a_p}\dot{w}^a_p \\
&= \sum_{p=1}^{M_{wa}}\sum_{m=1}^{M_{wa}} w^a_{0m} C\Bigg[\left(\frac{1}{b}\right)^2 I^{css}_{fpm} - \frac{1-\nu}{2}\frac{f\pi}{L}\frac{p\pi}{L}\frac{1}{b}\frac{b}{3} I^{css}_{pfm} \\
&\qquad + \nu\frac{p\pi}{L}\frac{m\pi}{L}\frac{1}{b}\frac{b}{3} I^{ccc}_{fpm} - \frac{1-\nu}{2}\frac{f\pi}{L}\frac{m\pi}{L}\frac{1}{b}\frac{b}{3} I^{css}_{mfp}\Bigg]\dot{w}^a_p \qquad (106) \\
&\quad + \sum_{p=1}^{M_{wa}}\sum_{m=1}^{M_{wb}}\sum_{n=1}^{N_{wb}} w^b_{0mn} C\Bigg[\nu\frac{p\pi}{L}\frac{m\pi}{L}\frac{1}{b} I^{ys}_n I^{ccc}_{fpm} \\
&\quad - \frac{1-\nu}{2}\frac{f\pi}{L}\frac{p\pi}{L}\frac{n\pi}{b} I^{yyc}_n I^{css}_{pfm} - \frac{1-\nu}{2}\frac{f\pi}{L}\frac{m\pi}{L}\frac{1}{b} I^{ys}_n I^{css}_{mfp}\Bigg]\dot{w}^a_p
\end{aligned}$$

$$\begin{aligned}
\mathbf{K}^{pmL}_{vawb}\dot{\mathbf{w}}^b &= \frac{\partial^2 U^{pmL}}{\partial v^a_f \partial w^b_{pq}}\dot{w}^b_{pq} \\
&= \sum_{p=1}^{M_{wb}}\sum_{q=1}^{N_{wb}}\sum_{m=1}^{M_{wa}} w^a_{0m} C\Bigg[\nu\frac{p\pi}{L}\frac{m\pi}{L}\frac{1}{b} I^{ys}_q I^{ccc}_{fpm} \\
&\qquad - \frac{1-\nu}{2}\frac{f\pi}{L}\frac{p\pi}{L}\frac{1}{b} I^{ys}_q I^{css}_{pfm} - \frac{1-\nu}{2}\frac{f\pi}{L}\frac{q\pi}{b}\frac{m\pi}{L} I^{yyc}_q I^{css}_{mfp}\Bigg]\dot{w}^b_{pq} \qquad (107) \\
&+ \sum_{p=1}^{M_{wb}}\sum_{q=1}^{N_{wb}}\sum_{m=1}^{M_{wb}}\sum_{n=1}^{N_{wb}} w^b_{0mn} C\Bigg[\frac{q\pi}{b}\frac{n\pi}{b}\frac{1}{b}\frac{b}{2}\delta_{qn} I^{css}_{fpm} - \frac{1-\nu}{2}\frac{f\pi}{L}\frac{p\pi}{L}\frac{n\pi}{b} I^{ycs}_{nq} I^{css}_{pfm} \\
&\qquad + \nu\frac{p\pi}{L}\frac{m\pi}{L}\frac{1}{b}\frac{b}{2}\delta_{qn} I^{ccc}_{fpm} - \frac{1-\nu}{2}\frac{f\pi}{L}\frac{q\pi}{b}\frac{m\pi}{L} I^{ycs}_{qn} I^{css}_{mfp}\Bigg]\dot{w}^b_{pq}
\end{aligned}$$

$$\begin{aligned}
\mathbf{K}^{pmL}_{vbwa}\dot{\mathbf{w}}^a &= \frac{\partial^2 U^{pmL}}{\partial v^b_{fg} \partial w^a_p}\dot{w}^a_p \\
&= \sum_{p=1}^{M_{wa}}\sum_{m=1}^{M_{wa}} w^a_{0m} C\Bigg[\frac{1-\nu}{2}\frac{f\pi}{L}\frac{p\pi}{L}\frac{1}{b} I^{ys}_g I^{scc}_{mfp} \\
&\quad + \nu\frac{g\pi}{b}\frac{p\pi}{L}\frac{m\pi}{L} I^{yyc}_g I^{scc}_{fpm} + \frac{1-\nu}{2}\frac{f\pi}{L}\frac{m\pi}{L}\frac{1}{b} I^{ys}_g I^{scc}_{pfm}\Bigg]\dot{w}^a_p \qquad (108) \\
&+ \sum_{p=1}^{M_{wa}}\sum_{m=1}^{M_{wb}}\sum_{n=1}^{N_{wb}} w^b_{0mn} C\Bigg[\frac{g\pi}{b}\frac{n\pi}{b}\frac{1}{b}\frac{b}{2}\delta_{gn} I^{sss}_{fpm} + \frac{1-\nu}{2}\frac{f\pi}{L}\frac{p\pi}{L}\frac{n\pi}{b} I^{ycs}_{ng} I^{scc}_{mfp} \\
&\qquad + \nu\frac{g\pi}{b}\frac{p\pi}{L}\frac{m\pi}{L} I^{ycs}_{gn} I^{scc}_{fpm} + \frac{1-\nu}{2}\frac{f\pi}{L}\frac{m\pi}{L}\frac{1}{b}\frac{b}{2}\delta_{gn} I^{scc}_{pfm}\Bigg]\dot{w}^a_p
\end{aligned}$$

$$\mathbf{K}_{vbwb}^{pmL}\dot{\mathbf{w}}^b = \frac{\partial^2 U^{pmL}}{\partial v_{fg}^b \partial w_{pq}^b}\dot{w}_{pq}^b$$

$$= \sum_{p=1}^{M_{wb}}\sum_{q=1}^{N_{wb}}\sum_{m=1}^{M_{wa}} w_{0m}^a C\left[\frac{g\pi}{b}\frac{q\pi}{b}\frac{1}{b}\frac{b}{2}\delta_{gn}I_{fpm}^{sss} + \frac{1-\nu}{2}\frac{f\pi}{L}\frac{p\pi}{L}\frac{1}{b}\frac{b}{2}\delta_{gn}I_{mfp}^{scc}\right.$$

$$\left. +\nu\frac{g\pi}{b}\frac{p\pi}{L}\frac{m\pi}{L}I_{gq}^{ycs}I_{fpm}^{scc} + \frac{1-\nu}{2}\frac{f\pi}{L}\frac{q\pi}{b}\frac{m\pi}{L}I_{qg}^{ycs}I_{pfm}^{scc}\right]\dot{w}_{pq}^b \tag{109}$$

$$+\sum_{p=1}^{M_{wb}}\sum_{q=1}^{N_{wb}}\sum_{m=1}^{M_{wb}}\sum_{n=1}^{N_{wb}} w_{0mn}^b C\left[\frac{g\pi}{b}\frac{q\pi}{b}\frac{n\pi}{b}I_{fpm}^{sss}I_{gqn}^{ccc} + \frac{1-\nu}{2}\frac{f\pi}{L}\frac{p\pi}{L}\frac{n\pi}{b}I_{mfp}^{scc}I_{ngq}^{css}\right.$$

$$\left. +\nu\frac{g\pi}{b}\frac{p\pi}{L}\frac{m\pi}{L}I_{fpm}^{scc}I_{gqn}^{css} + \frac{1-\nu}{2}\frac{f\pi}{L}\frac{q\pi}{b}\frac{m\pi}{L}I_{pfm}^{scc}I_{qgn}^{css}\right]\dot{w}_{pq}^b$$

$$\mathbf{K}_{vcwa}^{pmL}\dot{\mathbf{w}}^a = \frac{\partial^2 U^{pmL}}{\partial v^c \partial w_p^a}\dot{w}_p^a$$

$$= \sum_{p=1}^{M_{wa}} w_{0p}^a C\left[\left(\frac{1}{b}\right)^2\frac{L}{2} + \nu\left(\frac{p\pi}{L}\right)^2\frac{1}{b}\frac{Lb}{6}\right]\dot{w}_p^a \tag{110}$$

$$+\sum_{p=1}^{M_{wawb}}\sum_{n=1}^{N_{wb}} w_{0pn}^b C\left[\nu\left(\frac{p\pi}{L}\right)^2\frac{1}{b}I_n^{ys}\frac{L}{2}\right]\dot{w}_p^a$$

$$\mathbf{K}_{vcwb}^{pmL}\dot{\mathbf{w}}^b = \frac{\partial^2 U^{pmL}}{\partial v^c \partial w_{pq}^b}\dot{w}_{pq}^b$$

$$= \sum_{p=1}^{M_{wawb}}\sum_{q=1}^{N_{wb}} w_{0p}^a C\left[\nu\frac{1}{b}\left(\frac{p\pi}{L}\right)^2 I_q^{ys}\frac{L}{2}\right]\dot{w}_{pq}^b \tag{111}$$

$$+\sum_{p=1}^{M_{wb}}\sum_{q=1}^{N_{wb}} w_{0pq}^b C\left[\frac{1}{b}\left(\frac{q\pi}{b}\right)^2 + \nu\frac{1}{b}\left(\frac{p\pi}{L}\right)^2\right]\frac{Lb}{4}\dot{w}_{pq}^b$$

C.1.9 Definition of the $\mathbf{K}_{wv}^{pmL}$-matrix

Due to symmetry, the matrix can be given by

$$\mathbf{K}_{wv}^{pmL} = (\mathbf{K}_{vw}^{pmL})^T \tag{112}$$

where $\mathbf{K}_{vw}^{pmL}$ is given in Section C.1.8. The size of this matrix is $(M_{wa} + M_{wb}N_{wb}) \times (M_{va} + M_{vb}N_{vb} + 1)$.

C.1.10 Definition of the $\mathbf{K}_{ww}^{pmL}$-matrix

The matrix $\mathbf{K}_{ww}^{pmL}$ is symmetrical, and the size of this matrix is $(M_{wa} + M_{wb}N_{wb}) \times (M_{wa} + M_{wb}N_{wb})$. The matrix is a constant contribution and consists of the submatrices

given in index notation in the following expressions

$$
\begin{aligned}
&\mathbf{K}^{pmL}_{wawa}\dot{\mathbf{w}}^a = \frac{\partial^2 U^{pmL}}{\partial w^a_f \partial w^a_p}\dot{w}^a_p \\
&= \sum_{p=1}^{M_{wa}}\sum_{m=1}^{M_{wa}}\sum_{r=1}^{M_{wa}} w^a_{0m}w^a_{0r}C\Bigg[\frac{m\pi}{L}\frac{r\pi}{L}\frac{p\pi}{L}\frac{f\pi}{L}\frac{b}{5}I^{cccc}_{pfmr} + \frac{1-\nu}{2}\frac{m\pi}{L}\frac{r\pi}{L}\left(\frac{1}{b}\right)^2\frac{b}{3}I^{sscc}_{pfmr} \\
&\qquad + \left(\frac{1}{b}\right)^3 I^{ssss}_{pfmr} + \frac{1-\nu}{2}\left(\frac{1}{b}\right)^2\frac{p\pi}{L}\frac{f\pi}{L}\frac{b}{3}I^{sscc}_{mrpf} \\
&\qquad + \frac{1+\nu}{2}\frac{m\pi}{L}\frac{p\pi}{L}\left(\frac{1}{b}\right)^2\frac{b}{3}I^{sscc}_{mrpf} + \frac{1+\nu}{2}\frac{m\pi}{L}\frac{f\pi}{L}\left(\frac{1}{b}\right)^2\frac{b}{3}I^{sscc}_{prfm}\Bigg]\dot{w}^a_p \\
&+ \sum_{p=1}^{M_{wa}}\sum_{m=1}^{M_{wb}}\sum_{n=1}^{N_{wb}}\sum_{r=1}^{M_{wa}} w^b_{0mn}w^a_{0r}C\Bigg[2\frac{m\pi}{L}\frac{r\pi}{L}\frac{p\pi}{L}\frac{f\pi}{L}I^{yyys}_{n}I^{cccc}_{pfmr} \\
&\qquad + (1-\nu)\frac{m\pi}{L}\frac{r\pi}{L}\left(\frac{1}{b}\right)^2 I^{ys}_{n}I^{sscc}_{pfmr} + (1-\nu)\frac{n\pi}{b}\frac{p\pi}{L}\frac{f\pi}{L}\frac{1}{b}I^{yyc}_{n}I^{sscc}_{mrpf} \\
&\qquad + \frac{1+\nu}{2}\frac{r\pi}{L}\frac{n\pi}{b}\frac{p\pi}{L}\frac{1}{b}I^{yyc}_{n}I^{sscc}_{fmpr} + \frac{1+\nu}{2}\frac{m\pi}{L}\frac{p\pi}{L}\left(\frac{1}{b}\right)^2 I^{ys}_{n}I^{sscc}_{frmp} \\
&\qquad + \frac{1+\nu}{2}\frac{r\pi}{L}\frac{n\pi}{b}\frac{f\pi}{L}\frac{1}{b}I^{yyc}_{n}I^{sscc}_{pmfr} + \frac{1+\nu}{2}\frac{m\pi}{L}\frac{f\pi}{L}\left(\frac{1}{b}\right)^2 I^{ys}_{n}I^{sscc}_{prfm}\Bigg]\dot{w}^a_p \\
&+ \sum_{p=1}^{M_{wa}}\sum_{m=1}^{M_{wb}}\sum_{n=1}^{N_{wb}}\sum_{r=1}^{M_{wa}}\sum_{s=1}^{N_{wb}} w^b_{0mn}w^b_{0rs}C\Bigg[\frac{m\pi}{L}\frac{r\pi}{L}\frac{p\pi}{L}\frac{f\pi}{L}I^{yyss}_{ns}I^{cccc}_{pfmr} + \frac{1-\nu}{2}\frac{m\pi}{L}\frac{r\pi}{L}\left(\frac{1}{b}\right)^2\frac{b}{2}\delta_{ns}I^{sscc}_{pfmr} \\
&\qquad + \frac{n\pi}{b}\frac{s\pi}{b}\left(\frac{1}{b}\right)^2\frac{b}{2}\delta_{ns}I^{ssss}_{pfmr} + \frac{1-\nu}{2}\frac{n\pi}{b}\frac{s\pi}{b}\frac{p\pi}{L}\frac{f\pi}{L}I^{yycc}_{ns}I^{sscc}_{mrpf} \\
&\qquad + \frac{1+\nu}{2}\frac{m\pi}{L}\frac{s\pi}{b}\frac{p\pi}{L}\frac{1}{b}I^{ycs}_{sn}I^{sscc}_{frmp} + \frac{1+\nu}{2}\frac{m\pi}{L}\frac{s\pi}{b}\frac{f\pi}{L}\frac{1}{b}I^{ycs}_{sn}I^{sscc}_{prfm}\Bigg]\dot{w}^a_p
\end{aligned}
\tag{113}
$$

$$
\begin{aligned}
\mathbf{K}^{pmL}_{wawb}\dot{\mathbf{w}}^b =& \frac{\partial^2 U^{pmL}}{\partial w^a_f \partial w^b_{pq}}\dot{w}^b_{pq} \\
=& \sum_{p=1}^{M_{wb}}\sum_{q=1}^{N_{wb}}\sum_{m=1}^{M_{wa}}\sum_{r=1}^{M_{wa}} w^a_{0m}w^a_{0r}C\Bigg[\frac{m\pi}{L}\frac{r\pi}{L}\frac{p\pi}{L}\frac{f\pi}{L}I^{yyys}_{q}I^{cccc}_{fpmr} \\
&+\frac{1-\nu}{2}\frac{m\pi}{L}\frac{r\pi}{L}\frac{q\pi}{b}\frac{1}{b}I^{yyc}_{q}I^{sscc}_{fpmr}+\frac{1-\nu}{2}\left(\frac{1}{b}\right)^2\frac{f\pi}{L}\frac{p\pi}{L}I^{ys}_{q}I^{sscc}_{mrfp} \\
&+\frac{1+\nu}{2}\frac{m\pi}{L}\frac{f\pi}{L}\frac{q\pi}{b}I^{yyc}_{q}I^{sscc}_{prfm}+\frac{1+\nu}{2}\frac{m\pi}{L}\frac{p\pi}{L}\left(\frac{1}{b}\right)^2 I^{ys}_{q}I^{sscc}_{frpm}\Bigg]\dot{w}^b_{pq} \\
+\sum_{p=1}^{M_{wb}}\sum_{q=1}^{N_{wb}}\sum_{m=1}^{M_{wb}}\sum_{n=1}^{N_{wb}}\sum_{r=1}^{M_{wa}} & w^b_{0mn}w^a_{0r}C\Bigg[2\frac{m\pi}{L}\frac{r\pi}{L}\frac{p\pi}{L}\frac{f\pi}{L}I^{yyss}_{qn}I^{cccc}_{fpmr}+(1-\nu)\frac{m\pi}{L}\frac{r\pi}{L}\frac{q\pi}{b}\frac{1}{b}I^{ycs}_{qn}I^{sscc}_{fpmr} \\
&2\left(\frac{1}{b}\right)^2\frac{n\pi}{b}\frac{q\pi}{b}\frac{b}{2}\delta_{qn}I^{ssss}_{fpmr}+(1-\nu)\frac{n\pi}{b}\frac{f\pi}{L}\frac{p\pi}{L}\frac{1}{b}I^{ycs}_{nq}I^{sscc}_{mrfp} \\
&+\frac{1+\nu}{2}\frac{r\pi}{L}\frac{n\pi}{b}\frac{f\pi}{L}\frac{q\pi}{b}I^{yycc}_{qn}I^{sscc}_{pmfr}+\frac{1+\nu}{2}\frac{r\pi}{L}\frac{n\pi}{b}\frac{p\pi}{L}\frac{1}{b}I^{ycs}_{nq}I^{sscc}_{fmpr} \\
&+\frac{1+\nu}{2}\frac{m\pi}{L}\frac{f\pi}{L}\frac{q\pi}{b}\frac{1}{b}I^{ycs}_{qn}I^{sscc}_{prfm}+\frac{1+\nu}{2}\frac{m\pi}{L}\frac{p\pi}{L}\left(\frac{1}{b}\right)^2\frac{b}{2}\delta_{qn}I^{sscc}_{frpm}\Bigg]\dot{w}^b_{pq} \\
+\sum_{p=1}^{M_{wb}}\sum_{q=1}^{N_{wb}}\sum_{m=1}^{M_{wb}}\sum_{n=1}^{N_{wb}}\sum_{r=1}^{M_{wa}}\sum_{s=1}^{N_{wb}} & w^b_{0mn}w^b_{0rs}C\Bigg[\frac{m\pi}{L}\frac{r\pi}{L}\frac{p\pi}{L}\frac{f\pi}{L}I^{yyss}_{qns}I^{cccc}_{fpmr}+\frac{1-\nu}{2}\frac{m\pi}{L}\frac{r\pi}{L}\frac{q\pi}{b}\frac{1}{b}I^{css}_{qns}I^{sscc}_{fpmr} \\
&+\frac{n\pi}{b}\frac{s\pi}{b}\frac{q\pi}{b}\frac{1}{b}I^{ccc}_{qns}I^{ssss}_{pfmr}+\frac{1-\nu}{2}\frac{n\pi}{b}\frac{s\pi}{b}\frac{p\pi}{L}\frac{f\pi}{L}I^{yscc}_{qns}I^{sscc}_{mrpf} \\
&+\frac{1+\nu}{2}\frac{m\pi}{L}\frac{s\pi}{b}\frac{f\pi}{L}\frac{q\pi}{b}I^{yscc}_{nqs}I^{sscc}_{prfm}+\frac{1+\nu}{2}\frac{m\pi}{L}\frac{s\pi}{b}\frac{p\pi}{L}\frac{1}{b}I^{css}_{sqn}I^{sscc}_{frpm}\Bigg]\dot{w}^b_{pq}
\end{aligned}
\tag{114}
$$

$$
\mathbf{K}^{pmL}_{wbwa} = (\mathbf{K}^{pmL}_{wawb})^T \tag{115}
$$

$$
\begin{aligned}
\mathbf{K}^{pmL}_{wbwb}\dot{\mathbf{w}}^b =& \frac{\partial^2 U^{pmL}}{\partial w^b_{fg}\partial w^b_{pq}}\dot{w}^b_{pq} \\
=& \sum_{p=1}^{M_{wb}}\sum_{q=1}^{N_{wb}}\sum_{m=1}^{M_{wa}}\sum_{r=1}^{M_{wa}} w^a_{0m}w^a_{0r}C\Bigg[\frac{m\pi}{L}\frac{r\pi}{L}\frac{p\pi}{L}\frac{f\pi}{L}I^{yyss}_{qg}I^{cccc}_{fpmr} \\
&+\frac{1-\nu}{2}\frac{m\pi}{L}\frac{r\pi}{L}\frac{q\pi}{b}\frac{g\pi}{b}I^{yycc}_{qg}I^{sscc}_{fpmr} \\
&+\left(\frac{1}{b}\right)^2\left(\frac{q\pi}{b}\right)^2\frac{b}{2}\delta_{qg}I^{ssss}_{pfmr}+\frac{1-\nu}{2}\left(\frac{1}{b}\right)^2\frac{p\pi}{L}\frac{f\pi}{L}\frac{b}{2}\delta_{qg}I^{sscc}_{mrfp} \\
&+\frac{1+\nu}{2}\frac{m\pi}{L}\frac{p\pi}{L}\frac{g\pi}{b}\frac{1}{b}I^{ycs}_{gq}I^{sscc}_{frpm}+\frac{1+\nu}{2}\frac{m\pi}{L}\frac{f\pi}{L}\frac{q\pi}{b}\frac{1}{b}I^{ycs}_{qg}I^{sscc}_{prfm}\Bigg]\dot{w}^b_{pq} \\
&+\sum_{p=1}^{M_{wb}}\sum_{q=1}^{N_{wb}}\sum_{m=1}^{M_{wb}}\sum_{n=1}^{N_{wb}}\sum_{r=1}^{M_{wa}} w^b_{0mn}w^a_{0r}C\Bigg[2\frac{m\pi}{L}\frac{r\pi}{L}\frac{p\pi}{L}\frac{f\pi}{L}I^{ysss}_{qgn}I^{cccc}_{fpmr} \\
&+(1-\nu)\frac{m\pi}{L}\frac{r\pi}{L}\frac{q\pi}{b}\frac{g\pi}{b}I^{yscc}_{nqg}I^{sscc}_{fpmr} \\
&+2\frac{n\pi}{b}\frac{q\pi}{b}\frac{g\pi}{b}\frac{1}{b}I^{ccc}_{qgn}I^{ssss}_{fpmr}+(1-\nu)\frac{n\pi}{b}\frac{f\pi}{L}\frac{p\pi}{L}\frac{1}{b}I^{css}_{nqg}I^{sscc}_{mrfp} \\
&+\frac{1+\nu}{2}\frac{r\pi}{L}\frac{n\pi}{b}\frac{p\pi}{L}\frac{g\pi}{b}I^{yscc}_{qgn}I^{sscc}_{fmpr}+\frac{1+\nu}{2}\frac{m\pi}{L}\frac{p\pi}{L}\frac{g\pi}{b}\frac{1}{b}I^{css}_{gqn}I^{sscc}_{frpm} \\
&+\frac{1+\nu}{2}\frac{r\pi}{L}\frac{n\pi}{b}\frac{f\pi}{L}\frac{q\pi}{b}I^{yscc}_{gqn}I^{sscc}_{pmfr}+\frac{1+\nu}{2}\frac{m\pi}{L}\frac{f\pi}{L}\frac{q\pi}{b}\frac{1}{b}I^{css}_{qgn}I^{sscc}_{prfm}\Bigg]\dot{w}^b_{pq} \\
&+\sum_{p=1}^{M_{wb}}\sum_{q=1}^{N_{wb}}\sum_{m=1}^{M_{wb}}\sum_{n=1}^{N_{wb}}\sum_{r=1}^{M_{wa}}\sum_{s=1}^{N_{wb}} w^b_{0mn}w^b_{0rs}C\Bigg[\frac{m\pi}{L}\frac{r\pi}{L}\frac{p\pi}{L}\frac{f\pi}{L}I^{ssss}_{qgns}I^{cccc}_{fpmr} \\
&+\frac{1-\nu}{2}\frac{m\pi}{L}\frac{r\pi}{L}\frac{q\pi}{b}\frac{g\pi}{b}I^{sscc}_{pfmr}I^{sscc}_{nsqg} \\
&+\frac{n\pi}{b}\frac{s\pi}{b}\frac{q\pi}{b}\frac{g\pi}{b}I^{ssss}_{pfmr}I^{cccc}_{qgns}+\frac{1-\nu}{2}\frac{n\pi}{b}\frac{s\pi}{b}\frac{p\pi}{L}\frac{f\pi}{L}I^{sscc}_{mrpf}I^{sscc}_{qgns} \\
&+\frac{1+\nu}{2}\frac{m\pi}{L}\frac{s\pi}{b}\frac{p\pi}{L}\frac{g\pi}{b}I^{sscc}_{frpm}I^{sscc}_{qngs}+\frac{1+\nu}{2}\frac{m\pi}{L}\frac{s\pi}{b}\frac{f\pi}{L}\frac{q\pi}{b}I^{sscc}_{prfm}I^{sscc}_{gnqs}\Bigg]\dot{w}^b_{pq}
\end{aligned}
\tag{116}
$$

C.1.11 Definition of the $\mathbf{K}^{pmNL}_{uw}$-matrix

The size of the matrix $\mathbf{K}^{pmNL}_{uw}$ is $(M_{ua}+M_{ub}N_{ub}+1)\times(M_{wa}+M_{wb}N_{wb})$. The matrix is a nonlinear contribution and is dependent of the displacement amplitudes. It consists of

the submatrices given in index notation in the following expressions

$$\begin{aligned}
\mathbf{K}^{pmNL}_{uawa}\dot{\mathbf{w}}^a &= \frac{\partial^2 U^{pmNL}}{\partial u^a_f \partial w^a_p}\dot{w}^a_p \\
&= \sum_{p=1}^{M_{wa}}\sum_{m=1}^{M_{wa}} w^a_m C\left[\frac{f\pi}{L}\frac{p\pi}{L}\frac{m\pi}{L}\frac{b}{4}I^{ccc}_{fpm} + \frac{1-\nu}{2}\left(\frac{1}{b}\right)^2\frac{b}{2}\frac{m\pi}{L}I^{css}_{mfp}\right. \\
&\qquad \left. +\nu\frac{f\pi}{L}\left(\frac{1}{b}\right)^2\frac{b}{2}I^{css}_{fpm} + \frac{1-\nu}{2}\frac{p\pi}{L}\left(\frac{1}{b}\right)^2\frac{b}{2}I^{css}_{pfm}\right]\dot{w}^a_p \qquad (117)\\
&+ \sum_{p=1}^{M_{wa}}\sum_{m=1}^{M_{wb}}\sum_{n=1}^{N_{wb}} w^b_{mn} C\left[\frac{f\pi}{L}\frac{p\pi}{L}\frac{m\pi}{L}I^{yys}_{n}I^{ccc}_{fpm} + \frac{1-\nu}{2}\left(\frac{1}{b}\right)^2\frac{m\pi}{L}I^{s}_{n}I^{css}_{mfp}\right. \\
&\qquad \left. +\nu\frac{f\pi}{L}\frac{1}{b}\frac{n\pi}{b}I^{yc}_{n}I^{css}_{fpm} + \frac{1-\nu}{2}\frac{p\pi}{L}\frac{n\pi}{b}\frac{1}{b}I^{yc}_{n}I^{css}_{pfm}\right]\dot{w}^a_p
\end{aligned}$$

$$\begin{aligned}
\mathbf{K}^{pmNL}_{uawb}\dot{\mathbf{w}}^b &= \frac{\partial^2 U^{pmNL}}{\partial u^a_f \partial w^b_{pq}}\dot{w}^b_{pq} \\
&= \sum_{p=1}^{M_{wb}}\sum_{q=1}^{N_{wb}}\sum_{m=1}^{M_{wa}} w^a_m C\left[\frac{f\pi}{L}\frac{p\pi}{L}\frac{m\pi}{L}I^{yys}_{q}I^{ccc}_{fpm} + \frac{1-\nu}{2}\frac{q\pi}{b}\frac{m\pi}{L}\frac{1}{b}I^{yc}_{q}I^{css}_{mfp}\right. \\
&\qquad \left. +\nu\frac{f\pi}{L}\frac{q\pi}{b}\frac{1}{b}I^{yc}_{q}I^{css}_{fpm} + \frac{1-\nu}{2}\left(\frac{1}{b}\right)^2\frac{p\pi}{L}I^{s}_{q}I^{css}_{pfm}\right]\dot{w}^b_{pq} \qquad (118)\\
&+ \sum_{p=1}^{M_{wb}}\sum_{q=1}^{N_{wb}}\sum_{m=1}^{M_{wb}}\sum_{n=1}^{N_{wb}} w^b_{mn} C\left[\frac{f\pi}{L}\frac{p\pi}{L}\frac{m\pi}{L}I^{yss}_{qn}I^{ccc}_{fpm} + \frac{1-\nu}{2}\frac{1}{b}\frac{q\pi}{b}\frac{m\pi}{L}I^{cs}_{qn}I^{css}_{mfp}\right. \\
&\qquad \left. +\nu\frac{f\pi}{L}\frac{q\pi}{b}\frac{n\pi}{b}I^{ycc}_{qn}I^{css}_{fpm} + \frac{1-\nu}{2}\frac{p\pi}{L}\frac{n\pi}{b}\frac{1}{b}I^{cs}_{nq}I^{css}_{pfm}\right]\dot{w}^b_{pq}
\end{aligned}$$

$$\begin{aligned}
\mathbf{K}^{pmNL}_{ubwa}\dot{\mathbf{w}}^a &= \frac{\partial^2 U^{pmNL}}{\partial u^b_{fg} \partial w^a_p}\dot{w}^a_p \\
&= \sum_{p=1}^{M_{wa}}\sum_{m=1}^{M_{wa}} w^a_m C\left[\frac{f\pi}{L}\frac{p\pi}{L}\frac{m\pi}{L}I^{yys}_{g}I^{ccc}_{fpm} + \frac{1-\nu}{2}\frac{g\pi}{b}\frac{m\pi}{L}\frac{1}{b}I^{yc}_{g}I^{css}_{mfp}\right. \\
&\qquad \left. +\nu\frac{f\pi}{L}\left(\frac{1}{b}\right)^2 I^{s}_{g}I^{css}_{fpm} + \frac{1-\nu}{2}\frac{g\pi}{b}\frac{p\pi}{L}\frac{1}{b}I^{yc}_{g}I^{css}_{pfm}\right]\dot{w}^a_p \qquad (119)\\
&+ \sum_{p=1}^{M_{wa}}\sum_{m=1}^{M_{wb}}\sum_{n=1}^{N_{wb}} w^b_{mn} C\left[\frac{f\pi}{L}\frac{p\pi}{L}\frac{m\pi}{L}I^{yss}_{gn}I^{ccc}_{fpm} + \frac{1-\nu}{2}\frac{1}{b}\frac{g\pi}{b}\frac{m\pi}{L}I^{cs}_{gn}I^{css}_{mfp}\right. \\
&\qquad \left. +\nu\frac{f\pi}{L}\frac{n\pi}{b}\frac{1}{b}I^{cs}_{ng}I^{css}_{fpm} + \frac{1-\nu}{2}\frac{g\pi}{b}\frac{p\pi}{L}\frac{n\pi}{b}I^{ycc}_{gn}I^{css}_{pfm}\right]\dot{w}^a_p
\end{aligned}$$

$$\mathbf{K}_{ubwb}^{pmNL}\dot{\mathbf{w}}^b = \frac{\partial^2 U^{pmNL}}{\partial u_{fg}^b \partial w_{pq}^b}\dot{w}_{pq}^b$$

$$= \sum_{p=1}^{M_{wb}}\sum_{q=1}^{N_{wb}}\sum_{m=1}^{M_{wa}} w_m^a C\left[\frac{f\pi}{L}\frac{p\pi}{L}\frac{m\pi}{L}I_{gq}^{yss}I_{fpm}^{ccc} + \frac{1-\nu}{2}\frac{g\pi}{b}\frac{q\pi}{b}\frac{m\pi}{L}I_{gq}^{ycc}I_{mfp}^{css}\right.$$

$$\left. +\nu\frac{f\pi}{L}\frac{q\pi}{b}\frac{1}{b}I_{qg}^{cs}I_{fpm}^{css} + \frac{1-\nu}{2}\frac{g\pi}{b}\frac{p\pi}{L}\frac{1}{b}I_{gq}^{cs}I_{pfm}^{css}\right]\dot{w}_{pq}^b \tag{120}$$

$$+\sum_{p=1}^{M_{wb}}\sum_{q=1}^{N_{wb}}\sum_{m=1}^{M_{wb}}\sum_{n=1}^{N_{wb}} w_{mn}^b C\left[\frac{f\pi}{L}\frac{p\pi}{L}\frac{m\pi}{L}I_{fpm}^{ccc}I_{gqn}^{sss} + \frac{1-\nu}{2}\frac{g\pi}{b}\frac{q\pi}{b}\frac{m\pi}{L}I_{mfp}^{css}I_{ngq}^{scc}\right.$$

$$\left. +\nu\frac{f\pi}{L}\frac{q\pi}{b}\frac{n\pi}{b}I_{fpm}^{css}I_{gqn}^{scc} + \frac{1-\nu}{2}\frac{g\pi}{b}\frac{p\pi}{L}\frac{n\pi}{b}I_{qgn}^{scc}I_{pfm}^{css}\right]\dot{w}_{pq}^b$$

$$\mathbf{K}_{ucwa}^{pmNL}\dot{\mathbf{w}}^a = \frac{\partial^2 U^{pmNL}}{\partial u^c \partial w_p^a}\dot{w}_p^a$$

$$= \sum_{p=1}^{M_{wa}} w_p^a C\left[\frac{1}{L}\left(\frac{p\pi}{L}\right)^2\frac{Lb}{6} + \nu\frac{1}{L}\frac{1}{b}\frac{L}{2}\right]\dot{w}_p^a \tag{121}$$

$$+\sum_{p=1}^{M_{wawb}}\sum_{n=1}^{N_{wb}} w_{pn}^b C\left[\frac{1}{L}\left(\frac{p\pi}{L}\right)^2 I_n^{ys}\frac{L}{2}\right]\dot{w}_p^a$$

$$\mathbf{K}_{ucwb}^{pmNL}\dot{\mathbf{w}}^b = \frac{\partial^2 U^{pmNL}}{\partial u^c \partial w_{pq}^b}\dot{w}_{pq}^b$$

$$= \sum_{p=1}^{M_{wawb}}\sum_{q=1}^{N_{wb}} w_p^a C\left[\frac{1}{L}\left(\frac{p\pi}{L}\right)^2 I_q^{ys}\frac{L}{2}\right]\dot{w}_{pq}^b \tag{122}$$

$$+\sum_{p=1}^{M_{wb}}\sum_{q=1}^{N_{wb}} w_{pq}^b C\left[\frac{1}{L}\left(\frac{p\pi}{L}\right)^2 + \nu\frac{1}{L}\left(\frac{q\pi}{b}\right)^2\right]\frac{Lb}{4}\dot{w}_{pq}^b$$

C.1.12 Definition of the $\mathbf{K}_{wu}^{pmNL}$-matrix

Due to symmetry, the matrix can be given by

$$\mathbf{K}_{wu}^{pmNL} = (\mathbf{K}_{uw}^{pmNL})^T \tag{123}$$

where $\mathbf{K}_{uw}^{pmNL}$ is given in Section *C*.1.11. The size of this matrix is $(M_{wa} + M_{wb}N_{wb}) \times (M_{ua} + M_{ub}N_{ub} + 1)$.

C.1.13 Definition of the $\mathbf{K}_{vw}^{pmNL}$-matrix

The size of the matrix $\mathbf{K}_{vw}^{pmNL}$ is $(M_{va} + M_{vb}N_{vb} + 1) \times (M_{wa} + M_{wb}N_{wb})$. The matrix is a nonlinear contribution and is dependent of the displacement amplitudes. It consists of

the submatrices given in index notation in the following expressions

$$\begin{aligned}
\mathbf{K}^{pmNL}_{vawa}\dot{\mathbf{w}}^a &= \frac{\partial^2 U^{pmNL}}{\partial v^a_f \partial w^a_p}\dot{w}^a_p \\
&= \sum_{p=1}^{M_{wa}}\sum_{m=1}^{M_{wa}} w^a_m C\left[\left(\frac{1}{b}\right)^2 I^{css}_{fpm} - \frac{1-\nu}{2}\frac{f\pi}{L}\frac{p\pi}{L}\frac{1}{b}\frac{b}{3}I^{css}_{pfm}\right. \\
&\qquad \left. +\nu\frac{p\pi}{L}\frac{m\pi}{L}\frac{1}{b}\frac{b}{3}I^{ccc}_{fpm} - \frac{1-\nu}{2}\frac{f\pi}{L}\frac{m\pi}{L}\frac{1}{b}\frac{b}{3}I^{css}_{mfp}\right]\dot{w}^a_p \\
&\quad + \sum_{p=1}^{M_{wa}}\sum_{m=1}^{M_{wb}}\sum_{n=1}^{N_{wb}} w^b_{mn} C\left[\nu\frac{p\pi}{L}\frac{m\pi}{L}\frac{1}{b}I^{ys}_n I^{ccc}_{fpm}\right. \\
&\qquad \left. -\frac{1-\nu}{2}\frac{f\pi}{L}\frac{p\pi}{L}\frac{n\pi}{b}I^{yyc}_n I^{css}_{pfm} - \frac{1-\nu}{2}\frac{f\pi}{L}\frac{m\pi}{L}\frac{1}{b}I^{ys}_n I^{css}_{mfp}\right]\dot{w}^a_p
\end{aligned} \tag{124}$$

$$\begin{aligned}
\mathbf{K}^{pmNL}_{vawb}\dot{\mathbf{w}}^b &= \frac{\partial^2 U^{pmNL}}{\partial v^a_f \partial w^b_{pq}}\dot{w}^b_{pq} \\
&= \sum_{p=1}^{M_{wb}}\sum_{q=1}^{N_{wb}}\sum_{m=1}^{M_{wa}} w^a_m C\left[\nu\frac{p\pi}{L}\frac{m\pi}{L}\frac{1}{b}I^{ys}_q I^{ccc}_{fpm}\right. \\
&\qquad \left. -\frac{1-\nu}{2}\frac{f\pi}{L}\frac{p\pi}{L}\frac{1}{b}I^{ys}_q I^{css}_{pfm} - \frac{1-\nu}{2}\frac{f\pi}{L}\frac{q\pi}{b}\frac{m\pi}{L}I^{yyc}_q I^{css}_{mfp}\right]\dot{w}^b_{pq} \\
&\quad + \sum_{p=1}^{M_{wb}}\sum_{q=1}^{N_{wb}}\sum_{m=1}^{M_{wb}}\sum_{n=1}^{N_{wb}} w^b_{mn} C\left[\frac{q\pi}{b}\frac{n\pi}{b}\frac{1}{b}\frac{b}{2}\delta_{qn}I^{css}_{fpm} - \frac{1-\nu}{2}\frac{f\pi}{L}\frac{p\pi}{L}\frac{n\pi}{b}I^{ycs}_{nq}I^{css}_{pfm}\right. \\
&\qquad \left. +\nu\frac{p\pi}{L}\frac{m\pi}{L}\frac{1}{b}\frac{b}{2}\delta_{qn}I^{ccc}_{fpm} - \frac{1-\nu}{2}\frac{f\pi}{L}\frac{q\pi}{b}\frac{m\pi}{L}I^{ycs}_{qn}I^{css}_{mfp}\right]\dot{w}^b_{pq}
\end{aligned} \tag{125}$$

$$\begin{aligned}
\mathbf{K}^{pmNL}_{vbwa}\dot{\mathbf{w}}^a &= \frac{\partial^2 U^{pmNL}}{\partial v^b_{fg} \partial w^a_p}\dot{w}^a_p \\
&= \sum_{p=1}^{M_{wa}}\sum_{m=1}^{M_{wa}} w^a_m C\left[\frac{1-\nu}{2}\frac{f\pi}{L}\frac{p\pi}{L}\frac{1}{b}I^{ys}_g I^{scc}_{mfp}\right. \\
&\qquad \left. +\nu\frac{g\pi}{b}\frac{p\pi}{L}\frac{m\pi}{L}I^{yyc}_g I^{scc}_{fpm} + \frac{1-\nu}{2}\frac{f\pi}{L}\frac{m\pi}{L}\frac{1}{b}I^{ys}_g I^{scc}_{pfm}\right]\dot{w}^a_p \\
&\quad + \sum_{p=1}^{M_{wa}}\sum_{m=1}^{M_{wb}}\sum_{n=1}^{N_{wb}} w^b_{mn} C\left[\frac{g\pi}{b}\frac{n\pi}{b}\frac{1}{b}\frac{b}{2}\delta_{gn}I^{sss}_{fpm} + \frac{1-\nu}{2}\frac{f\pi}{L}\frac{p\pi}{L}\frac{n\pi}{b}I^{ycs}_{ng}I^{scc}_{mfp}\right. \\
&\qquad \left. +\nu\frac{g\pi}{b}\frac{p\pi}{L}\frac{m\pi}{L}I^{ycs}_{gn}I^{scc}_{fpm} + \frac{1-\nu}{2}\frac{f\pi}{L}\frac{m\pi}{L}\frac{1}{b}\frac{b}{2}\delta_{gn}I^{scc}_{pfm}\right]\dot{w}^a_p
\end{aligned} \tag{126}$$

$$\mathbf{K}_{vbwb}^{pmNL}\dot{\mathbf{w}}^b = \frac{\partial^2 U^{pmNL}}{\partial v_{fg}^b \partial w_{pq}^b}\dot{w}_{pq}^b$$

$$= \sum_{p=1}^{M_{wb}}\sum_{q=1}^{N_{wb}}\sum_{m=1}^{M_{wa}} w_m^a C\left[\frac{g\pi}{b}\frac{q\pi}{b}\frac{1}{b}\frac{b}{2}\delta_{gn}I_{fpm}^{sss} + \frac{1-\nu}{2}\frac{f\pi}{L}\frac{p\pi}{L}\frac{1}{b}\frac{b}{2}\delta_{gn}I_{mfp}^{scc}\right.$$

$$\left. +\nu\frac{g\pi}{b}\frac{p\pi}{L}\frac{m\pi}{L}I_{gq}^{ycs}I_{fpm}^{scc} + \frac{1-\nu}{2}\frac{f\pi}{L}\frac{q\pi}{b}\frac{m\pi}{L}I_{qg}^{ycs}I_{pfm}^{scc}\right]\dot{w}_{pq}^b \tag{127}$$

$$+\sum_{p=1}^{M_{wb}}\sum_{q=1}^{N_{wb}}\sum_{m=1}^{M_{wb}}\sum_{n=1}^{N_{wb}} w_{mn}^b C\left[\frac{g\pi}{b}\frac{q\pi}{b}\frac{n\pi}{b}I_{fpm}^{sss}I_{gqn}^{ccc} + \frac{1-\nu}{2}\frac{f\pi}{L}\frac{p\pi}{L}\frac{n\pi}{b}I_{mfp}^{scc}I_{ngq}^{css}\right.$$

$$\left. +\nu\frac{g\pi}{b}\frac{p\pi}{L}\frac{m\pi}{L}I_{fpm}^{scc}I_{gqn}^{css} + \frac{1-\nu}{2}\frac{f\pi}{L}\frac{q\pi}{b}\frac{m\pi}{L}I_{pfm}^{scc}I_{qgn}^{css}\right]\dot{w}_{pq}^b$$

$$\mathbf{K}_{vcwa}^{pmNL}\dot{\mathbf{w}}^a = \frac{\partial^2 U^{pmNL}}{\partial v^c \partial w_p^a}\dot{w}_p^a$$

$$= \sum_{p=1}^{M_{wa}} w_p^a C\left[\left(\frac{1}{b}\right)^2\frac{L}{2} + \nu\left(\frac{p\pi}{L}\right)^2\frac{1}{b}\frac{Lb}{6}\right]\dot{w}_p^a \tag{128}$$

$$+\sum_{p=1}^{M_{wawb}}\sum_{n=1}^{N_{wb}} w_{pn}^b C\left[\nu\left(\frac{p\pi}{L}\right)^2\frac{1}{b}I_n^{ys}\frac{L}{2}\right]\dot{w}_p^a$$

$$\mathbf{K}_{vcwb}^{pmNL}\dot{\mathbf{w}}^b = \frac{\partial^2 U^{pmNL}}{\partial v^c \partial w_{pq}^b}\dot{w}_{pq}^b$$

$$= \sum_{p=1}^{M_{wawb}}\sum_{q=1}^{N_{wb}} w_p^a C\left[\nu\frac{1}{b}\left(\frac{p\pi}{L}\right)^2 I_q^{ys}\frac{L}{2}\right]\dot{w}_{pq}^b \tag{129}$$

$$+\sum_{p=1}^{M_{wb}}\sum_{q=1}^{N_{wb}} w_{pq}^b C\left[\frac{1}{b}\left(\frac{q\pi}{b}\right)^2 + \nu\frac{1}{b}\left(\frac{p\pi}{L}\right)^2\right]\frac{Lb}{4}\dot{w}_{pq}^b$$

C.1.14 Definition of the $\mathbf{K}_{wv}^{pmNL}$-matrix

Due to symmetry, the matrix can be given by

$$\mathbf{K}_{wv}^{pmNL} = (\mathbf{K}_{vw}^{pmNL})^T \tag{130}$$

where $\mathbf{K}_{vw}^{pmNL}$ is given in Section *C*.1.13. The size of this matrix is $(M_{wa} + M_{wb}N_{wb}) \times (M_{va} + M_{vb}N_{vb} + 1)$.

C.1.15 Definition of the $\mathbf{K}_{ww}^{pmNL}$-matrix

The matrix $\mathbf{K}_{ww}^{pmNL}$ is symmetrical, and the size of this matrix is $(M_{wa} + M_{wb}N_{wb}) \times (M_{wa} + M_{wb}N_{wb})$. The matrix is a nonlinear contribution and is dependent of the dis-

placement amplitudes. It consists of the submatrices given in index notation in the following expressions

$$
\begin{aligned}
\mathbf{K}^{pmNL}_{wawa}\dot{\mathbf{w}}^a &= \frac{\partial^2 U^{pmNL}}{\partial w^a_f \partial w^a_p}\dot{w}^a_p \\
&= \sum_{p=1}^{M_{wa}}\sum_{m=1}^{M_{wa}}\sum_{r=1}^{M_{wa}}(w^a_m w^a_r + 2w^a_m w^a_{0r})C\left[\frac{3}{10}\frac{p\pi}{L}\frac{f\pi}{L}\frac{m\pi}{L}\frac{r\pi}{L}\,b\,I^{cccc}_{pfmr} + \frac{3}{2}\left(\frac{1}{b}\right)^3 I^{ssss}_{pfmr}\right. \\
&\quad + \frac{1}{6}\frac{f\pi}{L}\frac{p\pi}{L}\frac{1}{b}I^{sscc}_{mrfp} + \frac{1}{6}\frac{f\pi}{L}\frac{m\pi}{L}\frac{1}{b}I^{sscc}_{prfm} + \frac{1}{6}\frac{f\pi}{L}\frac{r\pi}{L}\frac{1}{b}I^{sscc}_{mpfr} \\
&\quad \left. + \frac{1}{6}\frac{m\pi}{L}\frac{r\pi}{L}\frac{1}{b}I^{sscc}_{fpmr} + \frac{1}{6}\frac{m\pi}{L}\frac{p\pi}{L}\frac{1}{b}I^{sscc}_{frmp} + \frac{1}{6}\frac{r\pi}{L}\frac{p\pi}{L}\frac{1}{b}I^{sscc}_{fmpr}\right]\dot{w}^a_p \\
&+ \sum_{p=1}^{M_{wa}}\sum_{m=1}^{M_{wa}}\sum_{r=1}^{M_{wb}}\sum_{s=1}^{N_{wb}}(w^a_m w^b_{rs} + w^a_{0m}w^b_{rs} + w^a_m w^b_{0rs})C\left[3\frac{p\pi}{L}\frac{f\pi}{L}\frac{m\pi}{L}\frac{r\pi}{L}I^{yyys}_{s}I^{cccc}_{pfmr}\right. \\
&\quad + \frac{p\pi}{L}\frac{f\pi}{L}\frac{s\pi}{b}\frac{1}{b}I^{yyc}_{s}I^{sscc}_{mrfp} + \frac{m\pi}{L}\frac{f\pi}{L}\frac{s\pi}{b}\frac{1}{b}I^{yyc}_{s}I^{sscc}_{prfm} + \frac{m\pi}{L}\frac{p\pi}{L}\frac{s\pi}{b}\frac{1}{b}I^{yyc}_{s}I^{sscc}_{frmp} \\
&\quad \left. + \frac{p\pi}{L}\frac{r\pi}{L}\left(\frac{1}{b}\right)^2 I^{ys}_{s}I^{sscc}_{fmpr} + \frac{m\pi}{L}\frac{r\pi}{L}\left(\frac{1}{b}\right)^2 I^{ys}_{s}I^{sscc}_{fpmr} + \frac{f\pi}{L}\frac{r\pi}{L}\left(\frac{1}{b}\right)^2 I^{ys}_{s}I^{sscc}_{mpfr}\right]\dot{w}^a_p \\
&+ \sum_{p=1}^{M_{wa}}\sum_{m=1}^{M_{wb}}\sum_{n=1}^{N_{wb}}\sum_{r=1}^{M_{wb}}\sum_{s=1}^{N_{wb}}\left[(w^b_{mn}w^b_{rs} + 2w^b_{mn}w^b_{0rs})C\left(\frac{3}{2}\frac{p\pi}{L}\frac{f\pi}{L}\frac{m\pi}{L}\frac{r\pi}{L}I^{yyss}_{ns}I^{cccc}_{pfmr} + \frac{3}{4}\frac{n\pi}{b}\frac{s\pi}{b}\frac{1}{b}\delta_{ns}I^{ssss}_{frmp}\right.\right. \\
&\quad + \frac{1}{2}\frac{p\pi}{L}\frac{f\pi}{L}\frac{n\pi}{b}\frac{s\pi}{b}I^{yycc}_{ns}I^{sscc}_{mrfp} + \frac{1}{4}\frac{m\pi}{L}\frac{r\pi}{L}\frac{1}{b}\delta_{ns}I^{sscc}_{fpmr} + \frac{1}{2}\frac{p\pi}{L}\frac{m\pi}{L}\frac{s\pi}{b}\frac{1}{b}I^{ycs}_{sn}I^{sscc}_{frmp} \\
&\quad \left.\left. + \frac{1}{2}\frac{f\pi}{L}\frac{m\pi}{L}\frac{s\pi}{b}\frac{1}{b}I^{ycs}_{sn}I^{sscc}_{prfm} + \frac{1}{2}\frac{f\pi}{L}\frac{r\pi}{L}\frac{n\pi}{b}\frac{1}{b}I^{ycs}_{ns}I^{sscc}_{mpfr} + \frac{1}{2}\frac{p\pi}{L}\frac{r\pi}{L}\frac{n\pi}{b}\frac{1}{b}I^{ycs}_{ns}I^{sscc}_{fmpr}\right)\dot{w}^a_p \\
&+ \sum_{p=1}^{M_{wa}}\sum_{i=1}^{M_{ua}}u^a_i C\left[\frac{i\pi}{L}\frac{p\pi}{L}\frac{f\pi}{L}\frac{b}{4}I^{ccc}_{ipf} + \nu\frac{i\pi}{L}\left(\frac{1}{b}\right)^2\frac{b}{2}I^{css}_{ipf} + \frac{1-\nu}{2}\frac{p\pi}{L}\left(\frac{1}{b}\right)^2\frac{b}{2}I^{css}_{pif} + \frac{1-\nu}{2}\frac{f\pi}{L}\left(\frac{1}{b}\right)^2\frac{b}{2}I^{css}_{fip}\right]\dot{w}^a_p \\
&+ \sum_{p=1}^{M_{wa}}\sum_{i=1}^{M_{ub}}\sum_{j=1}^{N_{ub}}u^b_{ij}C\left[\frac{i\pi}{L}\frac{p\pi}{L}\frac{f\pi}{L}I^{yys}_{j}I^{ccc}_{ipf} + \nu\frac{i\pi}{L}\left(\frac{1}{b}\right)^2 I^{s}_{j}I^{css}_{ipf} + \frac{1-\nu}{2}\frac{j\pi}{b}\frac{p\pi}{L}\frac{1}{b}I^{yc}_{j}I^{css}_{pif} + \frac{1-\nu}{2}\frac{j\pi}{b}\frac{f\pi}{L}\frac{1}{b}I^{yc}_{j}I^{css}_{fip}\right]\dot{w}^a_p \\
&+ \sum_{p=1}^{M_{wa}}u^c C\left[\frac{1}{L}\left(\frac{f\pi}{L}\right)^2\frac{Lb}{6} + \nu\frac{1}{L}\frac{1}{b}\frac{L}{2}\right]\delta_{fp}\dot{w}^a_p + \sum_{p=1}^{M_{wa}}\sum_{i=1}^{M_{va}}v^a_i C\left[\left(\frac{1}{b}\right)^2 I^{css}_{ipf} + \nu\frac{p\pi}{L}\frac{f\pi}{L}\frac{1}{b}\frac{b}{3}I^{ccc}_{ipf}\right. \\
&\quad \left. - \frac{1-\nu}{2}\frac{i\pi}{L}\frac{p\pi}{L}\frac{1}{b}\frac{b}{3}I^{css}_{pif} - \frac{1-\nu}{2}\frac{i\pi}{L}\frac{f\pi}{L}\frac{1}{b}\frac{b}{3}I^{css}_{fip}\right]\dot{w}^a_p + \sum_{p=1}^{M_{wa}}\sum_{i=1}^{M_{vb}}\sum_{j=1}^{N_{vb}}v^b_{ij}C\left[\nu\frac{j\pi}{b}\frac{p\pi}{L}\frac{f\pi}{L}I^{yyc}_{j}I^{scc}_{ipf}\right. \\
&\quad \left. + \frac{1-\nu}{2}\frac{i\pi}{L}\frac{p\pi}{L}\frac{1}{b}I^{ys}_{j}I^{scc}_{fip} + \frac{1-\nu}{2}\frac{i\pi}{L}\frac{f\pi}{L}\frac{1}{b}I^{ys}_{j}I^{scc}_{pif}\right]\dot{w}^a_p + \sum_{p=1}^{M_{wa}}v^c C\left[\left(\frac{1}{b}\right)^2\frac{L}{2} + \nu\left(\frac{f\pi}{L}\right)^2\frac{1}{b}\frac{Lb}{6}\right]\delta_{fp}\dot{w}^a_p
\end{aligned}
\tag{131}
$$

$$
\begin{aligned}
\mathbf{K}^{pmNL}_{wawb}\dot{\mathbf{w}}^b &= \frac{\partial^2 U^{pmNL}}{\partial w^a_f \partial w^b_{pq}}\dot{w}^b_{pq} \\
&= \sum_{p=1}^{M_{wb}}\sum_{q=1}^{N_{wb}}\sum_{m=1}^{M_{wa}}\sum_{r=1}^{M_{wa}}(w^a_m w^a_r + 2w^a_m w^a_{0r})C\left[\frac{3}{2}\frac{f\pi}{L}\frac{m\pi}{L}\frac{r\pi}{L}\frac{p\pi}{L}I^{yyys}_q I^{cccc}_{fpmr}\right. \\
&\quad +\frac{1}{2}\frac{m\pi}{L}\frac{r\pi}{L}\frac{q\pi}{b}\frac{1}{b}I^{yyc}_q I^{sscc}_{fpmr} + \frac{1}{2}\frac{f\pi}{L}\frac{r\pi}{L}\frac{q\pi}{b}\frac{1}{b}I^{yyc}_q I^{sscc}_{mpfr} + \frac{1}{2}\frac{f\pi}{L}\frac{m\pi}{L}\frac{q\pi}{b}\frac{1}{b}I^{yyc}_q I^{sscc}_{prfm} \\
&\quad \left.+\frac{1}{2}\frac{f\pi}{L}\frac{p\pi}{L}\left(\frac{1}{b}\right)^2 I^{ys}_q I^{sscc}_{mrfp} + \frac{1}{2}\frac{m\pi}{L}\frac{p\pi}{L}\left(\frac{1}{b}\right)^2 I^{ys}_q I^{sscc}_{frmp} + \frac{1}{2}\frac{r\pi}{L}\frac{p\pi}{L}\left(\frac{1}{b}\right)^2 I^{ys}_q I^{sscc}_{fmpr}\right]\dot{w}^b_{pq} \\
&\quad +\sum_{p=1}^{M_{wb}}\sum_{q=1}^{N_{wb}}\sum_{m=1}^{M_{wa}}\sum_{r=1}^{M_{wb}}\sum_{s=1}^{N_{wb}}(w^a_m w^b_{rs} + w^a_{0m}w^b_{rs} + w^a_m w^b_{0rs})C\left[3\frac{f\pi}{L}\frac{m\pi}{L}\frac{r\pi}{L}\frac{p\pi}{L}I^{yyss}_{sq}I^{cccc}_{fmrp}\right. \\
&\quad +3\frac{s\pi}{b}\frac{q\pi}{b}\left(\frac{1}{b}\right)^2\frac{b}{2}\delta_{sq}I^{ssss}_{fmrp} + \frac{f\pi}{L}\frac{m\pi}{L}\frac{s\pi}{b}\frac{q\pi}{b}I^{yycc}_{sq}I^{sscc}_{prfm} + \frac{f\pi}{L}\frac{r\pi}{L}\frac{q\pi}{b}\frac{1}{b}I^{ycs}_{qs}I^{sscc}_{mpfr} \\
&\quad +\frac{f\pi}{L}\frac{p\pi}{L}\frac{s\pi}{b}\frac{1}{b}I^{ycs}_{sq}I^{sscc}_{mrfp} + \frac{m\pi}{L}\frac{r\pi}{L}\frac{q\pi}{b}\frac{1}{b}I^{ycs}_{qs}I^{sscc}_{fpmr} + \frac{m\pi}{L}\frac{p\pi}{L}\frac{s\pi}{b}\frac{1}{b}I^{ycs}_{sq}I^{sscc}_{frmp} + \frac{r\pi}{L}\frac{p\pi}{L}\left(\frac{1}{b}\right)^2\frac{b}{2}\delta_{sq}I^{sscc}_{fmrp}\left.\right]\dot{w}^b_{pq} \\
&\quad +\sum_{p=1}^{M_{wb}}\sum_{q=1}^{N_{wb}}\sum_{m=1}^{M_{wb}}\sum_{n=1}^{N_{wb}}\sum_{r=1}^{M_{wb}}\sum_{s=1}^{N_{wb}}(w^b_{mn}w^b_{rs} + 2w^b_{mn}w^b_{0rs})C\left[\frac{3}{2}\frac{f\pi}{L}\frac{p\pi}{L}\frac{m\pi}{L}\frac{r\pi}{L}I^{ysss}_{qns}I^{cccc}_{fmpr} + \frac{3}{2}\frac{q\pi}{b}\frac{n\pi}{b}\frac{s\pi}{b}\frac{1}{b}I^{ccc}_{qns}I^{ssss}_{fpmr}\right. \\
&\quad +\frac{1}{2}\frac{f\pi}{L}\frac{p\pi}{L}\frac{n\pi}{b}\frac{s\pi}{b}I^{yscc}_{qns}I^{sscc}_{mrfp} + \frac{1}{2}\frac{f\pi}{L}\frac{m\pi}{L}\frac{q\pi}{b}\frac{s\pi}{b}I^{yscc}_{nqs}I^{sscc}_{prfm} + \frac{1}{2}\frac{f\pi}{L}\frac{r\pi}{L}\frac{q\pi}{b}\frac{n\pi}{b}I^{yscc}_{sqn}I^{sscc}_{mpfr} \\
&\quad \left.+\frac{1}{2}\frac{m\pi}{L}\frac{r\pi}{L}\frac{q\pi}{b}\frac{1}{b}I^{css}_{qns}I^{sscc}_{fpmr} + \frac{1}{2}\frac{p\pi}{L}\frac{r\pi}{L}\frac{n\pi}{b}\frac{1}{b}I^{css}_{nqs}I^{sscc}_{fmpr} + \frac{1}{2}\frac{m\pi}{L}\frac{p\pi}{L}\frac{s\pi}{b}\frac{1}{b}I^{css}_{sqn}I^{sscc}_{frmp}\right]\dot{w}^b_{pq} \\
&\quad +\sum_{p=1}^{M_{wb}}\sum_{q=1}^{N_{wb}}\sum_{i=1}^{M_{ua}}u^a_i C\left[\frac{i\pi}{L}\frac{p\pi}{L}\frac{f\pi}{L}I^{yys}_q I^{ccc}_{ipf} + \nu\frac{i\pi}{L}\frac{q\pi}{b}\frac{1}{b}I^{yc}_q I^{css}_{ipf} + \frac{1-\nu}{2}\frac{f\pi}{L}\frac{q\pi}{b}\frac{1}{b}I^{yc}_q I^{css}_{fip} + \frac{1-\nu}{2}\frac{p\pi}{L}\left(\frac{1}{b}\right)^2 I^{s}_q I^{css}_{pif}\right]\dot{w}^b_{pq} \\
&\quad +\sum_{p=1}^{M_{wb}}\sum_{q=1}^{N_{wb}}\sum_{i=1}^{M_{ub}}\sum_{j=1}^{N_{ub}}u^b_{ij}C\left[\frac{i\pi}{L}\frac{f\pi}{L}\frac{p\pi}{L}I^{yss}_{jq}I^{ccc}_{ifp} + \nu\frac{i\pi}{L}\frac{q\pi}{b}\frac{1}{b}I^{cs}_{qj}I^{css}_{ifp} + \frac{1-\nu}{2}\frac{j\pi}{b}\frac{f\pi}{L}\frac{q\pi}{b}I^{ycc}_{jq}I^{css}_{fip} + \frac{1-\nu}{2}\frac{j\pi}{b}\frac{p\pi}{L}\frac{1}{b}I^{cs}_{jq}I^{css}_{pif}\right]\dot{w}^b_{pq} \\
&\quad +\sum_{p=1}^{M_{wb}}\sum_{q=1}^{N_{wb}}u^c C\left[\frac{1}{L}\left(\frac{f\pi}{L}\right)^2 I^{ys}_q\frac{L}{2}\delta_{fp}\right]\dot{w}^b_{pq} + \sum_{p=1}^{M_{wb}}\sum_{q=1}^{N_{wb}}\sum_{i=1}^{M_{va}}v^a_i C\left[\nu\frac{f\pi}{L}\frac{p\pi}{L}\frac{1}{b}I^{ys}_q I^{ccc}_{ifp} - \frac{1-\nu}{2}\frac{i\pi}{L}\frac{f\pi}{L}\frac{q\pi}{b}I^{yyc}_q I^{css}_{fip}\right. \\
&\quad \left.-\frac{1-\nu}{2}\frac{i\pi}{L}\frac{p\pi}{L}\frac{1}{b}I^{ys}_q I^{css}_{pif}\right]\dot{w}^b_{pq} + \sum_{p=1}^{M_{wb}}\sum_{q=1}^{N_{wb}}\sum_{i=1}^{M_{vb}}\sum_{j=1}^{N_{vb}}v^b_{ij}C\left[\frac{j\pi}{b}\frac{q\pi}{b}\frac{1}{b}\frac{b}{2}\delta_{jq}I^{sss}_{ifp} + \nu\frac{j\pi}{b}\frac{f\pi}{L}\frac{p\pi}{L}I^{ycs}_{jq}I^{scc}_{ifp}\right. \\
&\quad \left.+\frac{1-\nu}{2}\frac{i\pi}{L}\frac{f\pi}{L}\frac{q\pi}{b}I^{ycs}_{qj}I^{scc}_{pif} + \frac{1-\nu}{2}\frac{i\pi}{L}\frac{p\pi}{L}\frac{1}{b}\frac{b}{2}\delta_{jq}I^{scc}_{fip}\right]\dot{w}^b_{pq} + \sum_{p=1}^{M_{wb}}\sum_{q=1}^{N_{wb}}v^c C\left[\nu\left(\frac{f\pi}{L}\right)^2\frac{1}{b}\frac{L}{2}I^{ys}_q\delta_{fp}\right]\dot{w}^b_{pq}
\end{aligned}
\tag{132}
$$

$$
\mathbf{K}^{pmNL}_{wbwa} = (\mathbf{K}^{pmNL}_{wawb})^T \tag{133}
$$

$$\mathbf{K}^{pmNL}_{wbwb}\dot{\mathbf{w}}^b = \frac{\partial^2 U^{pmNL}}{\partial w^b_{fg}\partial w^b_{pq}}\dot{w}^b_{pq}$$

$$= \sum_{p=1}^{M_{wb}}\sum_{q=1}^{N_{wb}}\sum_{m=1}^{M_{wb}}\sum_{n=1}^{N_{wb}}\sum_{r=1}^{M_{wb}}\sum_{s=1}^{N_{wb}}(w^b_{mn}w^b_{rs}+2w^b_{mn}w^b_{0rs})C\left[\frac{3}{2}\frac{f\pi}{L}\frac{m\pi}{L}\frac{r\pi}{L}\frac{p\pi}{L}I^{cccc}_{fpmr}I^{ssss}_{gqns}\right.$$
$$+\frac{3}{2}\frac{g\pi}{b}\frac{q\pi}{b}\frac{n\pi}{b}\frac{s\pi}{b}I^{ssss}_{fpmr}I^{cccc}_{gqns}+\frac{1}{2}\frac{f\pi}{L}\frac{p\pi}{L}\frac{n\pi}{b}\frac{s\pi}{b}I^{sscc}_{mrfp}I^{sscc}_{gqns}+\frac{1}{2}\frac{f\pi}{L}\frac{m\pi}{L}\frac{q\pi}{b}\frac{s\pi}{b}I^{sscc}_{prfm}I^{sscc}_{gnqs}$$
$$+\frac{1}{2}\frac{f\pi}{L}\frac{r\pi}{L}\frac{n\pi}{b}\frac{q\pi}{b}I^{sscc}_{mpfr}I^{sscc}_{gsnq}+\frac{1}{2}\frac{m\pi}{L}\frac{p\pi}{L}\frac{g\pi}{b}\frac{s\pi}{b}I^{sscc}_{frmp}I^{sscc}_{nqgs}+\frac{1}{2}\frac{m\pi}{L}\frac{r\pi}{L}\frac{q\pi}{b}\frac{g\pi}{b}I^{sscc}_{fpmr}I^{sscc}_{nsgq}$$
$$\left.+\frac{1}{2}\frac{p\pi}{L}\frac{r\pi}{L}\frac{g\pi}{b}\frac{n\pi}{b}I^{sscc}_{fmpr}I^{sscc}_{qsgn}\right]\dot{w}^b_{pq}$$

$$+\sum_{p=1}^{M_{wb}}\sum_{q=1}^{N_{wb}}\sum_{m=1}^{M_{wa}}\sum_{r=1}^{M_{wb}}\sum_{s=1}^{N_{wb}}(w^a_m w^b_{rs}+w^a_{0m}w^b_{rs}+w^a_m w^b_{0rs})C\left[3\frac{m\pi}{L}\frac{p\pi}{L}\frac{f\pi}{L}\frac{r\pi}{L}I^{ysss}_{qgs}I^{cccc}_{mpfr}\right.$$
$$+3\frac{q\pi}{b}\frac{g\pi}{b}\frac{s\pi}{b}\frac{1}{b}I^{ccc}_{qgs}I^{ssss}_{fmrp}+\frac{m\pi}{L}\frac{p\pi}{L}\frac{g\pi}{b}\frac{s\pi}{b}I^{yscc}_{qgs}I^{sscc}_{frmp}+\frac{m\pi}{L}\frac{f\pi}{L}\frac{q\pi}{b}\frac{s\pi}{b}I^{yscc}_{gqs}I^{sscc}_{prfm}$$
$$+\frac{m\pi}{L}\frac{r\pi}{L}\frac{g\pi}{b}\frac{q\pi}{b}I^{yscc}_{sgq}I^{sscc}_{fpmr}+\frac{f\pi}{L}\frac{r\pi}{L}\frac{q\pi}{b}\frac{1}{b}I^{css}_{qgs}I^{sscc}_{mpfr}+\frac{p\pi}{L}\frac{r\pi}{L}\frac{g\pi}{b}\frac{1}{b}I^{css}_{gqs}I^{sscc}_{fmpr}$$
$$\left.+\frac{p\pi}{L}\frac{f\pi}{L}\frac{s\pi}{b}\frac{1}{b}I^{css}_{sgq}I^{sscc}_{mrpf}\right]\dot{w}^b_{pq}$$

$$+\sum_{p=1}^{M_{wb}}\sum_{q=1}^{N_{wb}}\sum_{m=1}^{M_{wa}}\sum_{r=1}^{M_{wa}}\left[(w^a_m w^a_r+2w^a_m w^a_{0r})C\left(\frac{3}{2}\frac{m\pi}{L}\frac{r\pi}{L}\frac{p\pi}{L}\frac{f\pi}{L}I^{yyss}_{qg}I^{cccc}_{mrpf}+\frac{3}{4}\frac{q\pi}{b}\frac{g\pi}{b}\frac{1}{b}\delta_{qg}I^{ssss}_{mrpf}\right.\right.$$
$$+\frac{1}{2}\frac{p\pi}{L}\frac{f\pi}{L}\left(\frac{1}{b}\right)^2\frac{b}{2}\delta_{qg}I^{sscc}_{mrfp}+\frac{1}{2}\frac{m\pi}{L}\frac{r\pi}{L}\frac{q\pi}{b}\frac{g\pi}{b}I^{yycc}_{qg}I^{sscc}_{fpmr}+\frac{1}{2}\frac{m\pi}{L}\frac{p\pi}{L}\frac{g\pi}{b}\frac{1}{b}I^{ycs}_{gq}I^{sscc}_{frmp}$$
$$\left.\left.+\frac{1}{2}\frac{m\pi}{L}\frac{f\pi}{L}\frac{q\pi}{b}\frac{1}{b}I^{ycs}_{qg}I^{sscc}_{prfm}+\frac{1}{2}\frac{r\pi}{L}\frac{f\pi}{L}\frac{q\pi}{b}\frac{1}{b}I^{ycs}_{qg}I^{sscc}_{mpfr}+\frac{1}{2}\frac{r\pi}{L}\frac{p\pi}{L}\frac{g\pi}{b}\frac{1}{b}I^{ycs}_{gq}I^{sscc}_{fmpr}\right)\right]\dot{w}^b_{pq}$$

$$+\sum_{p=1}^{M_{wb}}\sum_{q=1}^{N_{wb}}\sum_{i=1}^{M_{ua}}u^a_i C\left[\frac{i\pi}{L}\frac{p\pi}{L}\frac{f\pi}{L}I^{yss}_{qg}I^{ccc}_{ipf}+\nu\frac{i\pi}{L}\frac{q\pi}{b}\frac{g\pi}{b}I^{ycc}_{qg}I^{css}_{ipf}+\frac{1-\nu}{2}\frac{p\pi}{L}\frac{g\pi}{b}\frac{1}{b}I^{cs}_{gq}I^{css}_{pif}+\frac{1-\nu}{2}\frac{f\pi}{L}\frac{q\pi}{b}\frac{1}{b}I^{cs}_{qg}I^{css}_{fip}\right]\dot{w}^b_{pq}$$

$$+\sum_{p=1}^{M_{wb}}\sum_{q=1}^{N_{wb}}\sum_{i=1}^{M_{ub}}\sum_{j=1}^{N_{ub}}u^b_{ij}C\left[\frac{i\pi}{L}\frac{p\pi}{L}\frac{f\pi}{L}I^{ccc}_{ipf}I^{sss}_{jqg}+\nu\frac{i\pi}{L}\frac{q\pi}{b}\frac{g\pi}{b}I^{css}_{ipf}I^{scc}_{jqg}+\frac{1-\nu}{2}\frac{j\pi}{b}\frac{p\pi}{L}\frac{g\pi}{b}I^{css}_{pif}I^{scc}_{qjg}+\frac{1-\nu}{2}\frac{j\pi}{b}\frac{f\pi}{L}\frac{q\pi}{b}I^{css}_{fip}I^{scc}_{gjq}\right]\dot{w}^b_{pq}$$

$$+\sum_{p=1}^{M_{wb}}\sum_{q=1}^{N_{wb}}u^c C\left[\left(\frac{f\pi}{L}\right)^2+\nu\left(\frac{g\pi}{b}\right)^2\right]\frac{1}{L}\frac{Lb}{4}\delta_{fp}\delta_{gq}\dot{w}^b_{pq}+\sum_{p=1}^{M_{wb}}\sum_{q=1}^{N_{wb}}\sum_{i=1}^{M_{va}}v^a_i C\left[\frac{q\pi}{b}\frac{g\pi}{b}\frac{1}{b}\frac{b}{2}\delta_{qg}I^{css}_{ipf}+\nu\frac{p\pi}{L}\frac{f\pi}{L}\frac{1}{b}\frac{b}{2}\delta_{qg}I^{ccc}_{ipf}\right.$$
$$\left.-\frac{1-\nu}{2}\frac{i\pi}{L}\frac{p\pi}{L}\frac{g\pi}{b}I^{ycs}_{gq}I^{css}_{pif}-\frac{1-\nu}{2}\frac{i\pi}{L}\frac{f\pi}{L}\frac{q\pi}{b}I^{ycs}_{qg}I^{css}_{fip}\right]\dot{w}^b_{pq}+\sum_{p=1}^{M_{wb}}\sum_{q=1}^{N_{wb}}\sum_{i=1}^{M_{vb}}\sum_{j=1}^{N_{vb}}v^b_{ij}C\left[\frac{j\pi}{b}\frac{q\pi}{b}\frac{g\pi}{b}I^{sss}_{ipf}I^{ccc}_{jqg}\right.$$
$$+\nu\frac{j\pi}{b}\frac{p\pi}{L}\frac{f\pi}{L}I^{scc}_{ipf}I^{css}_{jqg}+\frac{1-\nu}{2}\frac{i\pi}{L}\frac{p\pi}{L}\frac{g\pi}{b}I^{scc}_{fip}I^{css}_{gjq}+\frac{1-\nu}{2}\frac{i\pi}{L}\frac{f\pi}{L}\frac{q\pi}{b}I^{scc}_{pif}I^{css}_{qjg}\left.\right]\dot{w}^b_{pq}$$
$$+\sum_{p=1}^{M_{wb}}\sum_{q=1}^{N_{wb}}v^c C\left[\left(\frac{g\pi}{b}\right)^2+\nu\left(\frac{f\pi}{L}\right)^2\right]\frac{1}{b}\frac{Lb}{4}\delta_{fp}\delta_{gq}\dot{w}^b_{pq} \tag{134}$$

C.2 The generalised, incremental plate bending stiffness matrix $\mathbf{K}^{pb}$

C.2.1 Introduction

The generalised, incremental plate bending stiffness matrix is divided into the submatrices given below. The only non-zero submatrix is $\mathbf{K}^{pb}_{ww}$. In the solution procedure for postbuckling analysis described in Chapter 5, $\mathbf{K}^{pb}$ must be added to the generalised, incremental stiffness matrix $\mathbf{K}$ given in Eq. 41. Details on how to build the matrices is given in Appendix A and B.

C.2.2 Definition of the $\mathbf{K}^{pb}_{ww}$-matrix

The matrix $\mathbf{K}^{pb}_{ww}$ is symmetrical, and the size of this matrix is $(M_{wa} + M_{wb}N_{wb}) \times (M_{wa} + M_{wb}N_{wb})$. The matrix is a constant contribution and consists of the submatrices given in index notation in the following expressions

$$\mathbf{K}^{pb}_{wawa}\dot{\mathbf{w}}^a = \frac{\partial^2 U^{pb}}{\partial w^a_f \partial w^a_p}\dot{w}^a_p = \sum_{p=1}^{M_{wa}} D\left[\left(\frac{f\pi}{L}\right)^4 \frac{Lb}{6} + (1-\nu)\left(\frac{f\pi}{L}\right)^2 \frac{L}{b}\right]\delta_{fp}\dot{w}^a_p \tag{135}$$

$$\mathbf{K}^{pb}_{wawb}\dot{\mathbf{w}}^b = \frac{\partial^2 U^{pb}}{\partial w^a_f \partial w^{pb}_{pq}}\dot{w}^b_{pq} = \sum_{p=1}^{M_{wb}}\sum_{q=1}^{N_{wb}} D\left[\left(\frac{f\pi}{L}\right)^4 \frac{L}{2} I^{ys}_q + \nu\left(\frac{f\pi}{L}\right)^2\left(\frac{q\pi}{L}\right)^2 \frac{L}{2} I^{ys}_q\right]\delta_{fp}\dot{w}^b_{pq} \tag{136}$$

$$\mathbf{K}^{pb}_{wbwa}\dot{\mathbf{w}}^b = \frac{\partial^2 U^{pb}}{\partial w^b_{fg} \partial w^a_p}\dot{w}^a_p = \sum_{p=1}^{M_{wa}} D\left[\left(\frac{f\pi}{L}\right)^4 \frac{L}{2} I^{ys}_g + \nu\left(\frac{f\pi}{L}\right)^2\left(\frac{g\pi}{L}\right)^2 \frac{L}{2} I^{ys}_g\right]\delta_{fp}\dot{w}^a_p \tag{137}$$

$$\mathbf{K}^{pb}_{wbwb}\dot{\mathbf{w}}^b = \frac{\partial^2 U^{pb}}{\partial w^b_{fg} \partial w^b_{pq}}\dot{w}^b_{pq} = \sum_{p=1}^{M_{wb}}\sum_{q=1}^{N_{wb}} D\frac{Lb}{4}\left[\left(\frac{f\pi}{L}\right)^2 + \left(\frac{g\pi}{L}\right)^2\right]\delta_{fp}\delta_{gq}\dot{w}^b_{pq} \tag{138}$$

C.3 The generalised, incremental load vector $-\dot{\Lambda}\mathbf{G}^{p,x}$ of the plate

The incremental load vector $-\dot{\Lambda}\mathbf{G}^{p,x}$ of the plate due to an external load in x-direction is a constant contribution. It consists of the subvectors in the following expressions

$$-\dot{\Lambda}\mathbf{G}^{p,x}_{uc} = -\dot{\Lambda}\frac{\partial^2 T^{p,x}}{\partial u^c \partial \Lambda} = \dot{\Lambda} S_{0x} b t \tag{139}$$

$$\begin{aligned} &\mathbf{G}^{p,x}_{ua} = 0, \quad \mathbf{G}^{p,x}_{ub} = 0, \quad \mathbf{G}^{p,x}_{va} = 0, \quad \mathbf{G}^{p,x}_{vb} = 0, \\ &\mathbf{G}^{p,x}_{vc} = 0, \quad \mathbf{G}^{p,x}_{wa} = 0, \quad \mathbf{G}^{p,x}_{wb} = 0 \end{aligned} \tag{140}$$

Here, the subvector $-\dot{\Lambda}\mathbf{G}_{uc}^{p}$ is the only non-zero contribution for the load considered.

D Rate form of energy contributions of a stiffener

D.1 The generalised, incremental stiffness matrix $\mathbf{K}^{s,x}$ for stiffeners parallel to the free edge

D.1.1 Introduction

In the chosen coordinate system, defined in Fig. 4, stiffeners parallel to the free edge are oriented in the x-direction. In order to indicate the direction of the stiffeners, 'x' is included in the super index in the stiffener contributions.

In the expressions below, integrals are replace with simplified expressions, I_m^s, I_{mn}^{cs}, etc. For instance,

$$I_m^s = \int_0^b \sin(\frac{m\pi}{b}y)\, dy = \frac{b}{m\pi}[1-(-1)^m] \tag{141}$$

is introduced. The expressions for all the integrals can be found in Appendix F. In addition , the Kronecker delta defined by

$$\delta_{ij} = \begin{cases} 1 & \text{if } i = j \\ 0 & \text{otherwise} \end{cases} \tag{142}$$

is used. Details on how to build the matrices is given in Appendix A and B.

D.1.2 Definition of the $\mathbf{K}_{uu}^{sL,x}$-matrix

The matrix $\mathbf{K}_{uu}^{sL,x}$ is symmetrical, and the size of this matrix is $(M_{ua} + M_{ub}N_{ub} + 1) \times (M_{ua} + M_{ub}N_{ub} + 1)$. The matrix is a constant contribution and consists of the submatrices given in index notation in the following expressions

$$\mathbf{K}_{uaua}^{sL,x}\dot{\mathbf{u}}^a = \frac{\partial^2 U^{sL,x}}{\partial u_f^a \partial u_p^a}\dot{u}_p^a = \sum_{p=1}^{M_{ua}} EA_s\left[\left(\frac{f\pi}{L}\right)^2\left(\frac{y_s}{b}\right)^2\frac{L}{2}\right]\delta_{fp}\dot{u}_p^a \tag{143}$$

$$\mathbf{K}_{ubub}^{sL,x}\dot{\mathbf{u}}^b = \frac{\partial^2 U^{sL,x}}{\partial u_{fg}^b \partial u_{pq}^b}\dot{u}_{pq}^b = \sum_{p=1}^{M_{ub}}\sum_{q=1}^{N_{ub}} EA_s\left[\left(\frac{f\pi}{L}\right)^2\sin(\frac{g\pi}{b}y_s)\sin(\frac{q\pi}{b}y_s)\frac{L}{2}\right]\delta_{fp}\dot{u}_{pq}^b \tag{144}$$

$$\mathbf{K}_{ucuc}^{sL,x}\dot{\mathbf{u}}^c = \frac{\partial^2 U^{sL,x}}{\partial u^c \partial u^c}\dot{u}^c = EA_s\frac{1}{L}\dot{u}^c \tag{145}$$

$$\mathbf{K}^{sL,x}_{uaub}\dot{\mathbf{u}}^b = \frac{\partial^2 U^{sL,x}}{\partial u^a_f \partial u^b_{pq}}\dot{u}^b_{pq} = \sum_{p=1}^{M_{ub}}\sum_{q=1}^{N_{ub}} EA_s\left[\left(\frac{f\pi}{L}\right)^2 \frac{y_s}{b}\sin(\frac{q\pi}{b}y_s)\frac{L}{2}\right]\delta_{fp}\dot{u}^b_{pq} \tag{146}$$

$$\mathbf{K}^{sL,x}_{ubua}\dot{\mathbf{u}}^a = \frac{\partial^2 U^{sL,x}}{\partial u^b_{fg} \partial u^a_p}\dot{u}^a_p = \sum_{p=1}^{M_{ua}} EA_s\left[\left(\frac{f\pi}{L}\right)^2 \frac{y_s}{b}\sin(\frac{g\pi}{b}y_s)\frac{L}{2}\right]\delta_{fp}\dot{u}^a_p \tag{147}$$

$$\mathbf{K}^{sL,x}_{uauc} = 0, \quad \mathbf{K}^{sL,x}_{ucua} = 0, \quad \mathbf{K}^{sL,x}_{ubuc} = 0, \quad \mathbf{K}^{sL,x}_{ucub} = 0 \tag{148}$$

D.1.3 Definition of the $\mathbf{K}^{sL,x}_{uw}$-matrix

The size of the matrix $\mathbf{K}^{sL,x}_{uw}$ is $(M_{ua} + M_{ub}N_{ub} + 1) \times (M_{wa} + M_{wb}N_{wb})$. The matrix is a constant contribution and consists of the submatrices given in index notation in the following expressions

$$\begin{aligned}
\mathbf{K}^{sL,x}_{uawa}\dot{\mathbf{w}}^a &= \frac{\partial^2 U^{sL,x}}{\partial u^a_f \partial w^a_p}\dot{w}^a_p \\
&= \sum_{p=1}^{M_{wa}} e_c EA_s\left[\frac{f\pi}{L}\left(\frac{p\pi}{L}\right)^2\left(\frac{y_s}{b}\right)^2 I^{cs}_{fp}\right]\dot{w}^a_p \\
&+ \sum_{p=1}^{M_{wa}}\sum_{m=1}^{M_{wa}} w^a_{0m} EA_s\left[\frac{f\pi}{L}\frac{p\pi}{L}\frac{m\pi}{L}\left(\frac{y_s}{b}\right)^3 I^{ccc}_{fpm}\right]\dot{w}^a_p \\
&+ \sum_{p=1}^{M_{wa}}\sum_{m=1}^{M_{wb}}\sum_{n=1}^{N_{wb}} w^b_{0mn} EA_s\left[\frac{f\pi}{L}\frac{p\pi}{L}\frac{m\pi}{L}\left(\frac{y_s}{b}\right)^2 \sin(\frac{n\pi}{b}y_s) I^{ccc}_{fpm}\right]\dot{w}^a_p
\end{aligned} \tag{149}$$

$$\begin{aligned}
\mathbf{K}^{sL,x}_{uawb}\dot{\mathbf{w}}^b &= \frac{\partial^2 U^{sL,x}}{\partial u^a_f \partial w^b_{pq}}\dot{w}^b_{pq} \\
&= \sum_{p=1}^{M_{wb}}\sum_{q=1}^{N_{wb}} e_c EA_s\left[\frac{f\pi}{L}\left(\frac{p\pi}{L}\right)^2 \frac{y_s}{b}\sin(\frac{q\pi}{b}y_s) I^{cs}_{fp}\right]\dot{w}^b_{pq} \\
&+ \sum_{p=1}^{M_{wb}}\sum_{q=1}^{N_{wb}}\sum_{m=1}^{M_{wa}} w^a_{0m} EA_s\left[\frac{f\pi}{L}\frac{p\pi}{L}\frac{m\pi}{L}\left(\frac{y_s}{b}\right)^2 \sin(\frac{q\pi}{b}y_s) I^{ccc}_{fpm}\right]\dot{w}^b_{pq} \\
&+ \sum_{p=1}^{M_{wb}}\sum_{q=1}^{N_{wb}}\sum_{m=1}^{M_{wb}}\sum_{n=1}^{N_{wb}} w^b_{0mn} EA_s\left[\frac{f\pi}{L}\frac{p\pi}{L}\frac{m\pi}{L}\frac{y_s}{b}\sin(\frac{q\pi}{b}y_s)\sin(\frac{n\pi}{b}y_s) I^{ccc}_{fpm}\right]\dot{w}^b_{pq}
\end{aligned} \tag{150}$$

$$
\begin{aligned}
\mathbf{K}^{sL,x}_{ubwa}\dot{\mathbf{w}}^a &= \frac{\partial^2 U^{sL,x}}{\partial u^b_{fg}\partial w^a_p}\dot{w}^a_p \\
&= \sum_{p=1}^{M_{wa}} e_c E A_s \left[\frac{f\pi}{L}\left(\frac{p\pi}{L}\right)^2 \frac{y_s}{b}\sin(\frac{g\pi}{b}y_s) I^{cs}_{fp}\right]\dot{w}^a_p \\
&+ \sum_{p=1}^{M_{wa}}\sum_{m=1}^{M_{wa}} w^a_{0m} E A_s \left[\frac{f\pi}{L}\frac{p\pi}{L}\frac{m\pi}{L}\left(\frac{y_s}{b}\right)^2 \sin(\frac{g\pi}{b}y_s) I^{ccc}_{fpm}\right]\dot{w}^a_p \\
&+ \sum_{p=1}^{M_{wa}}\sum_{m=1}^{M_{wb}}\sum_{n=1}^{N_{wb}} w^b_{0mn} E A_s \left[\frac{f\pi}{L}\frac{p\pi}{L}\frac{m\pi}{L}\frac{y_s}{b}\sin(\frac{g\pi}{b}y_s)\sin(\frac{n\pi}{b}y_s) I^{ccc}_{fpm}\right]\dot{w}^a_p
\end{aligned}
\tag{151}
$$

$$
\begin{aligned}
\mathbf{K}^{sL,x}_{ubwb}\dot{\mathbf{w}}^b &= \frac{\partial^2 U^{sL,x}}{\partial u^b_{fg}\partial w^b_{pq}}\dot{w}^b_{pq} \\
&= \sum_{p=1}^{M_{wb}}\sum_{q=1}^{N_{wb}} e_c E A_s \left[\frac{f\pi}{L}\left(\frac{p\pi}{L}\right)^2 \sin(\frac{g\pi}{b}y_s)\sin(\frac{q\pi}{b}y_s) I^{cs}_{fp}\right]\dot{w}^b_{pq} \\
&+ \sum_{p=1}^{M_{wb}}\sum_{q=1}^{N_{wb}}\sum_{m=1}^{M_{wa}} w^a_{0m} E A_s \left[\frac{f\pi}{L}\frac{p\pi}{L}\frac{m\pi}{L}\frac{y_s}{b}\sin(\frac{g\pi}{b}y_s)\sin(\frac{q\pi}{b}y_s) I^{ccc}_{fpm}\right]\dot{w}^b_{pq} \\
&+ \sum_{p=1}^{M_{wb}}\sum_{q=1}^{N_{wb}}\sum_{m=1}^{M_{wb}}\sum_{n=1}^{N_{wb}} w^b_{0mn} E A_s \left[\frac{f\pi}{L}\frac{p\pi}{L}\frac{m\pi}{L}\sin(\frac{g\pi}{b}y_s)\sin(\frac{q\pi}{b}y_s)\sin(\frac{n\pi}{b}y_s) I^{ccc}_{fpm}\right]\dot{w}^b_{pq}
\end{aligned}
\tag{152}
$$

$$
\begin{aligned}
\mathbf{K}^{sL,x}_{ucwa}\dot{\mathbf{w}}^a &= \frac{\partial^2 U^{sL,x}}{\partial u^c \partial w^a_p}\dot{w}^a_p \\
&= \sum_{p=1}^{M_{wa}} e_c E A_s \left[\frac{1}{L}\left(\frac{p\pi}{L}\right)^2 \frac{y_s}{b} I^s_p\right]\dot{w}^a_p \\
&+ \sum_{p=1}^{M_{wa}} w^a_{0p} E A_s \left[\left(\frac{p\pi}{L}\right)^2 \left(\frac{y_s}{b}\right)^2 \frac{1}{2}\right]\dot{w}^a_p \\
&+ \sum_{p=1}^{M_{wawb}}\sum_{n=1}^{N_{wb}} w^b_{0pn} E A_s \left[\left(\frac{p\pi}{L}\right)^2 \frac{y_s}{b}\sin(\frac{n\pi}{b}y_s)\frac{1}{2}\right]\dot{w}^a_p
\end{aligned}
\tag{153}
$$

$$
\begin{aligned}
\mathbf{K}^{sL,x}_{ucwb}\dot{\mathbf{w}}^b &= \frac{\partial^2 U^{sL,x}}{\partial u^c \partial w^b_{pq}}\dot{w}^b_{pq} \\
&= \sum_{p=1}^{M_{wb}}\sum_{q=1}^{N_{wb}} e_c E A_s \left[\frac{1}{L}\left(\frac{p\pi}{L}\right)^2 \sin(\frac{q\pi}{b}y_s) I^s_p\right]\dot{w}^b_{pq} \\
&+ \sum_{p=1}^{M_{wawb}}\sum_{q=1}^{N_{wb}} w^a_{0p} E A_s \left[\left(\frac{p\pi}{L}\right)^2 \frac{y_s}{b}\sin(\frac{q\pi}{b}y_s)\frac{1}{2}\right]\dot{w}^b_{pq} \\
&+ \sum_{p=1}^{M_{wawb}}\sum_{q=1}^{N_{wb}}\sum_{n=1}^{N_{wb}} w^b_{0pn} E A_s \left[\left(\frac{p\pi}{L}\right)^2 \sin(\frac{q\pi}{b}y_s)\sin(\frac{n\pi}{b}y_s)\frac{1}{2}\right]\dot{w}^b_{pq}
\end{aligned}
\tag{154}
$$

D.1.4 Definition of the $\mathbf{K}^{sL,x}_{wu}$-matrix

Due to symmetry, the matrix can be given by

$$
\mathbf{K}^{sL,x}_{wu} = (\mathbf{K}^{sL,x}_{uw})^T \tag{155}
$$

where $\mathbf{K}^{sL,x}_{uw}$ is given in Section D.1.3. The size of this matrix is $(M_{wa} + M_{wb}N_{wb}) \times (M_{ua} + M_{ub}N_{ub} + 1)$.

D.1.5 Definition of the $\mathbf{K}^{sL,x}_{ww}$-matrix

The matrix $\mathbf{K}^{sL,x}_{ww}$ is symmetrical, and the size of this matrix is $(M_{wa} + M_{wb}N_{wb}) \times (M_{wa} + M_{wb}N_{wb})$. The matrix is a constant contribution and consists of the submatrices

given in index notation in the following expressions

$$
\begin{aligned}
\mathbf{K}^{sL,x}_{wawa}\dot{\mathbf{w}}^a &= \frac{\partial^2 U^{sL,x}}{\partial w^a_f \partial w^a_p}\dot{w}^a_p \\
&= \sum_{p=1}^{M_{wa}} EI\left(\frac{f\pi}{L}\right)^4\left(\frac{y_s}{b}\right)^2\frac{L}{2}\delta_{fp}\dot{w}^a_p \\
&+ \sum_{p=1}^{M_{wa}}\sum_{m=1}^{M_{wa}} w^a_{0m}e_c EA_s\left[\frac{f\pi}{L}\left(\frac{p\pi}{L}\right)^2\frac{m\pi}{L}I^{scc}_{pfm}\right. \\
&\qquad \left. + \frac{p\pi}{L}\left(\frac{f\pi}{L}\right)^2\frac{m\pi}{L}I^{scc}_{fpm}\right]\left(\frac{y_s}{b}\right)^3\dot{w}^a_p \\
&+ \sum_{p=1}^{M_{wa}}\sum_{m=1}^{M_{wb}}\sum_{n=1}^{N_{wb}} w^b_{0mn}e_c EA_s\left[\frac{f\pi}{L}\left(\frac{p\pi}{L}\right)^2\frac{m\pi}{L}I^{scc}_{pfm}\right. \\
&\qquad \left. + \frac{p\pi}{L}\left(\frac{f\pi}{L}\right)^2\frac{m\pi}{L}I^{scc}_{fpm}\right]\left(\frac{y_s}{b}\right)^2\sin(\frac{n\pi}{b}y_s)\dot{w}^a_p \qquad (156) \\
&+ \sum_{p=1}^{M_{wa}}\sum_{m=1}^{M_{wa}}\sum_{r=1}^{M_{wa}} w^a_{0m}w^a_{0r}EA_s\frac{f\pi}{L}\frac{p\pi}{L}\frac{m\pi}{L}\frac{r\pi}{L}\left(\frac{y_s}{b}\right)^4 I^{cccc}_{pfmr}\dot{w}^a_p \\
&+ \sum_{p=1}^{M_{wa}}\sum_{m=1}^{M_{wa}}\sum_{r=1}^{M_{wa}}\sum_{s=1}^{N_{wb}} w^a_{0m}w^b_{0rs}2EA_s\frac{f\pi}{L}\frac{p\pi}{L}\frac{m\pi}{L}\frac{r\pi}{L} \\
&\qquad \cdot\left(\frac{y_s}{b}\right)^3\sin(\frac{s\pi}{b}y_s)I^{cccc}_{pfmr}\dot{w}^a_p \\
&+ \sum_{p=1}^{M_{wa}}\sum_{m=1}^{M_{wb}}\sum_{n=1}^{N_{wb}}\sum_{r=1}^{M_{wa}}\sum_{s=1}^{N_{wb}} w^b_{0mn}w^b_{0rs}EA_s\frac{f\pi}{L}\frac{p\pi}{L}\frac{m\pi}{L}\frac{r\pi}{L} \\
&\qquad \cdot\left(\frac{y_s}{b}\right)^2\sin(\frac{n\pi}{b}y_s)\sin(\frac{s\pi}{b}y_s)I^{cccc}_{pfmr}\dot{w}^a_p
\end{aligned}
$$

$$
\begin{aligned}
\mathbf{K}^{sL,x}_{wawb}\dot{\mathbf{w}}^b &= \frac{\partial^2 U^{sL,x}}{\partial w^a_f \partial w^b_{pq}}\dot{w}^b_{pq} \\
&= \sum_{p=1}^{M_{wb}}\sum_{q=1}^{N_{wb}} EI\left(\frac{f\pi}{L}\right)^4 \frac{y_s}{b}\sin(\frac{q\pi}{b}y_s)\frac{L}{2}\delta_{fp}\dot{w}^b_{pq} \\
&+ \sum_{p=1}^{M_{wb}}\sum_{q=1}^{N_{wb}}\sum_{m=1}^{M_{wa}} w^a_{0m}e_c EA_s\left[\frac{f\pi}{L}\left(\frac{p\pi}{L}\right)^2\frac{m\pi}{L}I^{scc}_{pfm}\right. \\
&\qquad \left. + \left(\frac{f\pi}{L}\right)^2\frac{p\pi}{L}\frac{m\pi}{L}I^{scc}_{fpm}\right]\left(\frac{y_s}{b}\right)^2\sin(\frac{q\pi}{b}y_s)\dot{w}^b_{pq} \\
&+ \sum_{p=1}^{M_{wb}}\sum_{q=1}^{N_{wb}}\sum_{m=1}^{M_{wb}}\sum_{n=1}^{N_{wb}} w^b_{0mn}e_c EA_s\left[\frac{f\pi}{L}\left(\frac{p\pi}{L}\right)^2\frac{m\pi}{L}I^{scc}_{pfm}\right. \\
&\qquad \left. + \left(\frac{f\pi}{L}\right)^2\frac{p\pi}{L}\frac{m\pi}{L}I^{scc}_{fpm}\right]\frac{y_s}{b}\sin(\frac{q\pi}{b}y_s)\sin(\frac{n\pi}{b}y_s)\dot{w}^b_{pq} \\
&+ \sum_{p=1}^{M_{wb}}\sum_{q=1}^{N_{wb}}\sum_{m=1}^{M_{wa}}\sum_{r=1}^{M_{wa}} w^a_{0m}w^a_{0r}EA_s\frac{f\pi}{L}\frac{p\pi}{L}\frac{m\pi}{L}\frac{r\pi}{L} \\
&\qquad \cdot\left(\frac{y_s}{b}\right)^3\sin(\frac{q\pi}{b}y_s)I^{cccc}_{pfmr}\dot{w}^b_{pq} \\
&+ \sum_{p=1}^{M_{wb}}\sum_{q=1}^{N_{wb}}\sum_{m=1}^{M_{wa}}\sum_{r=1}^{M_{wa}}\sum_{s=1}^{N_{wb}} w^a_{0m}w^b_{0rs}2EA_s\frac{f\pi}{L}\frac{p\pi}{L}\frac{m\pi}{L}\frac{r\pi}{L} \\
&\qquad \cdot\left(\frac{y_s}{b}\right)^2\sin(\frac{q\pi}{b}y_s)\sin(\frac{s\pi}{b}y_s)I^{cccc}_{pfmr}\dot{w}^b_{pq} \\
&+ \sum_{p=1}^{M_{wb}}\sum_{q=1}^{N_{wb}}\sum_{m=1}^{M_{wb}}\sum_{n=1}^{N_{wb}}\sum_{r=1}^{M_{wa}}\sum_{s=1}^{N_{wb}} w^b_{0mn}w^b_{0rs}EA_s\frac{f\pi}{L}\frac{p\pi}{L}\frac{m\pi}{L}\frac{r\pi}{L} \\
&\qquad \cdot\frac{y_s}{b}\sin(\frac{q\pi}{b}y_s)\sin(\frac{n\pi}{b}y_s)\sin(\frac{s\pi}{b}y_s)I^{cccc}_{pfmr}\dot{w}^b_{pq}
\end{aligned} \tag{157}
$$

$$
\mathbf{K}^{sL,x}_{wbwa} = (\mathbf{K}^{sL,x}_{wawb})^T \tag{158}
$$

$$
\begin{aligned}
\mathbf{K}_{wbwb}^{sL,x}\dot{\mathbf{w}}^b &= \frac{\partial^2 U^{sL,x}}{\partial w_{fg}^b \partial w_{pq}^b}\dot{w}_{pq}^b \\
&= \sum_{p=1}^{M_{wb}}\sum_{q=1}^{N_{wb}} EI\left(\frac{f\pi}{L}\right)^4 \sin(\frac{g\pi}{b}y_s)\sin(\frac{q\pi}{b}y_s)\frac{L}{2}\delta_{fp}\dot{w}_{pq}^b \\
&\quad + \sum_{p=1}^{M_{wb}}\sum_{q=1}^{N_{wb}}\sum_{m=1}^{M_{wa}} w_{0m}^a e_c EA_s\left[\frac{f\pi}{L}\left(\frac{p\pi}{L}\right)^2\frac{m\pi}{L}I_{pfm}^{scc}\right. \\
&\quad \left. + \frac{p\pi}{L}\left(\frac{f\pi}{L}\right)^2\frac{m\pi}{L}I_{fpm}^{scc}\right]\frac{y_s}{b}\sin(\frac{g\pi}{b}y_s)\sin(\frac{q\pi}{b}y_s)\dot{w}_{pq}^b \\
&\quad + \sum_{p=1}^{M_{wb}}\sum_{q=1}^{N_{wb}}\sum_{m=1}^{M_{wb}}\sum_{n=1}^{N_{wb}} w_{0mn}^b e_c EA_s\left[\frac{f\pi}{L}\left(\frac{p\pi}{L}\right)^2\frac{m\pi}{L}I_{pfm}^{scc}\right. \\
&\quad \left. + \frac{p\pi}{L}\left(\frac{f\pi}{L}\right)^2\frac{m\pi}{L}I_{fpm}^{scc}\right]\sin(\frac{g\pi}{b}y_s)\sin(\frac{q\pi}{b}y_s)\sin(\frac{n\pi}{b}y_s)\dot{w}_{pq}^b \qquad (159) \\
&\quad + \sum_{p=1}^{M_{wb}}\sum_{q=1}^{N_{wb}}\sum_{m=1}^{M_{wa}}\sum_{r=1}^{M_{wa}} w_{0m}^a w_{0r}^a EA_s\frac{f\pi}{L}\frac{p\pi}{L}\frac{m\pi}{L}\frac{r\pi}{L} \\
&\quad \cdot\left(\frac{y_s}{b}\right)^2\sin(\frac{g\pi}{b}y_s)\sin(\frac{q\pi}{b}y_s)I_{pfmr}^{cccc}\dot{w}_{pq}^b \\
&\quad + \sum_{p=1}^{M_{wb}}\sum_{q=1}^{N_{wb}}\sum_{m=1}^{M_{wa}}\sum_{r=1}^{M_{wa}}\sum_{s=1}^{N_{wb}} w_{0m}^a w_{0rs}^b 2EA_s\frac{f\pi}{L}\frac{p\pi}{L}\frac{m\pi}{L}\frac{r\pi}{L} \\
&\quad \cdot\frac{y_s}{b}\sin(\frac{g\pi}{b}y_s)\sin(\frac{q\pi}{b}y_s)\sin(\frac{s\pi}{b}y_s)I_{pfmr}^{cccc}\dot{w}_{pq}^b \\
&\quad + \sum_{p=1}^{M_{wb}}\sum_{q=1}^{N_{wb}}\sum_{m=1}^{M_{wb}}\sum_{n=1}^{N_{wb}}\sum_{r=1}^{M_{wa}}\sum_{s=1}^{N_{wb}} w_{0mn}^b w_{0rs}^b EA_s\frac{f\pi}{L}\frac{p\pi}{L}\frac{m\pi}{L}\frac{r\pi}{L} \\
&\quad \cdot\sin(\frac{g\pi}{b}y_s)\sin(\frac{q\pi}{b}y_s)\sin(\frac{n\pi}{b}y_s)\sin(\frac{s\pi}{b}y_s)I_{pfmr}^{cccc}\dot{w}_{pq}^b
\end{aligned}
$$

D.1.6 Definition of the $\mathbf{K}_{uw}^{sNL,x}$-matrix

The size of the matrix $\mathbf{K}_{uw}^{sNL,x}$ is $(M_{ua} + M_{ub}N_{ub} + 1) \times (M_{wa} + M_{wb}N_{wb})$. The matrix is a nonlinear contribution and is dependent of the displacement amplitudes. It consists of

the submatrices given in index notation in the following expressions

$$\mathbf{K}^{sNL,x}_{uawa}\dot{\mathbf{w}}^a = \frac{\partial^2 U^{sNL,x}}{\partial u^a_f \partial w^a_p}\dot{w}^a_p$$
$$= \sum_{p=1}^{M_{wa}}\sum_{m=1}^{M_{wa}} w^a_m EA_s\left[\frac{f\pi}{L}\frac{p\pi}{L}\frac{m\pi}{L}\left(\frac{y_s}{b}\right)^3 I^{ccc}_{fpm}\right]\dot{w}^a_p \tag{160}$$
$$+\sum_{p=1}^{M_{wa}}\sum_{m=1}^{M_{wb}}\sum_{n=1}^{N_{wb}} w^b_{mn} EA_s\left[\frac{f\pi}{L}\frac{p\pi}{L}\frac{m\pi}{L}\left(\frac{y_s}{b}\right)^2 \sin(\frac{n\pi}{b}y_s) I^{ccc}_{fpm}\right]\dot{w}^a_p$$

$$\mathbf{K}^{sNL,x}_{uawb}\dot{\mathbf{w}}^b = \frac{\partial^2 U^{sNL,x}}{\partial u^a_f \partial w^b_{pq}}\dot{w}^b_{pq}$$
$$= \sum_{p=1}^{M_{wb}}\sum_{q=1}^{N_{wb}}\sum_{m=1}^{M_{wa}} w^a_m EA_s\left[\frac{f\pi}{L}\frac{p\pi}{L}\frac{m\pi}{L}\left(\frac{y_s}{b}\right)^2 \sin(\frac{q\pi}{b}y_s) I^{ccc}_{fpm}\right]\dot{w}^b_{pq} \tag{161}$$
$$+\sum_{p=1}^{M_{wb}}\sum_{q=1}^{N_{wb}}\sum_{m=1}^{M_{wb}}\sum_{n=1}^{N_{wb}} w^b_{mn} EA_s\left[\frac{f\pi}{L}\frac{p\pi}{L}\frac{m\pi}{L}\frac{y_s}{b}\sin(\frac{q\pi}{b}y_s)\sin(\frac{n\pi}{b}y_s) I^{ccc}_{fpm}\right]\dot{w}^b_{pq}$$

$$\mathbf{K}^{sNL,x}_{ubwa}\dot{\mathbf{w}}^a = \frac{\partial^2 U^{sNL,x}}{\partial u^b_{fg} \partial w^a_p}\dot{w}^a_p$$
$$= \sum_{p=1}^{M_{wa}}\sum_{m=1}^{M_{wa}} w^a_m EA_s\left[\frac{f\pi}{L}\frac{p\pi}{L}\frac{m\pi}{L}\left(\frac{y_s}{b}\right)^2 \sin(\frac{g\pi}{b}y_s) I^{ccc}_{fpm}\right]\dot{w}^a_p \tag{162}$$
$$+\sum_{p=1}^{M_{wa}}\sum_{m=1}^{M_{wb}}\sum_{n=1}^{N_{wb}} w^b_{mn} EA_s\left[\frac{f\pi}{L}\frac{p\pi}{L}\frac{m\pi}{L}\frac{y_s}{b}\sin(\frac{g\pi}{b}y_s)\sin(\frac{n\pi}{b}y_s) I^{ccc}_{fpm}\right]\dot{w}^a_p$$

$$\mathbf{K}^{sNL,x}_{ubwb}\dot{\mathbf{w}}^b = \frac{\partial^2 U^{sNL,x}}{\partial u^b_{fg} \partial w^b_{pq}}\dot{w}^b_{pq}$$
$$= \sum_{p=1}^{M_{wb}}\sum_{q=1}^{N_{wb}}\sum_{m=1}^{M_{wa}} w^a_m EA_s\left[\frac{f\pi}{L}\frac{p\pi}{L}\frac{m\pi}{L}\frac{y_s}{b}\sin(\frac{g\pi}{b}y_s)\sin(\frac{q\pi}{b}y_s) I^{ccc}_{fpm}\right]\dot{w}^b_{pq} \tag{163}$$
$$+\sum_{p=1}^{M_{wb}}\sum_{q=1}^{N_{wb}}\sum_{m=1}^{M_{wb}}\sum_{n=1}^{N_{wb}} w^b_{mn} EA_s\left[\frac{f\pi}{L}\frac{p\pi}{L}\frac{m\pi}{L}\sin(\frac{g\pi}{b}y_s)\sin(\frac{q\pi}{b}y_s)\sin(\frac{n\pi}{b}y_s) I^{ccc}_{fpm}\right]\dot{w}^b_{pq}$$

$$\mathbf{K}^{sNL,x}_{ucwa}\dot{\mathbf{w}}^a = \frac{\partial^2 U^{sNL,x}}{\partial u^c \partial w^a_p}\dot{w}^a_p$$
$$= \sum_{p=1}^{M_{wa}} w^a_p EA_s\left[\left(\frac{p\pi}{L}\right)^2\left(\frac{y_s}{b}\right)^2\frac{1}{2}\right]\dot{w}^a_p \tag{164}$$
$$+\sum_{p=1}^{M_{wawb}}\sum_{n=1}^{N_{wb}} w^b_{pn} EA_s\left[\left(\frac{p\pi}{L}\right)^2\frac{y_s}{b}\sin(\frac{n\pi}{b}y_s)\frac{1}{2}\right]\dot{w}^a_p$$

$$\mathbf{K}^{sNL,x}_{ucwb}\dot{\mathbf{w}}^b = \frac{\partial^2 U^{sNL,x}}{\partial u^c \partial w^b_{pq}}\dot{w}^b_{pq}$$
$$= \sum_{p=1}^{M_{wawb}}\sum_{q=1}^{N_{wb}} w^a_p EA_s\left[\left(\frac{p\pi}{L}\right)^2 \frac{y_s}{b}\sin(\frac{q\pi}{b}y_s)\frac{1}{2}\right]\dot{w}^b_{pq} \tag{165}$$
$$+ \sum_{p=1}^{M_{wawb}}\sum_{q=1}^{N_{wb}}\sum_{n=1}^{N_{wb}} w^b_{pn} EA_s\left[\left(\frac{p\pi}{L}\right)^2 \sin(\frac{q\pi}{b}y_s)\sin(\frac{n\pi}{b}y_s)\frac{1}{2}\right]\dot{w}^b_{pq}$$

D.1.7 Definition of the $\mathbf{K}^{sNL,x}_{wu}$-matrix

Due to symmetry, the matrix can be given by

$$\mathbf{K}^{sNL,x}_{wu} = (\mathbf{K}^{sNL,x}_{uw})^T \tag{166}$$

where $\mathbf{K}^{sNL,x}_{uw}$ is given in Section D.1.6. The size of this matrix is $(M_{wa} + M_{wb}N_{wb}) \times (M_{ua} + M_{ub}N_{ub} + 1)$.

D.1.8 Definition of the $\mathbf{K}^{sNL,x}_{ww}$-matrix

The matrix $\mathbf{K}^{sNL,x}_{ww}$ is symmetrical, and the size of this matrix is $(M_{wa} + M_{wb}N_{wb}) \times (M_{wa} + M_{wb}N_{wb})$. The matrix is a nonlinear contribution and is dependent of the displacement amplitudes. It consists of the submatrices given in index notation in the

following expressions

$$
\begin{aligned}
\mathbf{K}^{sNL,x}_{wawa}\dot{\mathbf{w}}^a &= \frac{\partial^2 U^{sNL,x}}{\partial w^a_f \partial w^a_p}\dot{w}^a_p \\
&= \sum_{p=1}^{M_{wa}}\sum_{m=1}^{M_{wa}} w^a_m e_c E A_s \left[\frac{f\pi}{L}\frac{p\pi}{L}\left(\frac{m\pi}{L}\right)^2 I^{scc}_{mfp}\right. \\
&\left. + \frac{m\pi}{L}\frac{p\pi}{L}\left(\frac{f\pi}{L}\right)^2 I^{scc}_{fmp} + \frac{m\pi}{L}\frac{f\pi}{L}\left(\frac{p\pi}{L}\right)^2 I^{scc}_{pfm}\right]\left(\frac{y_s}{b}\right)^3 \dot{w}^a_p \\
&+ \sum_{p=1}^{M_{wa}}\sum_{m=1}^{M_{wb}}\sum_{n=1}^{N_{wb}} w^b_{mn} e_c E A_s \left[\frac{f\pi}{L}\frac{p\pi}{L}\left(\frac{m\pi}{L}\right)^2 I^{scc}_{mfp}\right. \\
&\left. + \frac{m\pi}{L}\frac{p\pi}{L}\left(\frac{f\pi}{L}\right)^2 I^{scc}_{fmp} + \frac{m\pi}{L}\frac{f\pi}{L}\left(\frac{p\pi}{L}\right)^2 I^{scc}_{pfm}\right]\left(\frac{y_s}{b}\right)^2 \sin(\frac{n\pi}{b}y_s)\dot{w}^a_p \\
&+ \sum_{p=1}^{M_{wa}}\sum_{m=1}^{M_{wa}}\sum_{r=1}^{M_{wa}} E A_s \frac{f\pi}{L}\frac{p\pi}{L}\frac{m\pi}{L}\frac{r\pi}{L}\left(\frac{y_s}{b}\right)^4 I^{cccc}_{pfmr}\left[3w^a_m w^a_{0r} + \frac{3}{2}w^a_m w^a_r\right]\dot{w}^a_p \\
&+ \sum_{p=1}^{M_{wa}}\sum_{m=1}^{M_{wa}}\sum_{r=1}^{M_{wb}}\sum_{s=1}^{N_{wb}} E A_s \frac{f\pi}{L}\frac{p\pi}{L}\frac{m\pi}{L}\frac{r\pi}{L} \\
&\qquad \cdot\left(\frac{y_s}{b}\right)^3 \sin(\frac{s\pi}{b}y_s) I^{cccc}_{pfmr}\left[3w^a_m w^b_{0rs} + 3w^a_{0m}w^b_{rs} + 3w^a_m w^b_{rs}\right]\dot{w}^a_p \\
&+ \sum_{p=1}^{M_{wa}}\sum_{m=1}^{M_{wb}}\sum_{n=1}^{N_{wb}}\sum_{r=1}^{M_{wb}}\sum_{s=1}^{N_{wb}} E A_s \frac{f\pi}{L}\frac{p\pi}{L}\frac{m\pi}{L}\frac{r\pi}{L} \\
&\qquad \cdot\left(\frac{y_s}{b}\right)^2 \sin(\frac{n\pi}{b}y_s)\sin(\frac{s\pi}{b}y_s) I^{cccc}_{pfmr}\left[3w^b_{mn}w^b_{0rs} + \frac{3}{2}w^b_{mn}w^b_{rs}\right]\dot{w}^a_p \\
&+ \sum_{p=1}^{M_{wa}}\sum_{i=1}^{M_{ua}} u^a_i E A_s \frac{i\pi}{L}\frac{f\pi}{L}\frac{p\pi}{L}\left(\frac{y_s}{b}\right)^3 I^{ccc}_{ipf}\dot{w}^a_p \\
&+ \sum_{p=1}^{M_{wa}}\sum_{i=1}^{M_{ub}}\sum_{j=1}^{N_{ub}} u^b_{ij} E A_s \frac{i\pi}{L}\frac{f\pi}{L}\frac{p\pi}{L}\left(\frac{y_s}{b}\right)^2 \sin(\frac{j\pi}{b}y_s) I^{ccc}_{ipf}\dot{w}^a_p \\
&+ \sum_{p=1}^{M_{wa}} u^c E A_s \frac{1}{2}\left(\frac{f\pi}{L}\right)^2\left(\frac{y_s}{b}\right)^2 \delta_{fp}\dot{w}^a_p
\end{aligned}
\tag{167}
$$

$$
\begin{aligned}
\mathbf{K}^{sNL,x}_{wawb}\dot{\mathbf{w}}^b &= \frac{\partial^2 U^{sNL,x}}{\partial w^a_f \partial w^b_{pq}}\dot{w}^b_{pq} \\
&= \sum_{p=1}^{M_{wb}}\sum_{q=1}^{N_{wb}}\sum_{m=1}^{M_{wa}} w^a_m e_c E A_s \left[\frac{f\pi}{L}\frac{p\pi}{L}\left(\frac{m\pi}{L}\right)^2 I^{scc}_{mfp}\right. \\
&\quad \left. + \frac{m\pi}{L}\frac{p\pi}{L}\left(\frac{f\pi}{L}\right)^2 I^{scc}_{fmp} + \frac{m\pi}{L}\frac{f\pi}{L}\left(\frac{p\pi}{L}\right)^2 I^{scc}_{pfm}\right]\left(\frac{y_s}{b}\right)^2 \sin(\frac{q\pi}{b}y_s)\dot{w}^b_{pq} \\
&+ \sum_{p=1}^{M_{wb}}\sum_{q=1}^{N_{wb}}\sum_{m=1}^{M_{wb}}\sum_{n=1}^{N_{wb}} w^b_{mn} e_c E A_s \left[\frac{f\pi}{L}\frac{p\pi}{L}\left(\frac{m\pi}{L}\right)^2 I^{scc}_{mfp}\right. \\
&\quad \left. + \frac{m\pi}{L}\frac{p\pi}{L}\left(\frac{f\pi}{L}\right)^2 I^{scc}_{fmp} + \frac{m\pi}{L}\frac{f\pi}{L}\left(\frac{p\pi}{L}\right)^2 I^{scc}_{pfm}\right]\frac{y_s}{b}\sin(\frac{q\pi}{b}y_s)\sin(\frac{n\pi}{b}y_s)\dot{w}^b_{pq} \\
&\quad + \sum_{p=1}^{M_{wb}}\sum_{q=1}^{N_{wb}}\sum_{m=1}^{M_{wa}}\sum_{r=1}^{M_{wa}} E A_s \frac{f\pi}{L}\frac{p\pi}{L}\frac{m\pi}{L}\frac{r\pi}{L} \\
&\qquad \cdot\left(\frac{y_s}{b}\right)^3 \sin(\frac{q\pi}{b}y_s) I^{cccc}_{pfmr}\left[3w^a_m w^a_{0r} + \frac{3}{2}w^a_m w^a_r\right]\dot{w}^b_{pq} \\
&\quad + \sum_{p=1}^{M_{wb}}\sum_{q=1}^{N_{wb}}\sum_{m=1}^{M_{wa}}\sum_{r=1}^{M_{wb}}\sum_{s=1}^{N_{wb}} E A_s \frac{f\pi}{L}\frac{p\pi}{L}\frac{m\pi}{L}\frac{r\pi}{L} \\
&\qquad \cdot\left(\frac{y_s}{b}\right)^2 \sin(\frac{q\pi}{b}y_s)\sin(\frac{s\pi}{b}y_s) I^{cccc}_{pfmr}\left[3w^a_m w^b_{0rs} + 3w^a_{0m} w^b_{rs} + 3w^a_m w^b_{rs}\right]\dot{w}^b_{pq} \\
&+ \sum_{p=1}^{M_{wb}}\sum_{q=1}^{N_{wb}}\sum_{m=1}^{M_{wb}}\sum_{n=1}^{N_{wb}}\sum_{r=1}^{M_{wb}}\sum_{s=1}^{N_{wb}} E A_s \frac{f\pi}{L}\frac{p\pi}{L}\frac{m\pi}{L}\frac{r\pi}{L} \\
&\quad \cdot\frac{y_s}{b}\sin(\frac{n\pi}{b}y_s)\sin(\frac{s\pi}{b}y_s)\sin(\frac{q\pi}{b}y_s) I^{cccc}_{pfmr}\left[3w^b_{mn} w^b_{0rs} + \frac{3}{2}w^b_{mn} w^b_{rs}\right]\dot{w}^b_{pq} \\
&\quad + \sum_{p=1}^{M_{wb}}\sum_{q=1}^{N_{wb}}\sum_{i=1}^{M_{ua}} u^a_i E A_s \frac{i\pi}{L}\frac{f\pi}{L}\frac{p\pi}{L}\left(\frac{y_s}{b}\right)^2 \sin(\frac{q\pi}{b}y_s) I^{ccc}_{ipf}\dot{w}^b_{pq} \\
&+ \sum_{p=1}^{M_{wb}}\sum_{q=1}^{N_{wb}}\sum_{i=1}^{M_{ub}}\sum_{j=1}^{N_{ub}} u^b_{ij} E A_s \frac{i\pi}{L}\frac{f\pi}{L}\frac{p\pi}{L}\frac{y_s}{b}\sin(\frac{j\pi}{b}y_s)\sin(\frac{q\pi}{b}y_s) I^{ccc}_{ipf}\dot{w}^b_{pq} \\
&\quad + \sum_{p=1}^{M_{wb}}\sum_{q=1}^{N_{wb}} u^c E A_s \frac{1}{2}\left(\frac{f\pi}{L}\right)^2 \frac{y_s}{b}\sin(\frac{q\pi}{b}y_s)\delta_{fp}\dot{w}^b_{pq}
\end{aligned} \tag{168}
$$

$$
\mathbf{K}^{sNL,x}_{wbwa} = (\mathbf{K}^{sNL,x}_{wawb})^T \tag{169}
$$

$$
\begin{aligned}
&\mathbf{K}^{sNL,x}_{wbwb}\dot{\mathbf{w}}^b = \frac{\partial^2 U^{sNL,x}}{\partial w^b_{fg}\partial w^b_{pq}}\dot{w}^b_{pq} \\
&= \sum_{p=1}^{M_{wb}}\sum_{q=1}^{N_{wb}}\sum_{m=1}^{M_{wb}}\sum_{n=1}^{N_{wb}} w^b_{mn} e_c E A_s \left[\frac{f\pi}{L}\frac{p\pi}{L}\left(\frac{m\pi}{L}\right)^2 I^{scc}_{mfp}\right. \\
&\qquad \left. + \frac{m\pi}{L}\frac{p\pi}{L}\left(\frac{f\pi}{L}\right)^2 I^{scc}_{fmp} + \frac{m\pi}{L}\frac{f\pi}{L}\left(\frac{p\pi}{L}\right)^2 I^{scc}_{pfm}\right]\sin(\frac{g\pi}{b}y_s)\sin(\frac{q\pi}{b}y_s)\sin(\frac{n\pi}{b}y_s)\dot{w}^b_{pq} \\
&\quad + \sum_{p=1}^{M_{wb}}\sum_{q=1}^{N_{wb}}\sum_{m=1}^{M_{wa}} w^a_m e_c E A_s \left[\frac{f\pi}{L}\frac{p\pi}{L}\left(\frac{m\pi}{L}\right)^2 I^{scc}_{mfp}\right. \\
&\qquad \left. + \frac{m\pi}{L}\frac{p\pi}{L}\left(\frac{f\pi}{L}\right)^2 I^{scc}_{fmp} + \frac{m\pi}{L}\frac{f\pi}{L}\left(\frac{p\pi}{L}\right)^2 I^{scc}_{pfm}\right]\frac{y_s}{b}\sin(\frac{g\pi}{b}y_s)\sin(\frac{q\pi}{b}y_s)\dot{w}^b_{pq} \\
&\quad + \sum_{p=1}^{M_{wb}}\sum_{q=1}^{N_{wb}}\sum_{m=1}^{M_{wa}}\sum_{r=1}^{M_{wa}} E A_s \frac{f\pi}{L}\frac{p\pi}{L}\frac{m\pi}{L}\frac{r\pi}{L} \\
&\qquad \cdot\left(\frac{y_s}{b}\right)^2 \sin(\frac{g\pi}{b}y_s)\sin(\frac{q\pi}{b}y_s) I^{cccc}_{pfmr}\left[3w^a_m w^a_{0r} + \frac{3}{2}w^a_m w^a_r\right]\dot{w}^b_{pq} \\
&\quad + \sum_{p=1}^{M_{wb}}\sum_{q=1}^{N_{wb}}\sum_{m=1}^{M_{wa}}\sum_{r=1}^{M_{wb}}\sum_{s=1}^{N_{wb}} E A_s \frac{f\pi}{L}\frac{p\pi}{L}\frac{m\pi}{L}\frac{r\pi}{L} \\
&\qquad \cdot\frac{y_s}{b}\sin(\frac{g\pi}{b}y_s)\sin(\frac{q\pi}{b}y_s)\sin(\frac{s\pi}{b}y_s) I^{cccc}_{pfmr}\left[3w^a_m w^b_{0rs} + 3w^a_{0m} w^b_{rs} + 3w^a_m w^b_{rs}\right]\dot{w}^b_{pq} \\
&\quad + \sum_{p=1}^{M_{wb}}\sum_{q=1}^{N_{wb}}\sum_{m=1}^{M_{wb}}\sum_{n=1}^{N_{wb}}\sum_{r=1}^{M_{wb}}\sum_{s=1}^{N_{wb}} E A_s \frac{f\pi}{L}\frac{p\pi}{L}\frac{m\pi}{L}\frac{r\pi}{L} \\
&\qquad \cdot\sin(\frac{g\pi}{b}y_s)\sin(\frac{n\pi}{b}y_s)\sin(\frac{s\pi}{b}y_s)\sin(\frac{q\pi}{b}y_s) I^{cccc}_{pfmr}\left[3w^b_{mn} w^b_{0rs} + \frac{3}{2}w^b_{mn} w^b_{rs}\right]\dot{w}^b_{pq} \\
&\quad + \sum_{p=1}^{M_{wb}}\sum_{q=1}^{N_{wb}}\sum_{i=1}^{M_{ua}} u^a_i E A_s \frac{i\pi}{L}\frac{f\pi}{L}\frac{p\pi}{L}\frac{y_s}{b}\sin(\frac{g\pi}{b}y_s)\sin(\frac{q\pi}{b}y_s) I^{ccc}_{ipf}\dot{w}^b_{pq} \\
&\quad + \sum_{p=1}^{M_{wb}}\sum_{q=1}^{N_{wb}}\sum_{i=1}^{M_{ub}}\sum_{j=1}^{N_{ub}} u^b_{ij} E A_s \frac{i\pi}{L}\frac{f\pi}{L}\frac{p\pi}{L}\sin(\frac{j\pi}{b}y_s)\sin(\frac{g\pi}{b}y_s)\sin(\frac{q\pi}{b}y_s) I^{ccc}_{ipf}\dot{w}^b_{pq} \\
&\qquad + \sum_{p=1}^{M_{wb}}\sum_{q=1}^{N_{wb}} u^c E A_s \frac{1}{2}\left(\frac{f\pi}{L}\right)^2 \sin(\frac{g\pi}{b}y_s)\sin(\frac{q\pi}{b}y_s)\delta_{fp}\dot{w}^b_{pq}
\end{aligned}
\tag{170}
$$

D.2 The generalised, incremental stiffness matrix $\mathbf{K}^{s,y}$ for stiffeners perpendicular to the free edge

D.2.1 Introduction

In the chosen coordinate system, defined in Fig. 4, stiffeners perpendicular to the free edge are oriented in the y-direction. In order to indicate the direction of the stiffeners, 'y' is included in the super index in the stiffener contributions.

In the expressions below, integrals are replace with simplified expressions, I_m^s, I_{mn}^{cs}, etc. For instance,

$$I_m^s = \int_0^b \sin(\frac{m\pi}{b}y)\, dy = \frac{b}{m\pi}[1-(-1)^m] \tag{171}$$

is introduced. The expressions for all the integrals can be found in Appendix F. In addition , the Kronecker delta defined by

$$\delta_{ij} = \begin{cases} 1 & \text{if } i = j \\ 0 & \text{otherwise} \end{cases} \tag{172}$$

is used. Further, in order to simplify the expression of the contributions for the stiffeners perpendicular to the free edge, the following term

$$J_{ikmr}^{ssss} = \sin(\frac{i\pi}{L}x_s)\sin(\frac{k\pi}{L}x_s)\sin(\frac{m\pi}{L}x_s)\sin(\frac{r\pi}{L}x_s) \tag{173}$$

is introduced, since this term appears quite frequently in the expressions. Details on how to build the matrices is given in Appendix A and B.

D.2.2 Definition of the $\mathbf{K}_{vv}^{sL,y}$-matrix

The matrix $\mathbf{K}_{vv}^{sL,y}$ is symmetrical, and the size of this matrix is $(M_{va} + M_{vb}N_{vb} + 1) \times (M_{va} + M_{vb}N_{vb} + 1)$. The matrix is a constant contribution and consists of the sub-matrices given in index notation in the following expressions

$$\begin{aligned} \mathbf{K}_{vava}^{sL,y}\dot{\mathbf{v}}^a &= \frac{\partial^2 U^{sL,y}}{\partial v_f^a \partial v_p^a}\dot{v}_p^a \\ &= \sum_{p=1}^{M_{va}} EA_s \frac{1}{b}\cos(\frac{f\pi}{L}x_s)\cos(\frac{p\pi}{L}x_s)\dot{v}_p^a \end{aligned} \tag{174}$$

$$\begin{aligned} \mathbf{K}_{vbvb}^{sL,y}\dot{\mathbf{v}}^b &= \frac{\partial^2 U^{sL,y}}{\partial v_{fg}^b \partial v_{pq}^b}\dot{v}_{pq}^b \\ &= \sum_{p=1}^{M_{vb}}\sum_{q=1}^{N_{vb}} EA_s\left(\frac{g\pi}{b}\right)^2 \frac{b}{2}\sin(\frac{f\pi}{L}x_s)\sin(\frac{p\pi}{L}x_s)\delta_{gq}\dot{v}_{pq}^b \end{aligned} \tag{175}$$

$$\mathbf{K}^{sL,y}_{vcvc}\dot{\mathbf{v}}^c = \frac{\partial^2 U^{sL,y}}{\partial v^c \partial v^c}\dot{v}^c = EA_s\frac{1}{b}\dot{v}^c \tag{176}$$

$$\mathbf{K}^{sL,y}_{vavc}\dot{\mathbf{v}}^c = \frac{\partial^2 U^{sL,y}}{\partial v^a_f \partial v^c}\dot{v}^c = EA_s\frac{1}{b}\cos(\frac{f\pi}{L}x_s)\dot{v}^c \tag{177}$$

$$\mathbf{K}^{sL,y}_{vcva}\dot{\mathbf{v}}^a = \frac{\partial^2 U^{sL,y}}{\partial v^c \partial v^a_p}\dot{v}^a_p = \sum_{p=1}^{M_{va}} EA_s\frac{1}{b}\cos(\frac{p\pi}{L}x_s)\dot{v}^a_p \tag{178}$$

$$\mathbf{K}^{sL,y}_{vavb} = 0, \quad \mathbf{K}^{sL,y}_{vbva} = 0, \quad \mathbf{K}^{sL,y}_{vbvc} = 0, \quad \mathbf{K}^{sL,y}_{vcvb} = 0 \tag{179}$$

D.2.3 Definition of the $\mathbf{K}^{sL,y}_{vw}$-matrix

The size of the matrix $\mathbf{K}^{sL,y}_{vw}$ is $(M_{va} + M_{vb}N_{vb} + 1) \times (M_{wa} + M_{wb}N_{wb})$. The matrix is a constant contribution and consists of the submatrices given in index notation in the following expressions

$$\mathbf{K}^{sL,y}_{vawa}\dot{\mathbf{w}}^a = \frac{\partial^2 U^{sL,y}}{\partial v^a_f \partial w^a_p}\dot{w}^a_p = \sum_{p=1}^{M_{wa}}\sum_{m=1}^{M_{wa}} w^a_{0m} EA_s\left(\frac{1}{b}\right)^2\cos(\frac{f\pi}{L}x_s)\sin(\frac{p\pi}{L}x_s)\sin(\frac{m\pi}{L}x_s)\dot{w}^a_p \tag{180}$$

$$\begin{aligned}\mathbf{K}^{sL,y}_{vawb}\dot{\mathbf{w}}^b &= \frac{\partial^2 U^{sL,y}}{\partial v^a_f \partial w^b_{pq}}\dot{w}^b_{pq} \\ &= \sum_{p=1}^{M_{wb}}\sum_{q=1}^{N_{wb}} e_c EA_s\left(\frac{q\pi}{b}\right)^2\frac{1}{b}I^s_q\cos(\frac{f\pi}{L}x_s)\sin(\frac{p\pi}{L}x_s)\dot{w}^b_{pq} \\ &+ \sum_{p=1}^{M_{wb}}\sum_{q=1}^{N_{wb}}\sum_{m=1}^{M_{wb}} w^b_{0mq} EA_s\left(\frac{q\pi}{b}\right)^2\frac{1}{2}\cos(\frac{f\pi}{L}x_s)\sin(\frac{p\pi}{L}x_s)\sin(\frac{m\pi}{L}x_s)\dot{w}^b_{pq}\end{aligned} \tag{181}$$

$$\mathbf{K}^{sL,y}_{vbwa}\dot{\mathbf{w}}^a = \frac{\partial^2 U^{sL,y}}{\partial v^b_{fg} \partial w^a_p}\dot{w}^a_p = \sum_{p=1}^{M_{wa}}\sum_{m=1}^{M_{wa}} w^b_{0mg} EA_s\left(\frac{g\pi}{b}\right)^2\frac{1}{2}\sin(\frac{f\pi}{L}x_s)\sin(\frac{p\pi}{L}x_s)\sin(\frac{m\pi}{L}x_s)\dot{w}^a_p \tag{182}$$

$$\begin{aligned}\mathbf{K}^{sL,y}_{vbwb}\dot{\mathbf{w}}^b &= \frac{\partial^2 U^{sL,y}}{\partial v^b_{fg} \partial w^b_{pq}}\dot{w}^b_{pq} \\ &= \sum_{p=1}^{M_{wb}}\sum_{q=1}^{N_{wb}} e_c EA_s\left(\frac{q\pi}{b}\right)^2\frac{g\pi}{b}I^{cs}_{gq}\sin(\frac{f\pi}{L}x_s)\sin(\frac{p\pi}{L}x_s)\dot{w}^b_{pq} \\ &+ \sum_{p=1}^{M_{wb}}\sum_{q=1}^{N_{wb}}\sum_{m=1}^{M_{wa}} w^a_{0m} EA_s\left(\frac{g\pi}{b}\right)^2\frac{1}{2}\sin(\frac{f\pi}{L}x_s)\sin(\frac{p\pi}{L}x_s)\sin(\frac{m\pi}{L}x_s)\delta_{gq}\dot{w}^b_{pq} \\ &+ \sum_{p=1}^{M_{wb}}\sum_{q=1}^{N_{wb}}\sum_{m=1}^{M_{wb}}\sum_{m=1}^{M_{wb}} w^b_{0mn} EA_s\frac{g\pi}{b}\frac{q\pi}{b}\frac{n\pi}{b}I^{ccc}_{gqn}\sin(\frac{f\pi}{L}x_s)\sin(\frac{p\pi}{L}x_s)\sin(\frac{m\pi}{L}x_s)\dot{w}^b_{pq}\end{aligned} \tag{183}$$

$$\mathbf{K}^{sL,y}_{vcwa}\dot{\mathbf{w}}^a = \frac{\partial^2 U^{sL,y}}{\partial v^c \partial w^a_p}\dot{w}^a_p = \sum_{p=1}^{M_{wa}}\sum_{m=1}^{M_{wa}} w^a_{0m} EA_s \left(\frac{1}{b}\right)^2 \sin(\frac{p\pi}{L}x_s)\sin(\frac{m\pi}{L}x_s)\dot{w}^a_p \tag{184}$$

$$\begin{aligned}\mathbf{K}^{sL,y}_{vcwb}\dot{\mathbf{w}}^b &= \frac{\partial^2 U^{sL,y}}{\partial v^c \partial w^b_{pq}}\dot{w}^b_{pq} \\ &= \sum_{p=1}^{M_{wb}}\sum_{q=1}^{N_{wb}} e_c EA_s \left(\frac{q\pi}{b}\right)^2 \frac{1}{b} I^s_q \sin(\frac{p\pi}{L}x_s)\dot{w}^b_{pq} \\ &+ \sum_{p=1}^{M_{wb}}\sum_{q=1}^{N_{wb}}\sum_{m=1}^{M_{wb}} w^a_{0mq} EA_s \left(\frac{q\pi}{b}\right)^2 \frac{1}{2}\sin(\frac{p\pi}{L}x_s)\sin(\frac{m\pi}{L}x_s)\dot{w}^b_{pq}\end{aligned} \tag{185}$$

D.2.4 Definition of the $\mathbf{K}^{sL,y}_{wv}$-matrix

Due to symmetry, the matrix can be given by

$$\mathbf{K}^{sL,y}_{wv} = (\mathbf{K}^{sL,y}_{vw})^T \tag{186}$$

where $\mathbf{K}^{sL,y}_{vw}$ is given in Section D.2.3. The size of this matrix is $(M_{wa} + M_{wb}N_{wb}) \times (M_{va} + M_{vb}N_{vb} + 1)$.

D.2.5 Definition of the $\mathbf{K}^{sL,y}_{ww}$-matrix

The matrix $\mathbf{K}^{sL,y}_{ww}$ is symmetrical, and the size of this matrix is $(M_{wa} + M_{wb}N_{wb}) \times (M_{wa} + M_{wb}N_{wb})$. The matrix is a constant contribution and consists of the submatrices given in index notation in the following expressions

$$\begin{aligned}\mathbf{K}^{sL,y}_{wawa}\dot{\mathbf{w}}^a &= \frac{\partial^2 U^{sL,y}}{\partial w^a_f \partial w^a_p}\dot{w}^a_p \\ &= \sum_{p=1}^{M_{wa}}\sum_{m=1}^{M_{wa}}\sum_{r=1}^{M_{wa}} w^a_{0m} w^a_{0r} EA_s \left(\frac{1}{b}\right)^3 J^{ssss}_{fpmr}\dot{w}^a_p \\ &+ \sum_{p=1}^{M_{wa}}\sum_{m=1}^{M_{wb}}\sum_{n=1}^{N_{wb}}\sum_{r=1}^{M_{wb}} w^b_{0mn} w^b_{0rn} EA_s \frac{1}{b}\left(\frac{n\pi}{b}\right)^2 \frac{1}{2} J^{ssss}_{fpmr}\dot{w}^a_p\end{aligned} \tag{187}$$

$$\mathbf{K}^{sL,y}_{wawb}\dot{\mathbf{w}}^b = \frac{\partial^2 U^{sL,y}}{\partial w^a_f \partial w^b_{pq}}\dot{w}^b_{pq}$$

$$= \sum_{p=1}^{M_{wb}}\sum_{q=1}^{N_{wb}}\sum_{m=1}^{M_{wa}} w^a_{0m} e_c E A_s \left[\left(\frac{1}{b}\right)^2\left(\frac{q\pi}{b}\right)^2 I^s_q \sin(\frac{f\pi}{L}x_s)\sin(\frac{p\pi}{L}x_s)\sin(\frac{m\pi}{L}x_s)\right]\dot{w}^b_{pq}$$

$$+\sum_{p=1}^{M_{wb}}\sum_{q=1}^{N_{wb}}\sum_{m=1}^{M_{wb}}\sum_{n=1}^{N_{wb}} w^b_{0mn} e_c E A_s \left[\frac{1}{b}\left(\frac{q\pi}{b}\right)^2\frac{n\pi}{b} I^{cs}_{nq}\sin(\frac{f\pi}{L}x_s)\sin(\frac{p\pi}{L}x_s)\sin(\frac{m\pi}{L}x_s)\right]\dot{w}^b_{pq} \quad (188)$$

$$+\sum_{p=1}^{M_{wb}}\sum_{q=1}^{N_{wb}}\sum_{m=1}^{M_{wa}}\sum_{r=1}^{M_{wb}} w^a_{0m} w^b_{0rq} E A_s \frac{1}{b}\left(\frac{q\pi}{b}\right)^2 J^{ssss}_{fpmr}\dot{w}^b_{pq}$$

$$+\sum_{p=1}^{M_{wb}}\sum_{q=1}^{N_{wb}}\sum_{m=1}^{M_{wb}}\sum_{n=1}^{N_{wb}}\sum_{r=1}^{M_{wb}}\sum_{s=1}^{N_{wb}} w^b_{0mn} w^b_{0rs} E A_s \frac{1}{b}\frac{q\pi}{b}\frac{n\pi}{b}\frac{s\pi}{b} J^{ssss}_{fpmr} I^{ccc}_{qns}\dot{w}^b_{pq}$$

$$\mathbf{K}^{sL,y}_{wbwa} = (\mathbf{K}^{sL,y}_{wawb})^T \quad (189)$$

$$\mathbf{K}^{sL,y}_{wbwb}\dot{\mathbf{w}}^b = \frac{\partial^2 U^{sL,y}}{\partial w^b_{fg}\partial w^b_{pq}}\dot{w}^b_{pq}$$

$$= \sum_{p=1}^{M_{wb}}\sum_{q=1}^{N_{wb}} \frac{EI}{2}\left(\frac{g\pi}{b}\right)^4 b\,\sin(\frac{f\pi}{L}x_s)\sin(\frac{p\pi}{L}x_s)\delta_{gq}\dot{w}^b_{pq}$$

$$+\sum_{p=1}^{M_{wb}}\sum_{q=1}^{N_{wb}}\sum_{m=1}^{M_{wa}} w^a_{0m} e_c E A_s \left[\frac{1}{b}\left(\frac{q\pi}{b}\right)^2\frac{g\pi}{b} I^{cs}_{gq}\right.$$

$$\left.+\frac{1}{b}\left(\frac{g\pi}{b}\right)^2\frac{q\pi}{b} I^{cs}_{qg}\right]\sin(\frac{f\pi}{L}x_s)\sin(\frac{p\pi}{L}x_s)\sin(\frac{m\pi}{L}x_s)\Big]\dot{w}^b_{pq}$$

$$+\sum_{p=1}^{M_{wb}}\sum_{q=1}^{N_{wb}}\sum_{m=1}^{M_{wb}}\sum_{n=1}^{N_{wb}} w^b_{0mn} e_c E A_s \left[\left(\frac{q\pi}{b}\right)^2\frac{g\pi}{b}\frac{n\pi}{b} I^{scc}_{qgn}\right. \quad (190)$$

$$\left.+\left(\frac{g\pi}{b}\right)^2\frac{q\pi}{b}\frac{n\pi}{b} I^{scc}_{gqn}\right]\sin(\frac{f\pi}{L}x_s)\sin(\frac{p\pi}{L}x_s)\sin(\frac{m\pi}{L}x_s)\Big]\dot{w}^b_{pq}$$

$$+\sum_{p=1}^{M_{wb}}\sum_{q=1}^{N_{wb}}\sum_{m=1}^{M_{wa}}\sum_{r=1}^{M_{wa}} w^a_{0m} w^a_{0r} E A_s \frac{1}{b}\left(\frac{g\pi}{b}\right)^2\frac{1}{2} J^{ssss}_{fpmr}\delta_{gq}\dot{w}^b_{pq}$$

$$+\sum_{p=1}^{M_{wb}}\sum_{q=1}^{N_{wb}}\sum_{m=1}^{M_{wa}}\sum_{r=1}^{N_{wb}}\sum_{s=1}^{N_{wb}} w^a_{0m} w^b_{0rs} 2E A_s \frac{g\pi}{b}\frac{q\pi}{b}\frac{s\pi}{b}\frac{1}{b} J^{ssss}_{fpmr} I^{ccc}_{gqn}\dot{w}^b_{pq}$$

$$+\sum_{p=1}^{M_{wb}}\sum_{q=1}^{N_{wb}}\sum_{m=1}^{M_{wb}}\sum_{n=1}^{N_{wb}}\sum_{r=1}^{N_{wb}}\sum_{s=1}^{N_{wb}} w^b_{0mn} w^b_{0rs} E A_s \frac{g\pi}{b}\frac{q\pi}{b}\frac{n\pi}{b}\frac{s\pi}{b} J^{ssss}_{fpmr} I^{cccc}_{gqns}\dot{w}^b_{pq}$$

D.2.6 Definition of the $\mathbf{K}_{vw}^{sNL,y}$-matrix

The size of the matrix $\mathbf{K}_{vw}^{sNL,y}$ is $(M_{va} + M_{vb}N_{vb} + 1) \times (M_{wa} + M_{wb}N_{wb})$. The matrix is a nonlinear contribution and is dependent of the displacement amplitudes. It consists of the submatrices given in index notation in the following expressions

$$\mathbf{K}_{vawa}^{sNL,y}\dot{\mathbf{w}}^a = \frac{\partial^2 U^{sNL,y}}{\partial v_f^a \partial w_p^a}\dot{w}_p^a = \sum_{p=1}^{M_{wa}}\sum_{m=1}^{M_{wa}} w_m^a EA_s\left(\frac{1}{b}\right)^2 \cos(\frac{f\pi}{L}x_s)\sin(\frac{p\pi}{L}x_s)\sin(\frac{m\pi}{L}x_s)\dot{w}_p^a \tag{191}$$

$$\mathbf{K}_{vawb}^{sNL,y}\dot{\mathbf{w}}^b = \frac{\partial^2 U^{sNL,y}}{\partial v_f^a \partial w_{pq}^b}\dot{w}_{pq}^b = \sum_{p=1}^{M_{wb}}\sum_{q=1}^{N_{wb}}\sum_{m=1}^{M_{wb}} w_{mq}^b EA_s\left(\frac{q\pi}{b}\right)^2 \frac{1}{2}\cos(\frac{f\pi}{L}x_s)\sin(\frac{p\pi}{L}x_s)\sin(\frac{m\pi}{L}x_s)\dot{w}_{pq}^b \tag{192}$$

$$\mathbf{K}_{vbwa}^{sNL,y}\dot{\mathbf{w}}^a = \frac{\partial^2 U^{sNL,y}}{\partial v_{fg}^b \partial w_p^a}\dot{w}_p^a = \sum_{p=1}^{M_{wa}}\sum_{m=1}^{M_{wb}} w_{mg}^b EA_s\left(\frac{g\pi}{b}\right)^2 \frac{1}{2}\sin(\frac{f\pi}{L}x_s)\sin(\frac{p\pi}{L}x_s)\sin(\frac{m\pi}{L}x_s)\dot{w}_p^a \tag{193}$$

$$\begin{aligned}\mathbf{K}_{vbwb}^{sNL,y}\dot{\mathbf{w}}^b &= \frac{\partial^2 U^{sNL,y}}{\partial v_{fg}^b \partial w_{pq}^b}\dot{w}_{pq}^b \\ &= \sum_{p=1}^{M_{wb}}\sum_{q=1}^{N_{wb}}\sum_{m=1}^{M_{wb}}\sum_{n=1}^{N_{wb}} w_{mn}^b EA_s \frac{g\pi}{b}\frac{q\pi}{b}\frac{n\pi}{b}\sin(\frac{f\pi}{L}x_s)\sin(\frac{p\pi}{L}x_s)\sin(\frac{m\pi}{L}x_s) I_{gqn}^{ccc}\dot{w}_{pq}^b \\ &\quad + \sum_{p=1}^{M_{wb}}\sum_{q=1}^{N_{wb}}\sum_{m=1}^{M_{wa}} w_m^a EA_s\left(\frac{g\pi}{b}\right)^2 \frac{1}{2}\sin(\frac{f\pi}{L}x_s)\sin(\frac{p\pi}{L}x_s)\sin(\frac{m\pi}{L}x_s)\delta_{gq}\dot{w}_{pq}^b\end{aligned} \tag{194}$$

$$\mathbf{K}_{vcwa}^{sNL,y}\dot{\mathbf{w}}^a = \frac{\partial^2 U^{sNL,y}}{\partial v^c \partial w_p^a}\dot{w}_p^a = \sum_{p=1}^{M_{wa}}\sum_{m=1}^{M_{wa}} w_m^a EA_s\left(\frac{1}{b}\right)^2 \sin(\frac{p\pi}{L}x_s)\sin(\frac{m\pi}{L}x_s)\dot{w}_p^a \tag{195}$$

$$\mathbf{K}_{vcwb}^{sNL,y}\dot{\mathbf{w}}^b = \frac{\partial^2 U^{sNL,y}}{\partial v^c \partial w_{pq}^b}\dot{w}_{pq}^b = \sum_{p=1}^{M_{wb}}\sum_{q=1}^{N_{wb}}\sum_{m=1}^{M_{wb}} w_{mq}^b EA_s\left(\frac{g\pi}{b}\right)^2 \frac{1}{2}\sin(\frac{p\pi}{L}x_s)\sin(\frac{m\pi}{L}x_s)\dot{w}_{pq}^b \tag{196}$$

D.2.7 Definition of the $\mathbf{K}_{wv}^{sNL,y}$-matrix

Due to symmetry, the matrix can be given by

$$\mathbf{K}_{wv}^{sNL,y} = (\mathbf{K}_{vw}^{sNL,y})^T \tag{197}$$

where $\mathbf{K}_{vw}^{sNL,y}$ is given in Section D.2.6. The size of this matrix is $(M_{wa} + M_{wb}N_{wb}) \times (M_{va} + M_{vb}N_{vb} + 1)$.

D.2.8 Definition of the $\mathbf{K}_{ww}^{sNL,y}$-matrix

The matrix $\mathbf{K}_{ww}^{sNL,y}$ is symmetrical, and the size of this matrix is $(M_{wa} + M_{wb}N_{wb}) \times (M_{wa} + M_{wb}N_{wb})$. The matrix is a nonlinear contribution and is dependent of the displacement amplitudes. It consists of the submatrices given in index notation in the following expressions

$$
\begin{aligned}
\mathbf{K}_{wawa}^{sNL,y}\dot{\mathbf{w}}^a &= \frac{\partial^2 U^{sNL,y}}{\partial w_f^a \partial w_p^a}\dot{w}_p^a \\
&= \sum_{p=1}^{M_{wa}}\sum_{m=1}^{M_{wa}}\sum_{r=1}^{M_{wa}} EA_s\left(\frac{1}{b}\right)^3 J_{fpmr}^{ssss}\left[3w_m^a w_{0r}^a + \frac{3}{2}w_m^a w_r^a\right]\dot{w}_p^a \\
&+ \sum_{p=1}^{M_{wa}}\sum_{m=1}^{M_{wb}}\sum_{n=1}^{N_{wb}}\sum_{r=1}^{M_{wb}} EA_s\left(\frac{1}{b}\right)^2\left(\frac{n\pi}{b}\right)^2\frac{b}{2}J_{fpmr}^{ssss}\left[3w_{mn}^b w_{0rn}^b + \frac{3}{2}w_{mn}^b w_{rn}^b\right]\dot{w}_p^a \\
&+ \sum_{p=1}^{M_{wa}}\sum_{i=1}^{M_{va}} v_i^a EA_s\left(\frac{1}{b}\right)^2\cos(\frac{i\pi}{L}x_s)\sin(\frac{f\pi}{L}x_s)\sin(\frac{p\pi}{L}x_s)\dot{w}_p^a \\
&+ \sum_{p=1}^{M_{wb}} v^c EA_s\left(\frac{1}{b}\right)^2\sin(\frac{p\pi}{L}x_s)\sin(\frac{f\pi}{L}x_s)\dot{w}_p^a
\end{aligned}
\tag{198}
$$

$$
\begin{aligned}
\mathbf{K}_{wawb}^{sNL,y}\dot{\mathbf{w}}^b &= \frac{\partial^2 U^{sNL,y}}{\partial w_f^a \partial w_{pq}^b}\dot{w}_{pq}^b \\
&= \sum_{p=1}^{M_{wb}}\sum_{q=1}^{N_{wb}}\sum_{m=1}^{M_{wa}} w_m^a e_c EA_s\left[\left(\frac{1}{b}\right)^2\left(\frac{q\pi}{b}\right)^2 I_q^s\sin(\frac{f\pi}{L}x_s)\sin(\frac{p\pi}{L}x_s)\sin(\frac{m\pi}{L}x_s)\right]\dot{w}_{pq}^b \\
&+ \sum_{p=1}^{M_{wb}}\sum_{q=1}^{N_{wb}}\sum_{m=1}^{M_{wb}}\sum_{n=1}^{N_{wb}} w_{mn}^b e_c EA_s\left[\frac{1}{b}\left(\frac{n\pi}{b}\right)^2\frac{q\pi}{b}I_{qn}^{cs}\right. \\
&\qquad \left. + \frac{1}{b}\left(\frac{q\pi}{b}\right)^2\frac{n\pi}{b}I_{nq}^{cs}\right]\sin(\frac{f\pi}{L}x_s)\sin(\frac{p\pi}{L}x_s)\sin(\frac{m\pi}{L}x_s)\dot{w}_{pq}^b \\
&+ \sum_{p=1}^{M_{wb}}\sum_{q=1}^{N_{wb}}\sum_{m=1}^{M_{wa}}\sum_{r=1}^{M_{wb}} EA_s\left(\frac{q\pi}{b}\right)^2\left(\frac{1}{b}\right)^2\frac{b}{2}J_{fmpr}^{ssss}\left[3w_m^a w_{0rq}^b\right. \\
&\qquad \left. + 3w_{0m}^a w_{rq}^b + 3w_m^a w_{rq}^b\right]\dot{w}_{pq}^b \\
&+ \sum_{p=1}^{M_{wb}}\sum_{q=1}^{N_{wb}}\sum_{m=1}^{M_{wb}}\sum_{n=1}^{N_{wb}}\sum_{r=1}^{M_{wb}}\sum_{s=1}^{N_{wb}} EA_s\frac{1}{b}\frac{q\pi}{b}\frac{n\pi}{b}\frac{s\pi}{b}J_{fpmr}^{ssss}\left[3w_{mn}^b w_{0rs}^b + \frac{3}{2}w_{mn}^b w_{rs}^b\right]\dot{w}_{pq}^b \\
&+ \sum_{p=1}^{M_{wb}}\sum_{q=1}^{N_{vbwb}}\sum_{i=1}^{M_{vb}} v_{iq}^b EA_s\left(\frac{q\pi}{b}\right)^2\frac{1}{2}\sin(\frac{i\pi}{L}x_s)\sin(\frac{f\pi}{L}x_s)\sin(\frac{p\pi}{L}x_s)\dot{w}_{pq}^b
\end{aligned}
\tag{199}
$$

$$\mathbf{K}_{wbwa}^{sNL,y} = (\mathbf{K}_{wawb}^{sNL,y})^T \tag{200}$$

$$\begin{aligned}
\mathbf{K}_{wbwb}^{sNL,y}\dot{\mathbf{w}}^b &= \frac{\partial^2 U^{sNL,y}}{\partial w_{fg}^b \partial w_{pq}^b}\dot{w}_{pq}^b \\
&= \sum_{p=1}^{M_{wb}}\sum_{q=1}^{N_{wb}}\sum_{m=1}^{M_{wa}} w_m^a e_c E A_s \left[\frac{1}{b}\left(\frac{q\pi}{b}\right)^2 \frac{g\pi}{b} I_{gq}^{cs}\right. \\
&\qquad \left. + \frac{1}{b}\left(\frac{g\pi}{b}\right)^2 \frac{q\pi}{b} I_{qg}^{cs}\right] \sin(\frac{f\pi}{L}x_s)\sin(\frac{p\pi}{L}x_s)\sin(\frac{m\pi}{L}x_s)\dot{w}_{pq}^b \\
&+ \sum_{p=1}^{M_{wb}}\sum_{q=1}^{N_{wb}}\sum_{m=1}^{M_{wb}}\sum_{n=1}^{N_{wb}} w_{mn}^b e_c E A_s \left[\left(\frac{n\pi}{b}\right)^2 \frac{g\pi}{b}\frac{q\pi}{b} I_{ngq}^{scc} + \left(\frac{q\pi}{b}\right)^2 \frac{n\pi}{b}\frac{g\pi}{b} I_{qng}^{scc}\right. \\
&\qquad \left. + \left(\frac{g\pi}{b}\right)^2 \frac{n\pi}{b}\frac{q\pi}{b} I_{gnq}^{scc}\right] \sin(\frac{f\pi}{L}x_s)\sin(\frac{p\pi}{L}x_s)\sin(\frac{m\pi}{L}x_s)\dot{w}_{pq}^b \\
&+ \sum_{p=1}^{M_{wb}}\sum_{q=1}^{N_{wb}}\sum_{m=1}^{M_{wa}}\sum_{r=1}^{M_{wa}} E A_s \left(\frac{q\pi}{b}\right)^2 \left(\frac{1}{b}\right)^2 \frac{b}{2} J_{fpmr}^{ssss}\left[3w_{0m}^a w_r^a + \frac{3}{2}w_m^a w_r^a\right]\delta_{gq}\dot{w}_{pq}^b \\
&+ \sum_{p=1}^{M_{wb}}\sum_{q=1}^{N_{wb}}\sum_{m=1}^{M_{wb}}\sum_{n=1}^{N_{wb}}\sum_{r=1}^{M_{wa}} E A_s \frac{1}{b}\frac{q\pi}{b}\frac{g\pi}{b}\frac{n\pi}{b} J_{fpmr}^{ssss} I_{gqn}^{ccc}\left[3w_r^a w_{0mn}^b + 3w_{0r}^a w_{mn}^b + 3w_r^a w_{mn}^b\right]\dot{w}_{pq}^b \\
&+ \sum_{p=1}^{M_{wb}}\sum_{q=1}^{N_{wb}}\sum_{m=1}^{M_{wb}}\sum_{n=1}^{N_{wb}}\sum_{r=1}^{M_{wa}}\sum_{s=1}^{N_{wb}} E A_s \frac{g\pi}{b}\frac{q\pi}{b}\frac{n\pi}{b}\frac{s\pi}{b} J_{fpmr}^{ssss} I_{gqns}^{cccc}\left[3w_{mn}^b w_{0rs}^b + \frac{3}{2}w_{mn}^b w_{rs}^b\right]\dot{w}_{pq}^b \\
&+ \sum_{p=1}^{M_{wb}}\sum_{q=1}^{N_{wb}}\sum_{i=1}^{M_{va}} v_i^a E A_s \left(\frac{g\pi}{b}\right)^2 \frac{1}{2}\cos(\frac{i\pi}{L}x_s)\sin(\frac{f\pi}{L}x_s)\sin(\frac{p\pi}{L}x_s)\delta_{gq}\dot{w}_{pq}^b \\
&+ \sum_{p=1}^{M_{wb}}\sum_{q=1}^{N_{wb}}\sum_{i=1}^{M_{vb}}\sum_{i=1}^{N_{vb}} v_{ij}^b E A_s \frac{q\pi}{b}\frac{g\pi}{b}\frac{n\pi}{b}\sin(\frac{i\pi}{L}x_s)\sin(\frac{f\pi}{L}x_s)\sin(\frac{p\pi}{L}x_s) I_{qgn}^{ccc}\dot{w}_{pq}^b \\
&\qquad + \sum_{p=1}^{M_{wb}}\sum_{q=1}^{N_{wb}} v^c E A_s \left(\frac{g\pi}{b}\right)^2 \frac{1}{2}\sin(\frac{p\pi}{L}x_s)\sin(\frac{f\pi}{L}x_s)\delta_{gq}\dot{w}_{pq}^b
\end{aligned} \tag{201}$$

E The matrices of the eigenvalue problem

E.1 Introduction

The eigenmode is computed in the same manner as described in detail in Brubak et al. [19]. The resulting eigenvalue problem can be written in the common, bold face notation as

$$(\mathbf{K}_e^M + \Lambda^e \mathbf{K}_e^G)\mathbf{w}^e = \mathbf{0} \tag{202}$$

where Λ^e is the eigenvalue and $\mathbf{w}^e$ the corresponding eigenmode. $\mathbf{K}_e^M$ and $\mathbf{K}_e^G$ are the material and geometrical stiffness matrix, respectively. These matrices are divided into submatrices, and then, $\mathbf{K}_e^M$ and $\mathbf{K}_e^G$ can be written as

$$\mathbf{K}_e^M = \begin{bmatrix} \mathbf{K}_{wawa}^M & \mathbf{K}_{wawb}^M \\ \mathbf{K}_{wbwa}^M & \mathbf{K}_{wbwb}^M \end{bmatrix}, \quad \mathbf{K}_e^G = \begin{bmatrix} \mathbf{K}_{wawa}^G & \mathbf{K}_{wawb}^G \\ \mathbf{K}_{wbwa}^G & \mathbf{K}_{wbwb}^G \end{bmatrix} \tag{203}$$

More details on these matrices are given below. In this eigenvalue problem, the amplitudes for the out-of-plane displacements given in Eqs. 24-25 are the only unknowns.

E.2 The material stiffness matrix $\mathbf{K}_e^M$-matrix

The material stiffness matrix $\mathbf{K}_e^M$ consists of bending contributions of the plate and stiffeners. This can be expressed by

$$\mathbf{K}_e^M = \mathbf{K}_e^{pb} + \mathbf{K}_e^{sb,x} + \mathbf{K}_e^{sb,y} \tag{204}$$

where $\mathbf{K}_e^{pb}$ is the bending stiffness matrix of the plate, and $\mathbf{K}_e^{sb,x}$ and $\mathbf{K}_e^{sb,y}$ are the bending stiffness matrices of stiffeners parallel and perpendicular to the free edge, respectively.

The bending stiffness matrix of the plate, $\mathbf{K}_e^{pb}$, is identical to $\mathbf{K}_{ww}^{pb}$ given in Section C.2.2. The bending stiffness matrix of a stiffener parallel to the free edge, $\mathbf{K}_e^{sb,x}$, is identical to $\mathbf{K}_{ww}^{sL,x}$ in Section D.1.5 with $EA_s = 0$ (neglecting the membrane stiffness) and with the bending stiffness EI replaced by an effective bending stiffness EI_e in the same manner as in Brubak, Hellesland and Steen [19]. Similarly, bending stiffness matrix of the stiffeners perpendicular to the free edge, $\mathbf{K}_{ww}^{sL,y}$, is identical to $\mathbf{K}_{ww}^{sL,y}$ given in Section D.1.5 with $EA_s = 0$ and with an effective bending stiffness EI_e.

E.3 The geometrical stiffness matrix $\mathbf{K}_e^G$-matrix

The geometrical stiffness matrix $\mathbf{K}_e^G$ due the an applied reference stress S_{x0} at the plate edge consists of the submatrices given in index notation in the following expressions

$$\mathbf{K}^G_{wawa} = -\sum_{p=1}^{M_{wa}} \frac{S_{x0}Lbt}{6}\left(\frac{f\pi}{L}\right)^2 \delta_{fp} \tag{205}$$

$$\mathbf{K}^G_{wawb} = -\sum_{p=1}^{M_{wb}}\sum_{q=1}^{N_{wb}} \frac{S_{x0}Lt}{2}\left(\frac{f\pi}{L}\right)^2 I^{ys}_q \delta_{fp} \tag{206}$$

$$\mathbf{K}^G_{wbwa} = -\sum_{p=1}^{M_{wa}} \frac{S_{x0}Lt}{2}\left(\frac{f\pi}{L}\right)^2 I^{ys}_g \delta_{fp} \tag{207}$$

$$\mathbf{K}^G_{wbwb} = -\sum_{p=1}^{M_{wb}}\sum_{q=1}^{N_{wb}} \frac{S_{x0}Lbt}{4}\left(\frac{f\pi}{L}\right)^2 \delta_{fp}\delta_{gq} \tag{208}$$

F Integrals

The integrals in the expressions for all the submatrices are given below

$$I^s_j = \int_0^b \sin(\frac{j\pi}{b}y)\,dy = \frac{b}{j\pi}[1-(-1)^j] \tag{209}$$

$$I^{ys}_j = \int_0^b \frac{y}{b}\sin(\frac{j\pi}{b}y)\,dy = -\frac{b}{j\pi}(-1)^j \tag{210}$$

$$I^{yc}_j = \int_0^b \frac{y}{b}\cos(\frac{j\pi}{b}y)\,dy = \frac{b}{(j\pi)^2}[(-1)^j-1] \tag{211}$$

$$I^{yys}_j = \int_0^b \left(\frac{y}{b}\right)^2 \sin(\frac{j\pi}{b}y)\,dy = \frac{b}{(j\pi)^3}\Big([2-(j\pi)^2](-1)^j-2\Big) \tag{212}$$

$$I^{yyc}_j = \int_0^b \left(\frac{y}{b}\right)^2 \cos(\frac{j\pi}{b}y)\,dy = \frac{2b}{(j\pi)^2}(-1)^j \tag{213}$$

$$I_j^{yyys} = \int_0^b \left(\frac{y}{b}\right)^3 \sin(\frac{j\pi}{b}y)\, dy = \frac{b}{(j\pi)^3}[6-(j\pi)^2](-1)^j \tag{214}$$

$$I_{jl}^{cs} = \int_0^b \cos(\frac{j\pi}{b}y)\sin(\frac{l\pi}{b}y)\, dy = \begin{cases} 0 & \text{if } j = l \\ \frac{b[1-(-1)^j(-1)^l]l}{\pi(l^2-j^2)} & \text{if } j \neq l \end{cases} \tag{215}$$

$$I_{jl}^{ycc} = \int_0^b \frac{y}{b}\cos(\frac{j\pi}{b}y)\cos(\frac{l\pi}{b}y)\, dy = \begin{cases} \frac{b}{4} & \text{if } j = l \\ \frac{b[j^2+l^2][(-1)^{j+l}-1]}{\pi^2(j^2-l^2)^2} & \text{if } j \neq l \end{cases} \tag{216}$$

$$I_{jl}^{yss} = \int_0^b \frac{y}{b}\sin(\frac{j\pi}{b}y)\sin(\frac{l\pi}{b}y)\, dy = \begin{cases} \frac{b}{4} & \text{if } j = l \\ \frac{b2jl}{\pi^2(j^2-l^2)^2}[(-1)^{j+l}-1] & \text{if } j \neq l \end{cases} \tag{217}$$

$$I_{jl}^{ycs} = \int_0^b \frac{y}{b}\cos(\frac{j\pi}{b}y)\sin(\frac{l\pi}{b}y)\, dy = \begin{cases} -\frac{b}{4\pi j} & \text{if } j = l \\ \frac{b(-1)^j(-1)^l}{\pi(j^2-l^2)^2}[j^2l-l^3] & \text{if } j \neq l \end{cases} \tag{218}$$

$$I_{jl}^{yyss} = \int_0^b \left(\frac{y}{b}\right)^2 \sin(\frac{j\pi}{b}y)\sin(\frac{l\pi}{b}y)\, dy = \begin{cases} \frac{b[2(\pi j)^2-3]}{12(\pi j)^2} & \text{if } j = l \\ \frac{b4[j^3l-l^3j](-1)^{j+l}}{\pi^2(j^6-l^6+3j^2l^4-3j^4l^2)} & \text{if } j \neq l \end{cases} \tag{219}$$

$$I_{jl}^{yycc} = \int_0^b \left(\frac{y}{b}\right)^2 \cos(\frac{j\pi}{b}y)\cos(\frac{l\pi}{b}y)\, dy = \begin{cases} \frac{b[3+2(\pi j)^2]}{12(\pi j)^2} & \text{if } j = l \\ \frac{b2[j^4-l^4](-1)^{j+l}}{\pi^2(j^6-l^6+3j^2l^4-3j^4l^2)} & \text{if } j \neq l \end{cases} \tag{220}$$

$$I_{jln}^{sss} = \int_0^b \sin(\frac{j\pi}{b}y)\sin(\frac{l\pi}{b}y)\sin(\frac{n\pi}{b}y)\, dy = \begin{cases} 0 & \text{if } \frac{j^4+l^4+n^4}{2(j^2l^2+j^2n^2+l^2n^2)} = 1 \\ \frac{b2jln[(-1)^j(-1)^l(-1)^n-1]}{\pi[j^4+l^4+n^4-2(j^2l^2+j^2n^2+l^2n^2)]} & \text{otherwise} \end{cases} \tag{221}$$

$$I_{jln}^{ccc} = \int_0^b \cos(\frac{j\pi}{b}y)\cos(\frac{l\pi}{b}y)\cos(\frac{n\pi}{b}y)\, dy = \begin{cases} \frac{b}{4} & \text{if } \frac{j^4+l^4+n^4}{2(j^2l^2+j^2n^2+l^2n^2)} = 1 \\ 0 & \text{otherwise} \end{cases} \tag{222}$$

$$I_{jln}^{css} = \int_0^b \cos(\frac{j\pi}{b}y)\sin(\frac{l\pi}{b}y)\sin(\frac{n\pi}{b}y)\, dy = \begin{cases} \frac{b}{4} & \text{if } \frac{j^4+l^4+n^4}{2(j^2l^2+j^2n^2+l^2n^2)} = 1 \text{ and } l^2+n^2 > j^2 \\ -\frac{b}{4} & \text{if } \frac{j^4+l^4+n^4}{2(j^2l^2+j^2n^2+l^2n^2)} = 1 \text{ and } l^2+n^2 < j^2 \\ 0 & \text{otherwise} \end{cases} \tag{223}$$

$$I_{jln}^{scc} = \int_0^b \sin(\frac{j\pi}{b}y)\cos(\frac{l\pi}{b}y)\cos(\frac{n\pi}{b}y)\,dy = \begin{cases} 0 & \text{if } \frac{j^4+l^4+n^4}{2(j^2l^2+j^2n^2+l^2n^2)} = 1 \\ \frac{bj[l^2+n^2-j^2][(-1)^j(-1)^l(-1)^n-1]}{\pi[j^4+l^4+n^4-2(j^2l^2+j^2n^2+l^2n^2)]} & \text{otherwise} \end{cases} \tag{224}$$

$$I_{jln}^{ysss} = \int_0^b \frac{y}{b}\sin(\frac{j\pi}{b}y)\sin(\frac{l\pi}{b}y)\sin(\frac{n\pi}{b}y)\,dy = \Phi_1 + \Phi_2 + \Phi_3 + \Phi_4 \tag{225}$$

where

$$\Phi_1 = \begin{cases} 0 & \text{if } n+l-j = 0 \\ -\frac{b(-1)^{j+l-j}}{4\pi(n+l-j)} & \text{otherwise} \end{cases}, \quad \Phi_2 = \begin{cases} 0 & \text{if } n+j-l = 0 \\ -\frac{b(-1)^{n+j-l}}{4\pi(n+j-l)} & \text{otherwise} \end{cases} \tag{226}$$

$$\Phi_3 = \begin{cases} 0 & \text{if } n-j-l = 0 \\ \frac{b(-1)^{n-j-l}}{4\pi(n-j-l)} & \text{otherwise} \end{cases}, \quad \Phi_4 = \frac{b(-1)^{n+j+l}}{4\pi(n+j+l)} \tag{227}$$

$$I_{jln}^{yscc} = \int_0^b \frac{y}{b}\sin(\frac{j\pi}{b}y)\cos(\frac{l\pi}{b}y)\cos(\frac{n\pi}{b}y)\,dy = \Psi_1 + \Psi_2 + \Psi_3 + \Psi_4 \tag{228}$$

where

$$\Psi_1 = \begin{cases} 0 & \text{if } j-l-n = 0 \\ -\frac{b(-1)^{j-l-n}}{4\pi(j-l-n)} & \text{otherwise} \end{cases}, \quad \Psi_2 = \begin{cases} 0 & \text{if } j-l+n = 0 \\ -\frac{b(-1)^{j-l+n}}{4\pi(j-l+n)} & \text{otherwise} \end{cases} \tag{229}$$

$$\Psi_3 = \begin{cases} 0 & \text{if } j+l-n = 0 \\ -\frac{b(-1)^{j+l-n}}{4\pi(j+l-n)} & \text{otherwise} \end{cases}, \quad \Psi_4 = -\frac{b(-1)^{n+j+l}}{4\pi(n+j+l)} \tag{230}$$

$$I_{jlns}^{cccc} = \int_0^b \cos(\frac{j\pi}{b}y)\cos(\frac{l\pi}{b}y)\cos(\frac{n\pi}{b}y)\cos(\frac{s\pi}{b}y)\,dy = \Theta_1 + \Theta_2 + \Theta_3 + \Theta_4 + \Theta_5 + \Theta_6 + \Theta_7 \tag{231}$$

where

$$\Theta_1 = \begin{cases} \frac{b}{8} & \text{if } j+l = n+s \\ 0 & \text{otherwise} \end{cases}, \quad \Theta_2 = \begin{cases} \frac{b}{8} & \text{if } j+l = -n+s \\ 0 & \text{otherwise} \end{cases} \tag{232}$$

$$\Theta_3 = \begin{cases} \frac{b}{8} & \text{if } j+l = n-s \\ 0 & \text{otherwise} \end{cases}, \quad \Theta_4 = \begin{cases} \frac{b}{8} & \text{if } j-l = -n-s \\ 0 & \text{otherwise} \end{cases} \tag{233}$$

$$\Theta_5 = \begin{cases} \frac{b}{8} & \text{if } j-l=n+s \\ 0 & \text{otherwise} \end{cases}, \quad \Theta_6 = \begin{cases} \frac{b}{8} & \text{if } j-l=-n+s \\ 0 & \text{otherwise} \end{cases} \tag{234}$$

$$\Theta_7 = \begin{cases} \frac{b}{8} & \text{if } j-l=n-s \\ 0 & \text{otherwise} \end{cases} \tag{235}$$

$$I_{jlns}^{ssss} = \int_0^b \sin(\frac{j\pi}{b}y)\sin(\frac{l\pi}{b}y)\sin(\frac{n\pi}{b}y)\sin(\frac{s\pi}{b}y)\,dy = \Omega_1+\Omega_2+\Omega_3+\Omega_4+\Omega_5+\Omega_6+\Omega_7 \tag{236}$$

where

$$\Omega_1 = \begin{cases} -\frac{b}{8} & \text{if } j+l=-n+s \\ 0 & \text{otherwise} \end{cases}, \quad \Omega_2 = \begin{cases} -\frac{b}{8} & \text{if } j+l=n-s \\ 0 & \text{otherwise} \end{cases} \tag{237}$$

$$\Omega_3 = \begin{cases} \frac{b}{8} & \text{if } j+l=n+s \\ 0 & \text{otherwise} \end{cases}, \quad \Omega_4 = \begin{cases} \frac{b}{8} & \text{if } j-l=-n+s \\ 0 & \text{otherwise} \end{cases} \tag{238}$$

$$\Omega_5 = \begin{cases} \frac{b}{8} & \text{if } j-l=n-s \\ 0 & \text{otherwise} \end{cases}, \quad \Theta_6 = \begin{cases} -\frac{b}{8} & \text{if } j-l=-n-s \\ 0 & \text{otherwise} \end{cases} \tag{239}$$

$$\Omega_7 = \begin{cases} -\frac{b}{8} & \text{if } j-l=n+s \\ 0 & \text{otherwise} \end{cases} \tag{240}$$

$$I_{jlns}^{sscc} = \int_0^b \sin(\frac{j\pi}{b}y)\sin(\frac{l\pi}{b}y)\cos(\frac{n\pi}{b}y)\cos(\frac{s\pi}{b}y)\,dy = \Upsilon_1+\Upsilon_2+\Upsilon_3+\Upsilon_4+\Upsilon_5+\Upsilon_6+\Upsilon_7 \tag{241}$$

where

$$\Upsilon_1 = \begin{cases} -\frac{b}{8} & \text{if } j+l=n+s \\ 0 & \text{otherwise} \end{cases}, \quad \Upsilon_2 = \begin{cases} -\frac{b}{8} & \text{if } j+l=-n+s \\ 0 & \text{otherwise} \end{cases} \tag{242}$$

$$\Upsilon_3 = \begin{cases} -\frac{b}{8} & \text{if } j+l=n-s \\ 0 & \text{otherwise} \end{cases}, \quad \Upsilon_4 = \begin{cases} \frac{b}{8} & \text{if } j-l=-n-s \\ 0 & \text{otherwise} \end{cases} \tag{243}$$

$$\Upsilon_5 = \begin{cases} \frac{b}{8} & \text{if } j-l=n+s \\ 0 & \text{otherwise} \end{cases}, \quad \Upsilon_6 = \begin{cases} \frac{b}{8} & \text{if } j-l=-n+s \\ 0 & \text{otherwise} \end{cases} \tag{244}$$

$$\Upsilon_7 = \begin{cases} \frac{b}{8} & \text{if } j-l=n-s \\ 0 & \text{otherwise} \end{cases} \tag{245}$$